SELECTION OF μ-MESONS BY A ČERENKOV COUNTER SYSTEM AND AN INVESTIGATION OF THE INTERACTIONS PRODUCED BY THEM IN LEAD PLATES IN A WILSON CLOUD CHAMBER.

Thesis

submitted by

Michael John Landels

B.Sc., (Edinburgh).

for the Degree of

Doctor of Philosophy.

University of Edinburgh

May, 1964.

PREFACE

The research described in this thesis has been carried out in the Department of Natural Philosophy of the University of Edinburgh, under the joint direction of Professor N. Feather, F.R.S. and Dr. G. R. Evans.

CONTENTS

Chapter 1.

INTRODUCTION

1.1. Čerenkov Radiation.

In recent years, the Čerenkov detector has become one of the most important instruments for the detection of charged particles. The counter is based on the fact that a small amount of light is emitted when a charged particle traverses a medium with a velocity which is greater that the velocity of light in that medium. The amount of light emitted, depends on the charge of the particle, (usually e, the electronic charge), the velocity of the particle and the refractive index of the medium being traversed.

The first systematic attempt to study the phenomenon was made by Mallet, who observed that light emitted from a large number of transparent bodies, placed close to a radio-active source, always had the same bluish-white quality and that the spectrum was continuous. In 1934, Čerenkov commenced a series of experiments on the phenomenon which was later designated by his name. These experiments involved the effect of a flux of particles and they continued until 1938. The experimental results were in excellent agreement with the theory of the effect which had been proposed in 1937 by Frank and Tamm.

Frank and Tamm considered a charged particle slowly traversing a transparent medium. The atoms in the region close to the passing particle will be distorted, and the medium polarised about the instantaneous position of the particle. Thus, as the particle passes through the medium, each portion of the

dielectric along the track will, in turn, receive an electromagnetic pulse. Owing to the symmetry of the polarisation field about the particle, there will be no resultant field at large distances, and therefore, no radiation.

If, however, the particle is travelling with a velocity comparable with the velocity of light in the medium, the polarisation field is no longer symmetrical. Along the axis, there is a resultant dipole field, which will be apparent even at large distances from the particle track.

In general, the radiated wavelets will interfere destructively, to give a zero field intensity, but if the velocity of the particle is greater than the velocity of light in the medium, it is possible for the wavelets from all portions of the track to be in phase, so that there is now a resultant field at some distant point. It can easily be calculated from a Huygen's construction, that the relation for Čerenkov radiation is:-

$$\cos\Theta = \frac{1}{\beta n} \qquad (1.1)$$

where Θ is the angle from the direction of the particle track, at which wavelets from points on the track are coherent.

n is the refractive index of the medium.

β is the ratio of the velocity of the particle to the velocity of light in vacuo, c.

Frank and Tamm also obtained the following result, for the number of photons emitted per unit path length, within wavelength limits, λ and $\lambda + d\lambda$

$$\frac{dN}{dl} = \frac{2\pi e^2}{\hbar c}\left(1 - \frac{1}{\beta^2 n^2}\right)\frac{d\lambda}{\lambda^2}$$

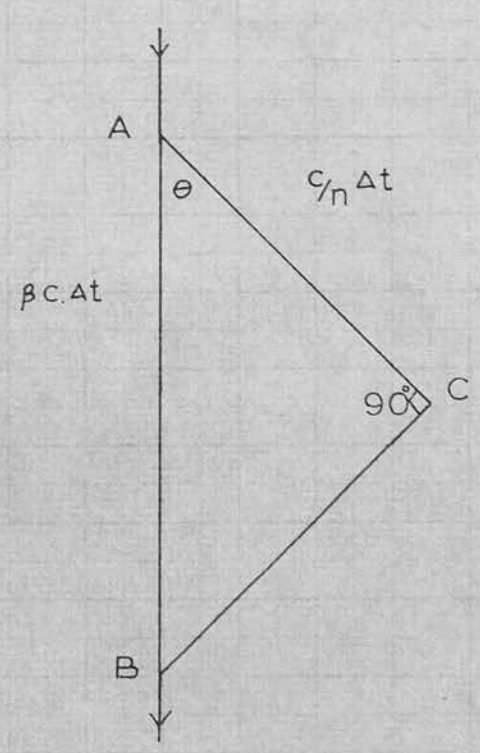

Fig 1·1 Diagram to illustrate
Cerenkov Relation

From these results, certain conclusions can be drawn. These are enumerated below:-

1. The light from each point on the track will be emitted along the surface of a cone of semi-angle Θ, the axis of the cone being the track of the particle.

2. There will be a critical velocity β_{crit}, below which no radiation occurs (equal to the velocity of light in the medium). At this velocity, the angle is equal to 0^{o}.

$$\beta_{crit} = \frac{1}{n} \qquad (1.3).$$

3. As the velocity of the particle increases above β_{crit}, the angle Θ will also increase (Fig. 1.2 and 1.3). This effect will be discussed in more detail below. It will be seen, however, that for a particular medium, there will be a maximum value of Θ, i.e. Θ_{MAX}, which corresponds to a particle travelling with the velocity of light c.

It will be seen from relation (1.3), that a critical velocity, and therefore radiation can only exist when $n > 1$. For all substances likely to be used in these experiments, the refractive index is greater than one in the visible and near-ultraviolet regions of the spectrum. Thus, these regions will be suitable for the production of Čerenkov radiation. Of course, the absorption lines for the elements present, will ensure that certain wavelengths within these regions will not contribute to the light output, since, although photons of these frequencies are radiated, they will be absorbed in a short distance. These lines are so narrow, however, that their total width compared to the width of the spectral range studied, is very small and can be

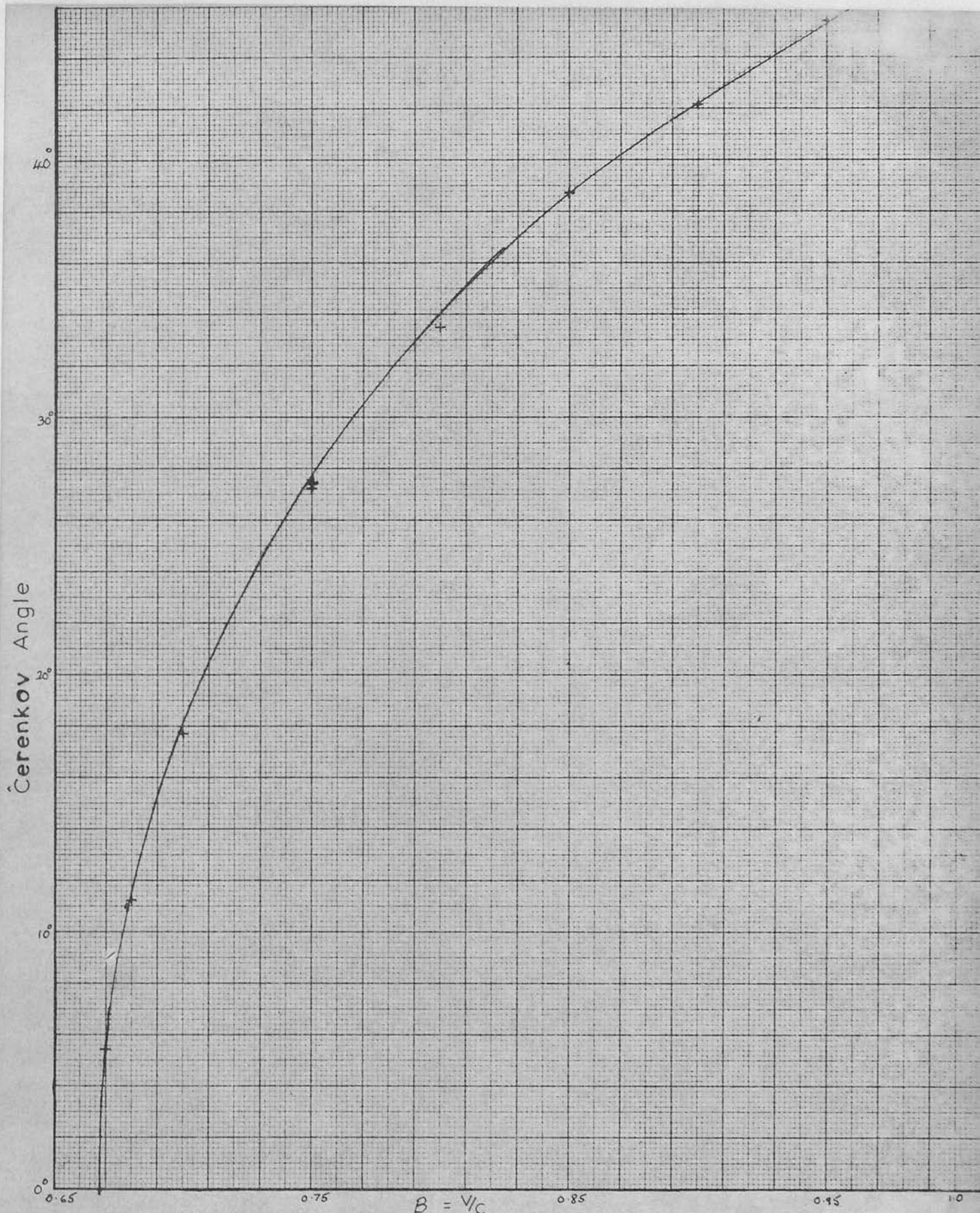

Fig 1·2 Cerenkov Angle Variation with Velocity(n = 1·50

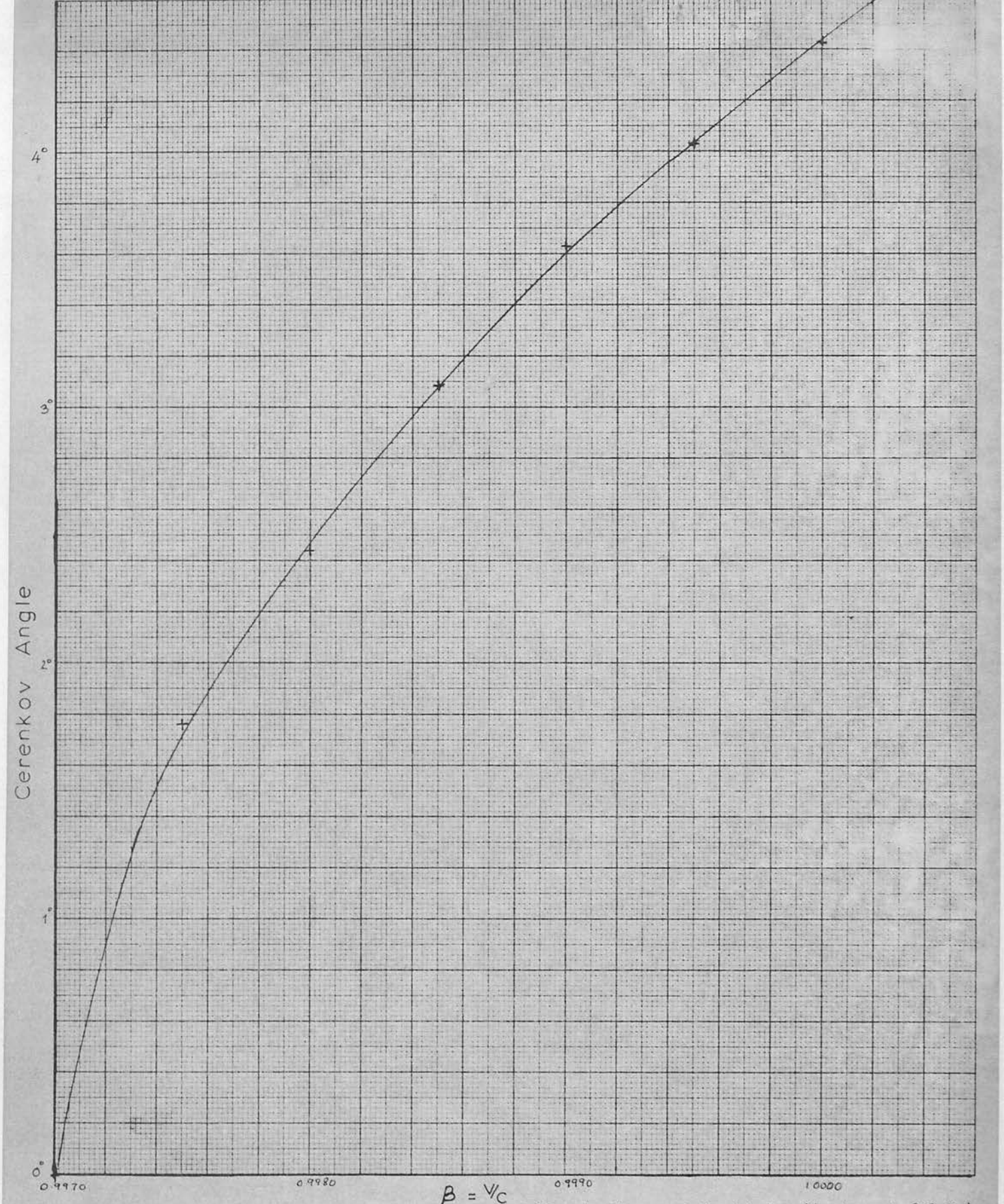

Fig 1·3 Cerenkov Angle Variation with Velocity (n = 1·003)

neglected. Thus, for substances such as glass, water, gases etc., the refractive index in the visible and near-ultraviolet regions, is such as to make Čerenkov light production possible. It is also possible, however, that other regions of the spectrum satisfy the condition that $n > 1$.

If a medium is considered, which is more or less transparent in the visible region, a curve can be drawn of the variation of the refractive index of the medium against wavelength. Although this curve is different for different substances, there are certain general features in common. At $\lambda = 0$, the index of refraction is 1; for γ-rays and short X-rays, the index is slightly less than 1. Thus, no Čerenkov radiation is possible in these regions of the spectrum, except perhaps in the neighbourhood of absorption bands. If the refractive index is measured in the neighbourhood of an absorption band, it will be observed that the index decreases more rapidly as it approaches the band from the short wavelength side. On the long wavelength side of the band, the refractive index is found to be very high, decreasing at first rapidly and then more slowly, as the wavelength is increased beyond the absorption band. It will be seen that although generally, the index of refraction might be less than 1, it may be considerably higher, in the region of absorption bands and therefore, in such regions, Čerenkov light is capable of being produced. The first absorption is found in the X-ray region, at a wavelength depending on the atomic weight of the heaviest element in the material. For silicon, it reaches its maximum at 6.731A$^{\circ}$. This absorption rises sharply to a maximum, and then falls off rapidly at the K-absorption limit of the element. Beyond this,

will lie the other absorption discontinuities L, M, --- of this element, as well as the K, L, M, --- limits of the other elements present in the medium. Thus, although at these absorption bands radiation is possible, it would be strongly absorbed, and therefore can be neglected in this region. The refractive index remains less than unity for the remainder of the X-ray region and also in the far ultraviolet. When it does exceed unity again, in the ultraviolet, it is in a region of strong absorption once more.

Somewhere in the near infra-red, there will be another absorption band. The centre of this band for quartz is at 8.5μ, but the absorption begins to become strong at 4.5μ. Beyond this first absorption band, there usually exist one or more others. In passing each of these bands, the index of refraction increases.

At wavelengths beyond all of the infra-red bands, the index decreases slowly and uniformly, through the region of radio waves, approaching a limiting value for infinitely long waves equal to $\sqrt{k}$, the square root of the dielectric constant.

Thus, it will be seen that Čerenkov radiation is concentrated in certain wavelength bands, the visible region extended into the near ultraviolet and infra-red, parts of the far infra-red and the radio wave region. In our experiments, only Čerenkov radiation in the visible part of the spectrum will be considered. This was decided originally due to the choice of glass as the window material, to withstand the pressures envisaged in the counters. The glass imposes a low wavelength cut off in the neighbourhood of 3700A$^{\circ}$.

If the effects of the refractive index variation within the visible part of the spectrum are considered, it can be seen that they are twofold. Firstly, there will be different threshold

velocities for different wavelengths; thus a particle could have a velocity above threshold, for the blue end of the spectrum, and yet have its velocity below threshold for the red end. Secondly, the number of photons produced in the blue region will be greater than the number in the red region. This relation can be rewritten as:-

$$\frac{dN}{dl} = c\left\{1 - \frac{1}{\beta^2 n^2}\right\}\frac{d\lambda}{\lambda^2} \qquad (1.4)$$

where c is a constant.

If the velocity of a particle is increased, an idea of the contributions made by these effects can be obtained. If the particle velocity is less than $\frac{1}{n}$, no radiation is possible. When the velocity reaches a value equal to $\frac{1}{n}$ for the short wavelengths, light within these wavelengths will be produced and as the velocity increases, longer and longer wavelengths will be included. In the case of a gas, this region between the critical velocity for blue light and the critical velocity for red light is extremely small and for practical purposes can be neglected. At still higher velocities, there is, effectively, a linear increase in the number of photons produced, with increasing velocity. These effects are due to the term in the brackets in relation (1.4). If the other term in the expression, consisting of the wavelength variation is considered, one can see why the radiation is concentrated in the blue region of the spectrum. The number of photons will be seen to be inversely proportional to the square of the wavelength.

The Čerenkov angle relation (1.1) can be rewritten as:-

$$\cos\theta = \frac{\beta_{crit}}{\beta}$$

It will be seen that until $\beta > \beta_{crit}$, i.e. $\beta > \frac{1}{n}$, no light is

emitted, and thereafter cos θ is equal to the ratio of the critical velocity to the velocity of the particle. This shows that θ initially increases rapidly with increasing velocity but as $\beta \rightarrow 1$, the variation becomes less and less marked. (Figs. 1.2 and 1.3). Some examples of the magnitudes involved for a particle travelling with the velocity of light, through 30 cms. path length in the medium, are shown in Figure 1.4.

Substance	Critical Velocity	No. of Photons.	Čerenkov Angle.
Glass	0.67c	9,100	48° 11'
Nitrogen 100 atmospheres	0.9700c	940	14° 6'
Nitrogen 1 atmosphere	0.9997c	9.8	1° 18'

Figure 1.4.

In the initial experiments, Čerenkov detected the effects of a flux of electrons and he was able to measure the relative intensities of the light emitted from 16 pure liquids. He found the range of intensities to be rather small, and also showed that spectral distribution varied little, from liquid to liquid. He also proved that the radiation was not fluorescence, and in a later experiment, made a crude check on the $\cos \theta = \frac{1}{\beta n}$ relation. Čerenkov also measured the absolute intensity of the radiation and found excellent agreement with the theory of Frank and Tamm. The first clear evidence that single fast particles could be detected with high efficiency, was produced by Jelley (1951). By this time, the light detecting device was, of course,

the photomultiplier tube, In Jelleys experiments, a water detector was used to select cosmic ray particles. The first experiments to detect the radiation from gaseous substances, were made by Ascoli Balzanelli and Ascoli (1953). They selected high energy cosmic ray particles passing through chloroform vapour. They obtained a refractive index in the region 1.01 to 1.02 and the light pulses produced in the vapour, were detected by a photomultiplier, run in coincidence with the Geiger counter telescope used to select the particles. In these experiments, Čerenkov radiation was being studied as a phenomenon, but in the meantime counters making use of the Čerenkov effect were being developed.

The Čerenkov counter has certain properties which make it unique among the various detectors of charged particles. Firstly, it has directional properties, emitting light only in the direction of the particles motion. Thus, it is able to distinguish between two particles moving anti-parallel to each other. The second difference is that the Čerenkov counter can distinguish between particles with different velocities, in the high velocity range (the relativistic region).

In the case of the cloud chamber (the drop count), the emulsion (the grain count) and the scintillation counter (the light production), the measured quantity is a function of the ionisation loss of the particle, in traversing the medium. This ionisation loss, as given by the Bethe-Block formula, can be used in the low velocity region, $\beta = 0.10$ to $\beta = 0.90$, to distinguish between particles with velocities within this range. At high velocities, $\beta > 0.96$, however, the Bethe-Bloch formula only gives

a very slight variation of ionisation loss with increasing velocity and it is no longer possible, using these techniques, to distinguish between particles in the higher velocity range. Thus, the Čerenkov counter is able to operate in a region where the resolution of the above detectors is small. The only other method of distinguishing between particles of different velocity, in this high velocity range, is by magnetic deflection and this depends on the momentum of the particle, not the velocity. Thus, if a beam from an accelerator, which has a small amount of impurity is considered, the Čerenkov detector can be used to eliminate the impurity. For example, if there is a 122 Mev. muon beam, with a contamination of pions, the corresponding velocities would be $\beta = 0.8919$ for muons and $\beta = 0.8573$ for pions, Therefore, if a pulse from a Čerenkov detector, of critical velocity $\beta_{crit} = 0.86$ is required, the pion contamination could be eliminated by a coincidence arrangement.

The Čerenkov pulses are very much sharper than the scintillation pulses, the response time being limited by the electronic circuits, rather than inherently. The intrinsic speed of a Cerenkov counter may be as short as $10^{-11} - 10^{-13}$ sec.

One of the most striking properties of Čerenkov radiation is the angular effect. The angle at which the light is emitted, depends on the ratio of the velocity of the particle, to the critical velocity, hence, in principle, it is possible to construct a detecting medium and an optical system, which will focus light emitted along the particle track at a certain chosen angle, and eliminate light emitted at any other angle.

An example of this type of counter is one due to Marshall. The apparatus is shown in Figure 1.5, and consists of a combined

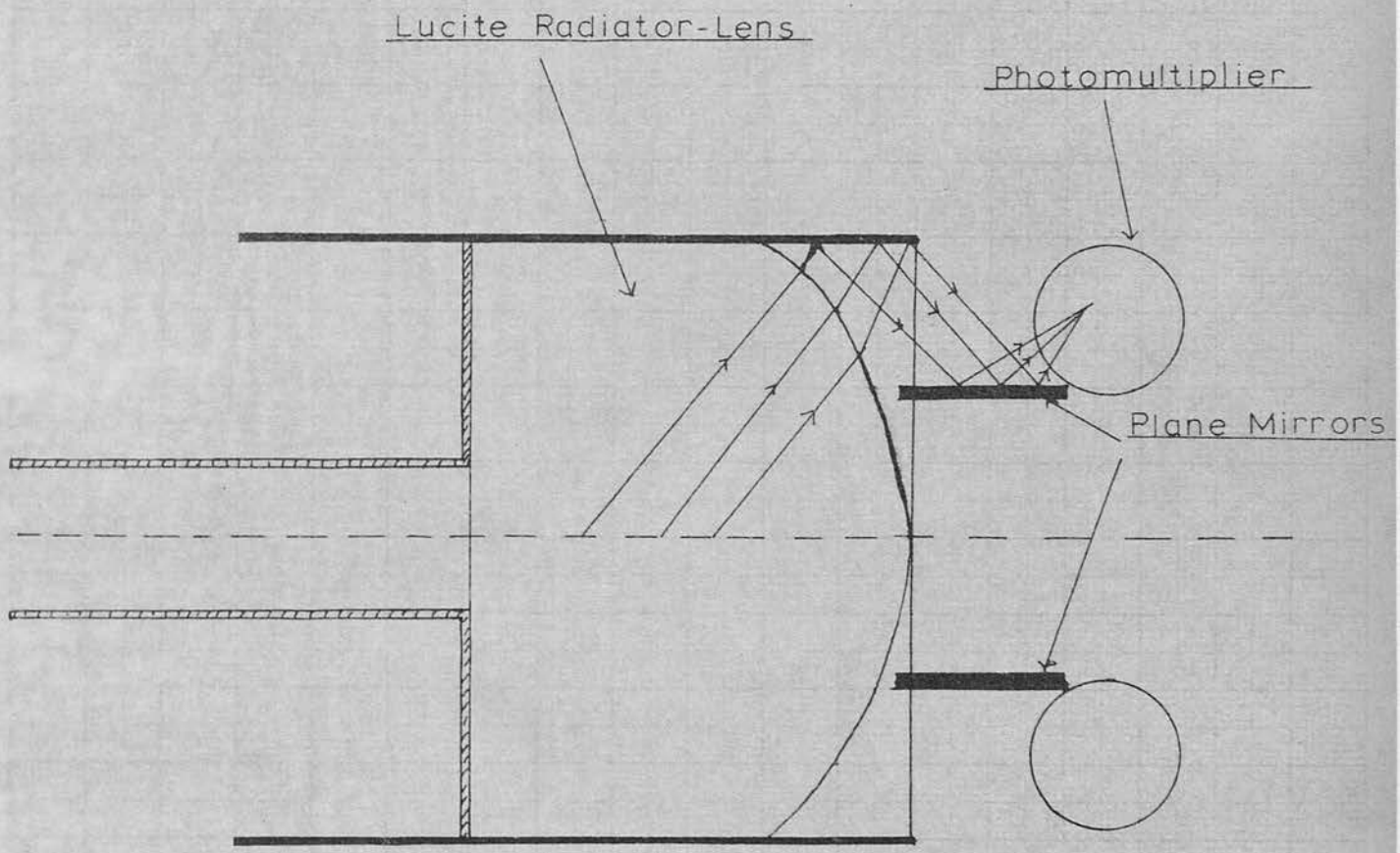

Fig. 1·5 Apparatus of Marshall

radiator and lens of Lucite. Surrounding the radiator-lens combination is a cylindrical mirror, and between the lens and the photomultipliers, there are two plane mirrors for splitting the light. A coincidence count, from the two photomultipliers, is required, and the various angles can be selected by varying the position of the radiator-lens, with respect to the plane mirrors and photomultipliers. It should be noticed, that with this arrangement, the photomultipliers are not on the direct particle path, which is a great advantage, from the point of view of reducing the background count. With such an arrangement, Marshall was able to resolve 145 Mev. from 121 Mev. pions, the two Čerenkov angles measured being 39.9° and 38.0° respectively. The resolution in this experiment was approximately 19 Mev. or ~ 13% at 145 Mev.

1.2. Experimental Considerations.

In the previous section, it has been shown that particles can be selected by their Čerenkov angle. However, in the case considered above, it will be noticed that the velocities of the particles were comparatively low. In the extremely high velocity region, the difficulties associated with the angular selection method, will be discussed, when cosmic rays are used as the particle flux.

Consideration of the variation of Čerenkov angle against velocity for glass (n = 1.500), shows that there is a rapid increase in angle with increasing velocity, in the region just above the critical velocity, but the curve begins to flatten out at higher velocities. For example, an increase in velocity from $\beta = 0.67$ to $\beta = 0.69$, gives a change in the Čerenkov angle from $\sim 5\frac{1}{2}^{\circ}$ to $\sim 15^{\circ}$,

whereas a corresponding velocity change, in the high velocity region, say $\beta = 0.93 - 0.95$, changes the angle from $44\frac{1}{2}^{\circ}$ to $45\frac{1}{2}^{\circ}$. Hence, it will be seen, that this method is best applied to particles, whose velocity is just greater than the critical velocity, i.e. in this case, the low velocity range.

If a medium is chosen, whose critical velocity is itself very high, i.e. nitrogen at a pressure of 10 atmospheres, ($\beta = 0.9970$), the position is not improved, as the maximum possible angle in this case is only approximately 4.3°, so this does not give a good angle to velocity ratio.

There is also another disadvantage to be found with the angular discrimination method, from the point of view of a selection experiment. The velocity range of interest is $\beta > 0.99$, and the cosmic radiation had to be used as the source of particle flux. Now, in the angular method, the particles are assumed to pass along the axis of the optical system or parallel to it. This is not a drawback, in the case of an accelerator source, but in the case of cosmic rays, where the particles are orientated at all angles, the counting rate would be very small if such a great limitation on the angle was imposed. The position and size of the scintillators in our telescope is such as to select particles travelling within a cone of semi-angle $2^{\circ}\ 30'$, about the vertical. Thus, if we are to select all suitable particles within this cone by the angular method, it is required that the selected angle be indeterminate to this amount. If a counter with critical velocity 0.97c (100 atmospheres of nitrogen) is considered, a 1 Gev. muon would produce light at an angle $\Theta = 12^{\circ}\ 57'$. If all particles

orientated up to 2° 30' to the vertical are to be included, the apparatus should be arranged to accept particles travelling at this angle. Thus, in the limiting case, this means accepting light produced at 10° 27' to the vertical. This would mean accepting vertical muons of energy 0.536 Gev. Thus, instead of having a limit fixed at 1 Gev., muons would be selected whose energy was as low as 0.536 Gev. Likewise, the angle could be as large as 15° 3', before the particle was eliminated.

If the pressure is reduced to make the critical velocity nearer the required selected velocity, the situation is improved slightly. At 20 atmospheres of nitrogen, a 1 Gev. muon produces light at a Čerenkov angle of 3°. Thus, it would be possible to count muons orientated at 2° 30' to the vertical, that are producing light at 0° 30'. The selection energy would thus be dropped to 0.86 Gev. Therefore, it will be seen, that if this method of selection was adopted, there would be a region of indeterminacy dependant on the telescope angle. Of course, this angle could be reduced to make the indeterminacy less, but this would correspondingly reduce the counting rate.

The practical difficulties could, perhaps, be seen more clearly, if an actual angle measuring counter is considered. In a counter of this nature, if there is a lens symmetrically placed with respect to the counter axis, and a particle travelling along or parallel to the axis, all the Čerenkov light emitted at a certain angle θ, will be focussed onto a ring of fixed radius, $f\theta$, where f is the focal length of the lens. Of course, this ring will not be infinitely thin, but due to diffraction, etc., will have a finite thickness and a fixed radius depending on the angle of emission. If the particle

is orientated at an angle φ to the vertical, the centre of the focal ring will be displaced by an amount equal to $f\varphi$.

The method of selection used in such counters is to block the view of the photomultiplier, except for an annulus corresponding to the focal ring for the particles required. As this annulus will have finite thickness defined by r and r + dr, it will accept a range of angles, θ to $\theta + d\theta$, at which light is emitted by vertical particles. The relation is that

$$r + dr = f(\theta + d\theta).$$

As well as this, however, certain sections of the rings produced by inclined particles, could overlap portions of the annular hole, and therefore, inclined particles of various velocities could count, with an efficiency depending on the proportion of their focal ring overlapping the annular hole.

It will be seen that this problem is extremely complicated and it was considered that a better cut off could be obtained by threshold discrimination.

In the threshold discriminator, any light produced, irrespective of angle, is collected and is focussed onto the photomultiplier. The criterion adopted is not the angle at which the light is emitted, but whether or not light is produced. Thus, if such a counter is available, theoretically, it should be possible to separate particles, the velocity of which is greater than the critical velocity, from those moving at less than the critical velocity. The impossibility of achieving this condition on practical grounds will be discussed later.

In the experiments to be considered, it was intended to

develop a counter, which would select particles travelling in the range $0.9900 < \beta < 1$ and in fact, an even higher bottom limit 0.9970 was concentrated on. In order to eliminate all particles below these limits, a medium with a refractive index in the neighbourhood of unity was required. Another consideration was that a medium in which the refractive index could be readily varied in the above critical velocity range, $(n - 1.0100 - 1.0000)$, was needed. The medium which best suited these requirements was obviously a gas, and the one chosen was nitrogen. The refractive index of nitrogen, at atmospheric pressure is 1.0003 and the variation of refractive index with pressure, at comparatively low pressures, is linear (the case with all pressures used in these experiments). The refractive index also varies with temperature, so it is essential to know the temperature at which the counter is filled. Temperature variations after filling do not matter if there are no leaks in the apparatus, because, the refractive index can be taken as being proportional to $\frac{1}{1+aT}$ where a is a constant. Thus, if the temperature increases, the pressure will increase and the two effects tend to cancel out. For a rise of as much as 5° C, no appreciable change in the refractive index would be noticed.

It has been stated that the variation of the refractive index of nitrogen with wavelength at atmospheric pressure is very small, (1.000288 at 3200 A° to 1.000276 at 6800 A°), and thus, a constant refractive index over the whole wavelength range of photomultiplier sensitivity can be assumed. In order to cover the above range in refractive index, and therefore critical velocity, it is required

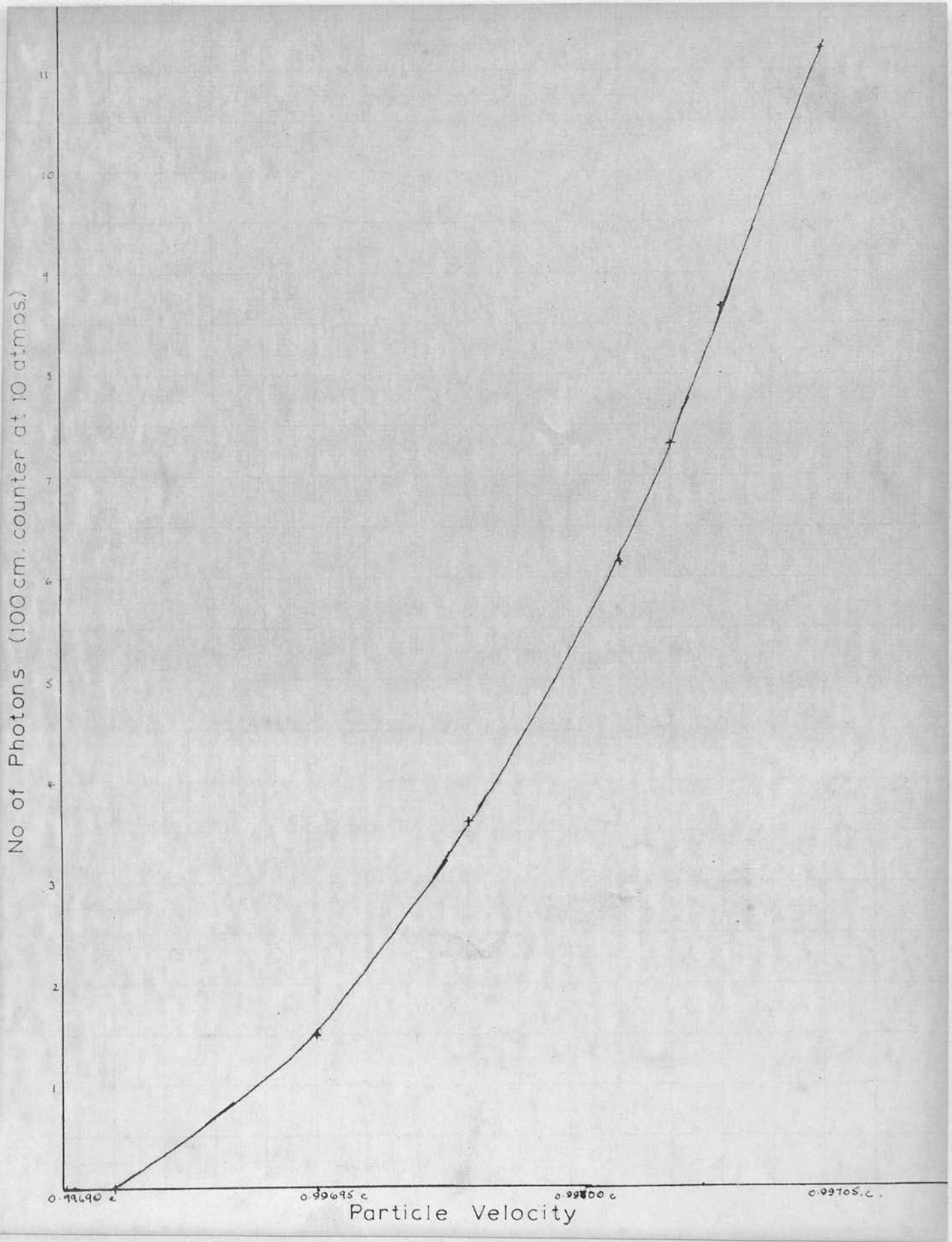
No of Photons (100 cm. counter at 10 atmos.)
1
2
3
4
5
6
7
8
9
10
11
0·99690 c
0·99695 c
0·99700 c
0·99705 c.
Particle Velocity

Fig.1·6

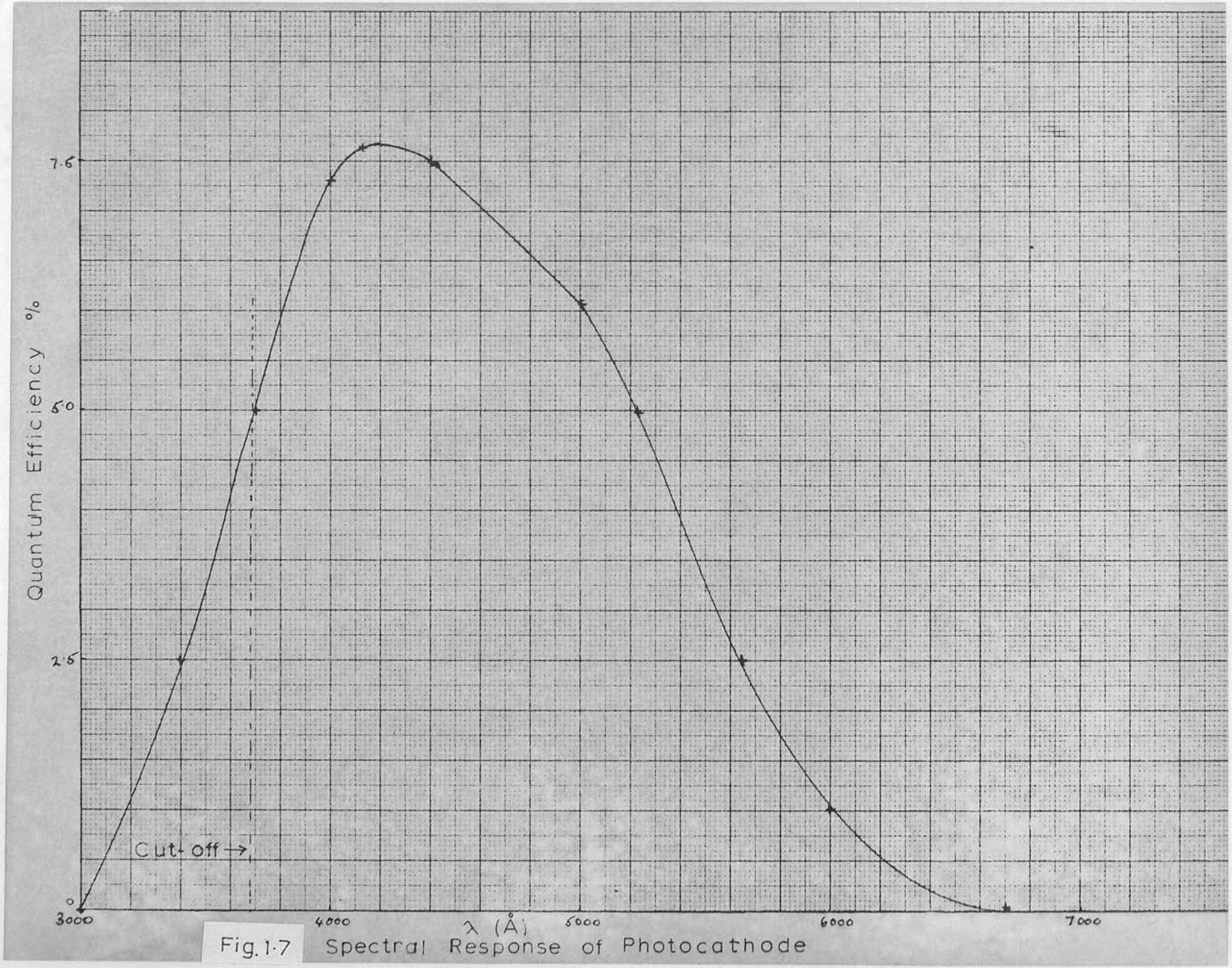

Fig. 1.7 Spectral Response of Photocathode

that the counter should be able to take a pressure of up to ~ 33 atmospheres.

It has been mentioned previously, that theoretically, one should not count any particle travelling at a velocity lower than the critical velocity for the counter, and should count every particle travelling at a velocity higher than the critical velocity. Thus, there should be a selection efficiency of 0% up to β_{crit}, and an efficiency of 100% at and above β_{crit}. In the practical case, however, these conditions are not obtained due to several considerations. Firstly, by equation (1.2), it will be seen that the number of photons emitted at the critical velocity is 0, and the number increases, as the particle velocity is increased with respect to the critical velocity. This means that no pulse could be obtained at the critical velocity, or immediately above, as the number of photons emitted would be very small. Secondly, as the refractive index varies with wavelength, there will be a complicated function describing the increase in photon number with increasing velocity (Figure 1.6). Thirdly, as the quantum conversion efficiency of the photomultiplier is low (7.5% at maximum - Figure 1.7), a large number of photons are required to produce a small number of photoelectrons. Also, due to statistical fluctuations in this process, the same number of photons arriving at the photocathode at different times, need not always produce the same number of photoelectrons.

If we consider, a nitrogen counter at a pressure of 10 atmospheres, it will be seen that the critical velocity is 0.9970c. If the assumption is made that if 60 or more photons reach the

photomultiplier, there will always be an identifiable pulse, and if less than 60 photons arrive, no pulse is produced, (Fig. 1.8) is obtained In this graph, perfect optical properties for the collection of the light have been assumed, i.e. all the photons emitted reach the photocathode. Obviously, this is still an idealised picture of the situation, but it enables some insight to be obtained on the effect the practical limitations impose. The number of 60 photons for 100% efficiency can be taken, at this stage, as an example, although it was later proved to be approximately the correct value for one of the counters. With these assumptions, the efficiency curve (Figure 1.8), has been drawn, the manner of construction being as follows. Firstly, a path length in the counter of 100 cms. is considered, this being approximately the length of one of the counters used in the experiments. If, for example, a particle velocity corresponding to $\beta = 0.9972$, is considered, the number of photons emitted would be 20 ± 5 and the percentage of particles emitting 60 or more photons would be ~ 0. At $\beta = 0.9977$, 68 ± 8 photons would be emitted giving more than 60 photons in $\sim 95\%$ of the cases.

In Figure (1.8), it will be seen that instead of the sharp rise at 0.9970, there is no appreciable rise until 0.9973 and thereafter, a finite gradient which is reduced, as the efficiency reaches 100%. Full efficiency is only obtained at approximately $\beta = 0.9978$, so if 100% efficiency is taken as the criterion, the critical velocity is displaced by an amount $\Delta\beta = 0.0008$. This effect becomes important when two counters are considered.

In the testing of the counters, there were a large number of

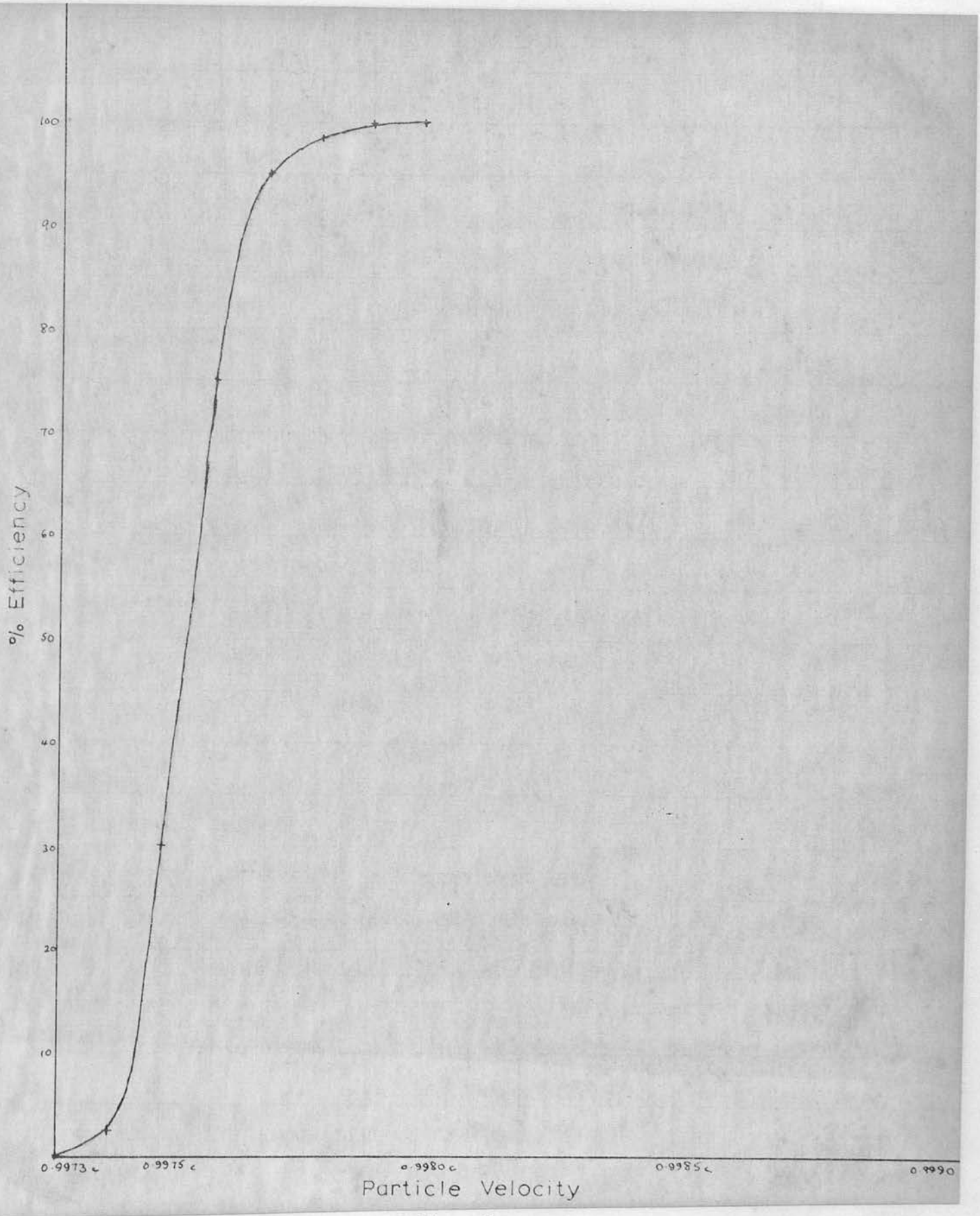
100
90
80
70
60
50
40
30
20
10
% Efficiency
0.9973c
0.9975c
0.9980c
0.9985c
0.9990
Particle Velocity

Fig. 1·8

experiments with a single Čerenkov detector, but the actual intention of the main experiment was to select particles within a certain band width of velocities, rather than those with a velocity greater than some critical velocity. Obviously, with a single counter, particles are being selected within the band of velocities between the critical velocity and the velocity of light in vacuo c. However, if there are two counters, one whose pressure is arranged to give a critical velocity β_{c1}, and another counter whose pressure is different, corresponding to a critical velocity β_{c2} ($\beta_{c1} > \beta_{c2}$), theoretically particles can be selected within the range $\beta_{c_2} < \beta < \beta_{c1}$, by putting the two counters, one in anti-coincidence with the other. If β is in the above range, the particle will be able to produce light in the second counter, giving a pulse from the photomultiplier, whereas the first counter will receive no light pulse. Thus, an anti-coincidence circuit would give a count for a particle in the above range. If $\beta > \beta_{c1}$, both counters would give a pulse and the anti-coincidence circuit would eliminate such a particle, whereas if $\beta < \beta_{c2}$, neither of the counters would be triggered.

If the efficiency curves for two identical counters, where the refractive indices are slightly different are considered, two similar efficiency curves, will be obtained slightly displaced from each other (by the separation of their critical velocities). If the efficiency characteristic of the first counter is denoted by ε_1 and that of the second counter by ε_2, the efficiency for an anti-coincidence arrangement is given by $\varepsilon_1 (1 - \varepsilon_2)$. This function is calculated for different values of $\Delta\beta$, the difference in velocity between the critical velocities of the two counters. The results

are shown in Figure (1.9). By consideration of these curves, it will be seen that two effects occur. Firstly, if there are two counters whose critical velocities are different by an amount $\Delta\beta = 0.0010$, i.e. the pressures in the counters being 10 atmospheres and $6\frac{2}{3}$ atmospheres, efficiency curve 1 will be obtained. It will be seen on comparing this curve with the dotted theoretical curve, that the region selected would be displaced, and no particle would be selected below a value of ~ 0.9973. Likewise, particles would be selected at a higher velocity than would be expected in the perfect efficiency case i.e. up to 0.9989c. However, in this case it will be noticed that 100% efficiency is attained and that the curve has approximately the same shape as the dotted one, except for the finite slope and rounded corners.

If curve 2 is considered, where the pressures in the counters are 10 atmospheres and $8\frac{1}{3}$ atmospheres respectively, it will be seen that a maximum efficiency of $\sim 99\%$ is attained as well as the shift to the higher velocity of selection. This effect of not attaining 100% efficiency becomes greater as $\Delta\beta$ is decreased. For example, in curve 3, for pressures of 10 atmospheres and $9\frac{2}{3}$ atmospheres, the maximum efficiency is only $\sim 57.5\%$, and over most of the range, it is considerably less than this value.

Thus, it would appear from these considerations that two effects occur. Firstly, the anti-coincidence region is displaced and secondly, as the two critical velocities are brought closer together, the maximum possible efficiency and also, the average efficiency over the region, became greatly reduced. This obviously puts a limitation on the possible band width $\Delta\beta$.

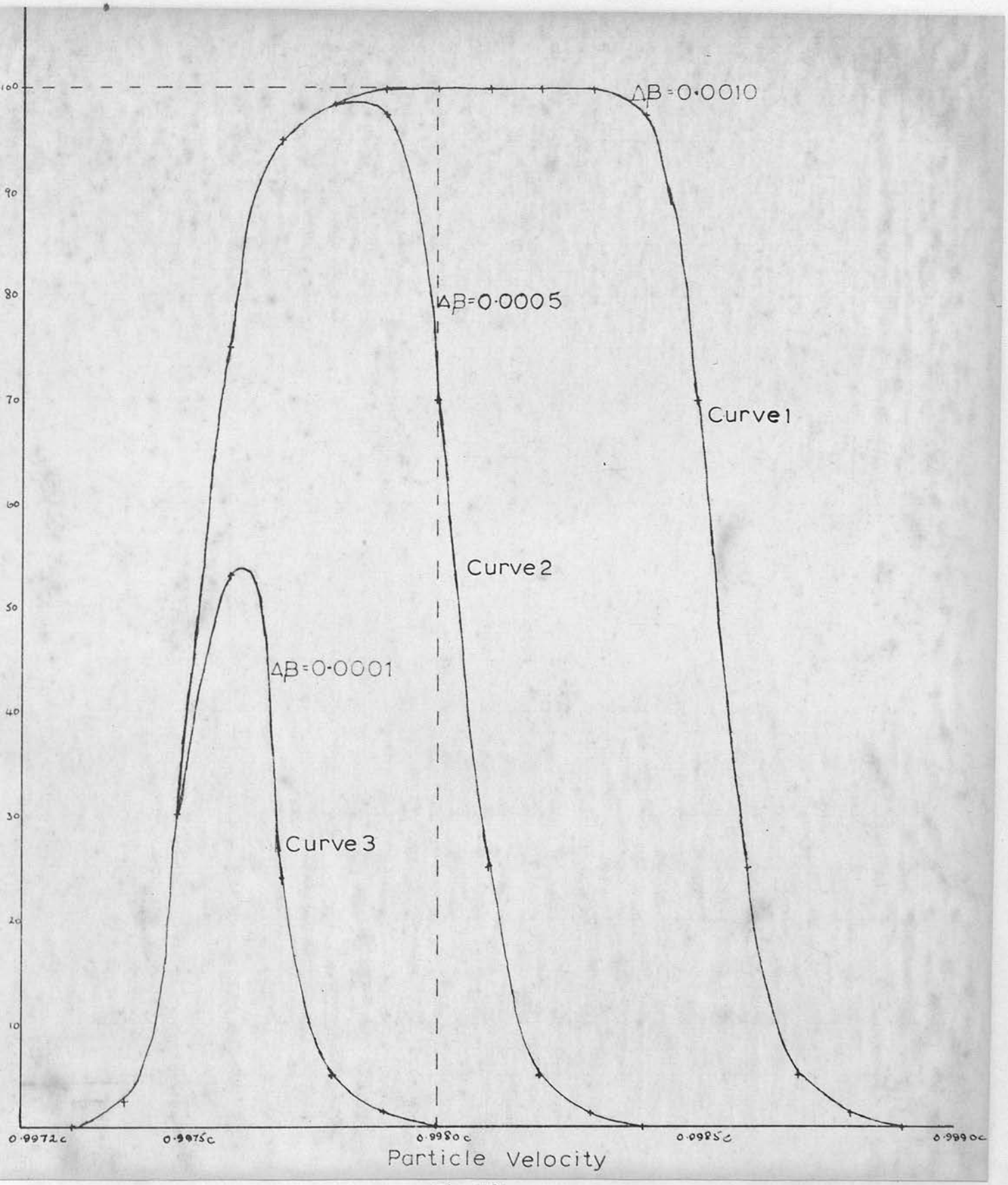
ΔB = 0·0010
ΔB = 0·0005
ΔB = 0·0001
Curve 1
Curve 2
Curve 3
100
90
80
70
60
50
40
30
20
10
0·9972c
0·9975c
0·9980c
0·9985c
0·9990c
Particle Velocity

Fig. 1·9

Thus, it would appear from the above considerations that for selecting particles in the high velocity range, the threshold discrimination method is in principle,possible. At a later stage, the experimental efficiency of the counters will be discussed in more detail.

Chapter 2.

DESCRIPTION OF THE COUNTERS.

In this chapter, the counters used in the experiments will be described. In preliminary experiments, to decide on the best design for the Čerenkov counters, a high pressure Wilson cloud chamber was used, firstly as a pressure holding device, to provide the sensitive medium for a Čerenkov counter, then as a combined cloud chamber - Čerenkov counter. These experiments on the design of the Čerenkov counter, will be described in Appendix 1. It is sufficient to state here, that these experiments proved that Čerenkov light, emitted by a single particle in a gaseous medium could be detected. Also, no significant scintillation effects were observed in the gas, or in a glass window. It was also proved that particles passing through the glass envelope of the photomultiplier could be counted by the Čerenkov light they emit, and therefore, the photomultiplier had to be placed out of the particle path. The counters used in the experiments can be divided into two groups, the Čerenkov counters and the scintillation counters.

2.1. The Čerenkov Counters.

These counters were designed purely for the efficient production and collection of Cerenkov light. Two identical counters were originally built, although certain modifications, described below, were carried out on one of the counters. The counters in the original form, were capable of holding pressures up to approximately 400 lb./sq. in.

In calculating the size of the Čerenkov counters, use was made

of the photomultiplier data, which gave ~ 4 photoelectrons, as the mimimum number which could be counted with an efficiency approaching 100%. The average number of photons, producing 4 photoelectrons, is approximately 60. The counters were to be used to select muons in the energy range 1 to 1.5 Gev., (β = 0.9954 - 0.9979). Thus, if it was required that 60 photons be produced in the counter, and there was a pressure giving a critical velocity just below the required velocity, few photons would be produced per unit path length, and a very long counter would be required. On the other hand, there could be a pressure, giving a critical velocity well below the required velocity, in which case a shorter counter would suffice. If for example, a 1 Gev. muon is considered, and the pressure of the counter is 16 atmospheres, it would require the counter to be ~ 220 cms. long, in order to obtain 60 photons. If the counters were to be as long as this, the counting rate from the counter telescope would be impossibly low, therefore a balance has to be obtained between these effects. A pressure of 25 atmospheres was a reasonable figure, in which case the counter would have to be ~18 cms. long. It will be realised that these figures were approximate, and just gave the order of magnitude for the counter. In actual fact, the counters when constructed had a sensitive length of ~40 cms. This was to enable the selection of particles below 1 Gev. if required, without increasing the pressure in the counter. With such lengths, it was found that the counting rate from the telescope was reasonable.

The other problem concerns the collection of light. In the previous experiments (Appendix 1), it was shown that the phototube

must be removed from the particle path, and for this reason, the light was deflected by a mirror, through 90° into a side tube. It is essential that as much light as possible is collected, and therefore, the absorption and scattering of the light by the black cylinder walls has to be overcome. If particles travelling down the axis of the tube are considered, it will be seen that the Čerenkov light, produced in the lower region of the tube, would strike the mirror directly. However, the light produced further up the tube, would strike the side walls and be scattered, before it reached the mirror. In the case of particles travelling along the tube axis, this is not a serious problem, with the length of counter and pressure envisaged. However, there will be some particles travelling parallel to the axis, but displaced to the side, and others which are inclined to the axis, for which a proportion of the light emitted, would strike the walls and be scattered or absorbed. For this reason, it becomes essential to have a reflecting surface, lining the cylinder wall, in order that as many of the emitted photons as possible are collected. Such a reflecting surface has interesting optical properties for particles travelling parallel to the tube axis. It will be seen that the angle at which light would be reflected from the walls would be such, that all light, whether direct or reflected once or more times, would be travelling parallel to the sides of the Čerenkov cone. Thus, such a surface, as well as increasing the amount of light being reflected down the tube, also ensures that all the light, direct or reflected, is being propagated at the same angle to the particle track i.e. the Čerenkov angle θ. If, therefore, a lens

is placed above the reflecting mirror, it will focus all the light onto a ring of radius $f\theta$, where f is the focal length of the lens. The focal length of the lens, and its position and that of the mirror, can be arranged in such a way, that the focal ring is positioned in the centre of the side tube. This side tube should likewise be lined with a reflecting surface. The reflecting surface chosen for the counters was a hollow glass cylinder aluminised on the inside surface, in order to prevent any Čerenkov light, produced in the walls of the glass cylinder, escaping into the sensitive region and perhaps, reaching the photomultiplier.

Each counter, (Figure 2.1), consisted of a steel cylindrical tube, of diameter 3 inches, length 19 inches, and wall thickness 3/10 inch. A short side tube, 2 inches in diameter and 2½ inches long, is joined to the first, 2 inches above the base, by a hard soldered joint. The main tube is closed at both ends, by end pieces bolted to flanges; the seals being made by O-rings. The side tube is closed by an armoured plate glass window. The pressure seal being made by 2 O-rings. Six inches above the base of the main tube there is a gas entry pipe and pressure tap, through which the cylinder can be filled. The reflecting mirror set at 45° to the axis of the main tube, was set opposite the side tube entrance. The mirror, aluminised on its front surface, to ensure that no Čerenkov light produced in the glass of the mirror, could reach the phototube, was 2¾ inches in diameter. The converging lens, of diameter 2¾ inches and focal length 4 inches was placed above the mirror, with its axis coincident with the axis of the tube. The focal length of the lens was chosen so that the light

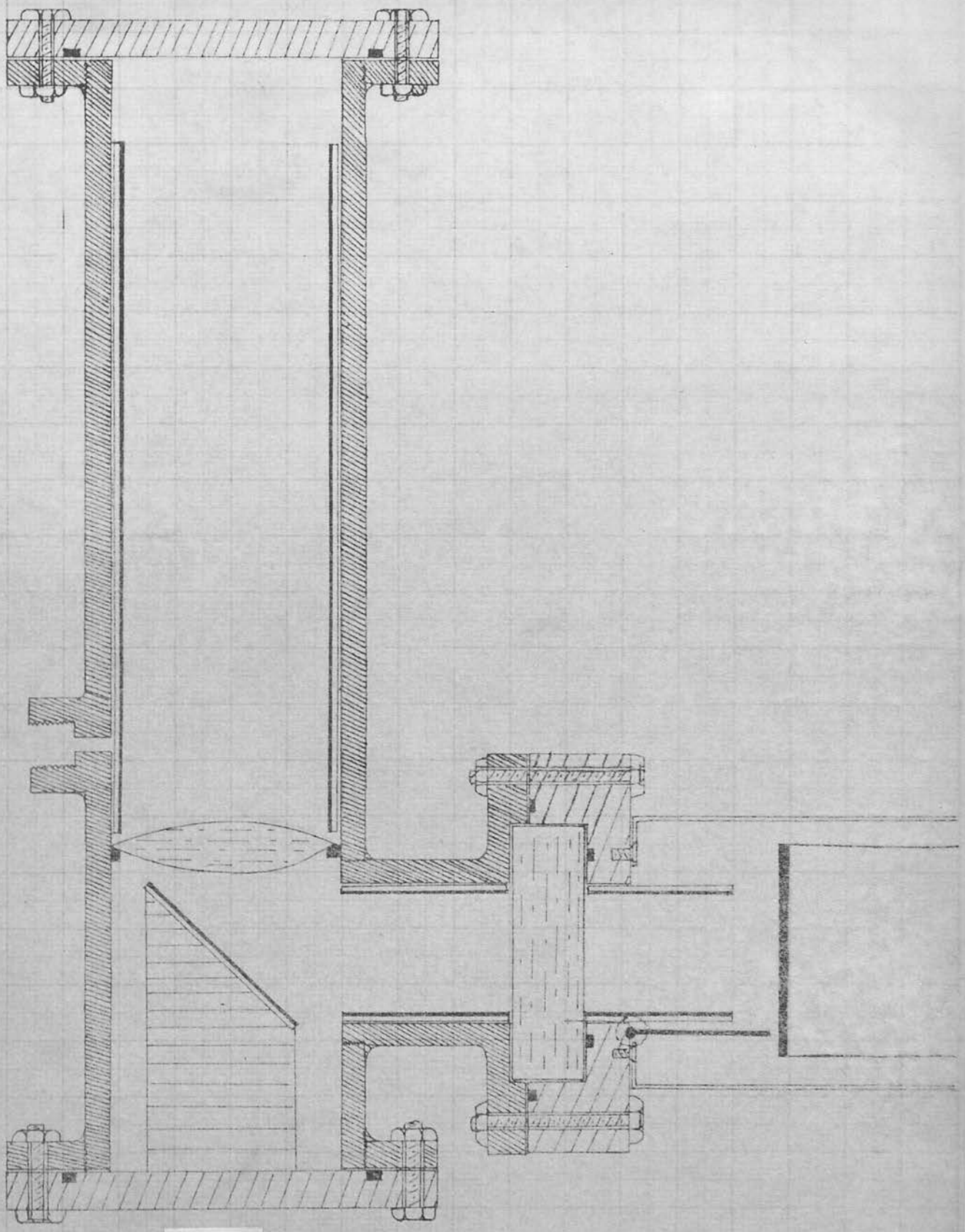

Fig. 2·1 Nitrogen Čerenkov Counter

ring was focussed in the centre of the entrance to the side tube. The apparatus was set up with the main tube vertical and therefore, the side tube horizontal.

The above description applies to both Čerenkov counters, except that one counter had an additional brass tube clamped to the top of the steel tube, the seal being made by a rubber gasket. This increased the sensitive length of this counter to 100 cms. and obviously increased the number of photons produced at any particular pressure. The pressure attainable in this counter was less than in the unmodified counter, due to the strength of the brass. It will be convenient in what follows, to call the unmodified counter, the small counter, and the counter modified by the addition of the brass tube, the large counter.

The Čerenkov light, reflected into the side tube, falls onto the photocathode of a 13 - stage photomultiplier tube (E.M.I. 9514S). The pulses from the photomultiplier are passed, in turn, to a cathode follower, a commercial wide band amplifier of band width 250 Mc/s. and gain 40, (Fleming Radio Developments 2002), and finally to a commercial coincidence unit with an input pulse discriminator of minimum height 2 volts.

The photomultiplier, for convenience, and also to keep it light tight, was included in the Čerenkov counter assembly. The photomultiplier base connections are shown in Figure 2.2. The E.H.T. voltage is applied to the anode of the photomultiplier, and the interstage voltages are provided by a resistance chain, the whole circuit being included in the light tight box. The cathode follower is used to match the high output impedence of the photo-

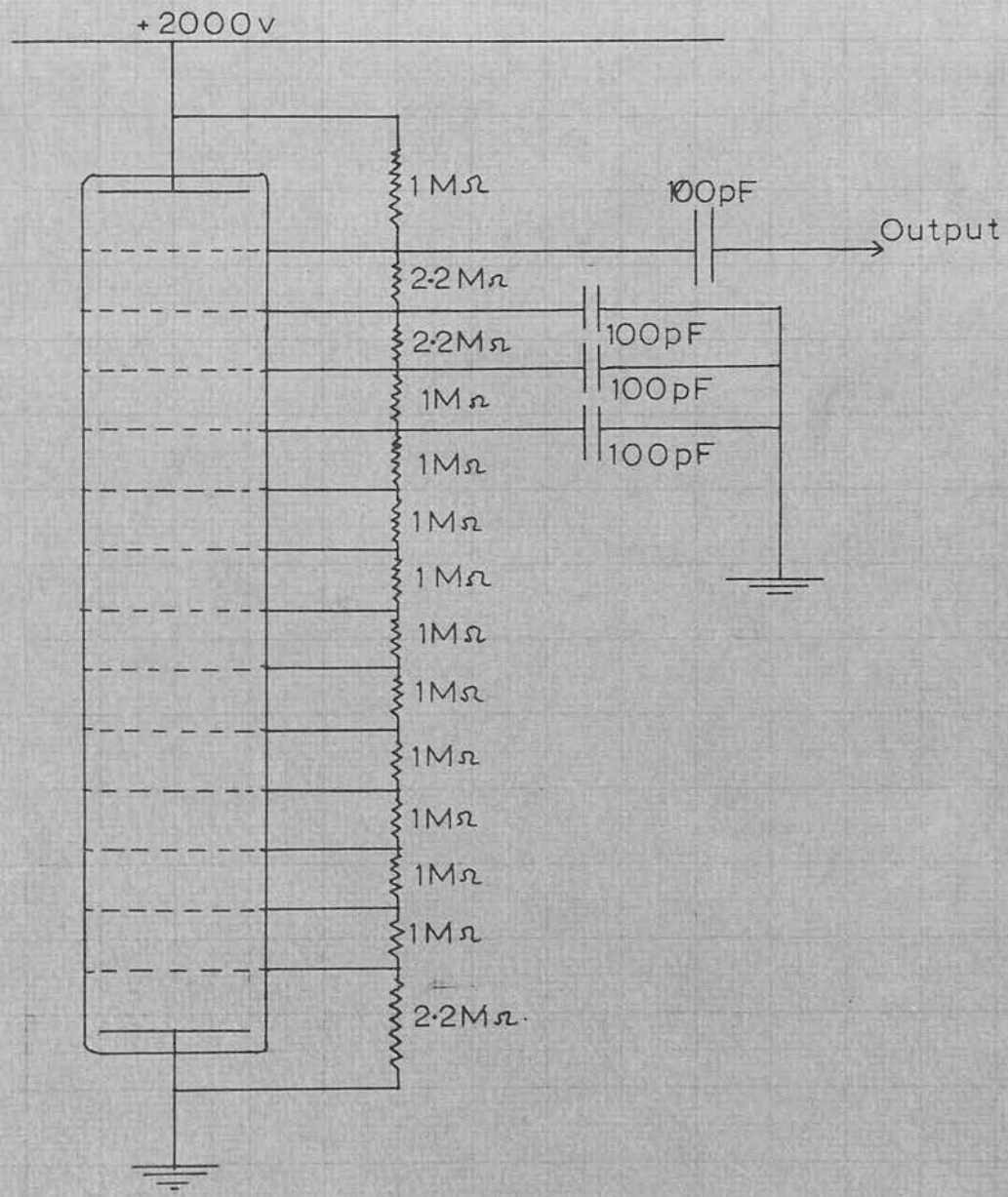

Fig.2·2 Photomultiplier Base Circuit

multiplier to the low input impedence of the amplifier. The circuit for the original cathode follower is shown in Figure (2.3a), and for a later model in Figure (2.3b).

If a pulse of say 2.8 volts, incident on the coincidence unit, is required in order to count, and it is assumed that the amplifier is being run at its maximum gain of 40, this means that a pulse of height 0.07 volts must leave the last dynode. This corresponds to a charge of 7.2×10^{-12} coulombs on the last dynode, and assuming the gain of the phototube to be 10^7, when run in this fashion, this gives a figure of 4.5 photoelectrons leaving the photocathode. By comparing the quantum conversion curves for the photomultiplier, it will be seen that, on average, 4.5 photoelectrons are produced by 60 photons. Thus, it will be seen that if 60 photons are collected by the photocathode, this should be sufficient to enable a count to be observed with the system as described.

2.2. Scintillation Counters.

The scintillation counters all had the same basic physical arrangement, i.e. a photomultiplier tube in good optical contact with a piece of plastic scintillator (NE 101). When a charged particle passed through the scintillating medium, pulses of light were produced which could be converted into electrical pulses, by the photomultiplier tube. For details of the scintillation process see Birks. An important property of the scintillation effect is that the light is emitted in all directions, and is, therefore, unlike Čerenkov radiation, where the light is only emitted in the forward direction of the particle motion.

The photomultiplier tubes used in all but one of the

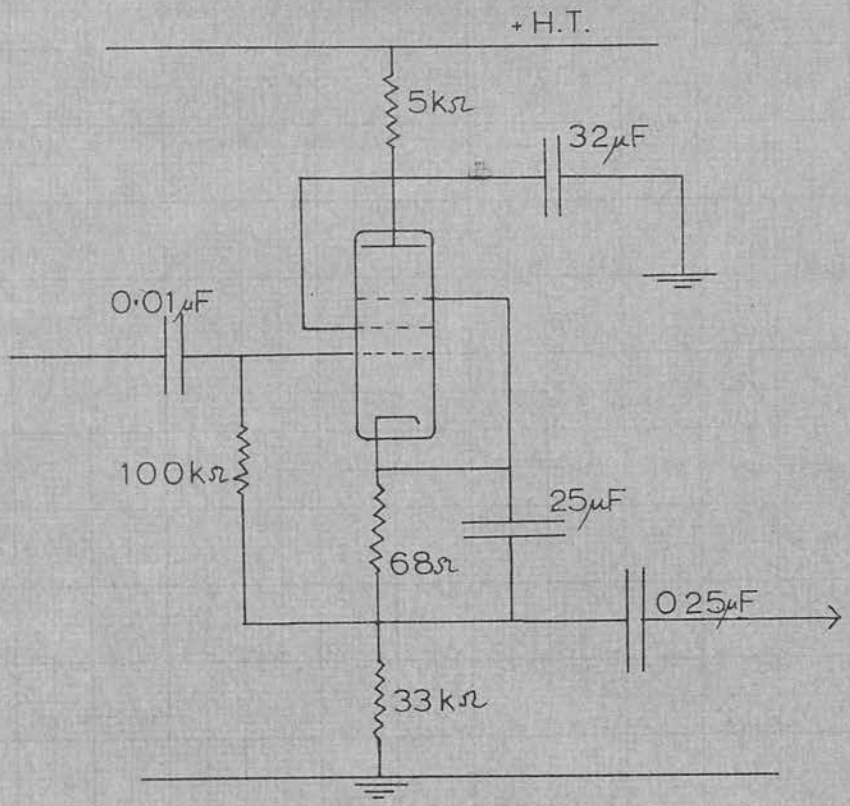

Fig. 2·3a Cathode Follower (Type 1)

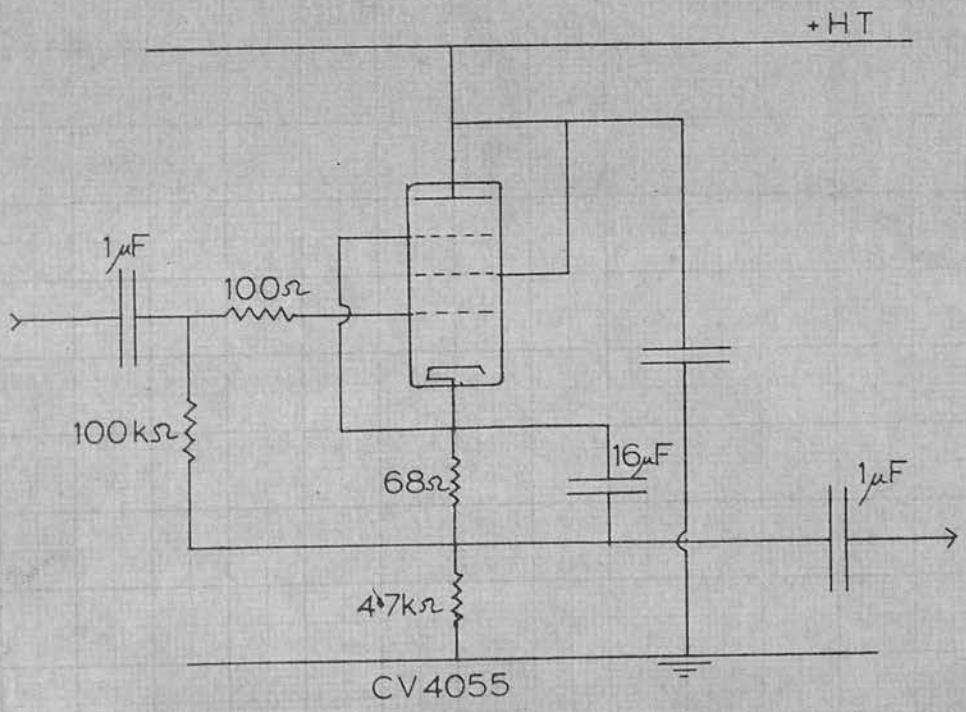

Fig. 2·3b Cathode Follower (Type 2)

scintillation counters, were of type E.M.I.9514S, the exception being an 11-stage E.M.I.6099B. The vertical counter had the following construction. The photomultiplier and scintillator were enclosed in a light tight box, usually cylindrical in shape, of height about 15 inches and diameter 6 inches. The photomultiplier was held upright, along the axis of the box, by means of the photomultiplier base which was screwed to a piece of tufnol. The tufnol was held in position by several O.B.A.threaded rods, which extended through the base and lid of the counter. The plastic scintillator was held in position against the end window of the phototube, by another, similar piece of tufnol. The optical contact, between the end window of the phototube and the scintillating medium was originally made by a thin layer of vaseline. This, however, was replaced in all the later experiments, by a layer of glycerine, which was found to have better optical properties. It was essential, in the setting up of the counter, to ensure that no air bubbles existed in the connecting optical layer. In this respect, the glycerine was far better than vaseline.

Also connected inside the light tight box, were the photomultiplier base connections, identical to those in the Čerenkov counters, and the output and E.H.T. plugs were attached to the lid of the box. These plugs had Apiezon packed around them, in order to keep the box light tight. The complete internal structure was fitted to the lid of the box, to make examination of the scintillator simpler. A diagram of this counter is shown in Figure (2.4). In this type of counter, the direction of particle motion is parallel to the axis of the cylindrical box, and therefore,

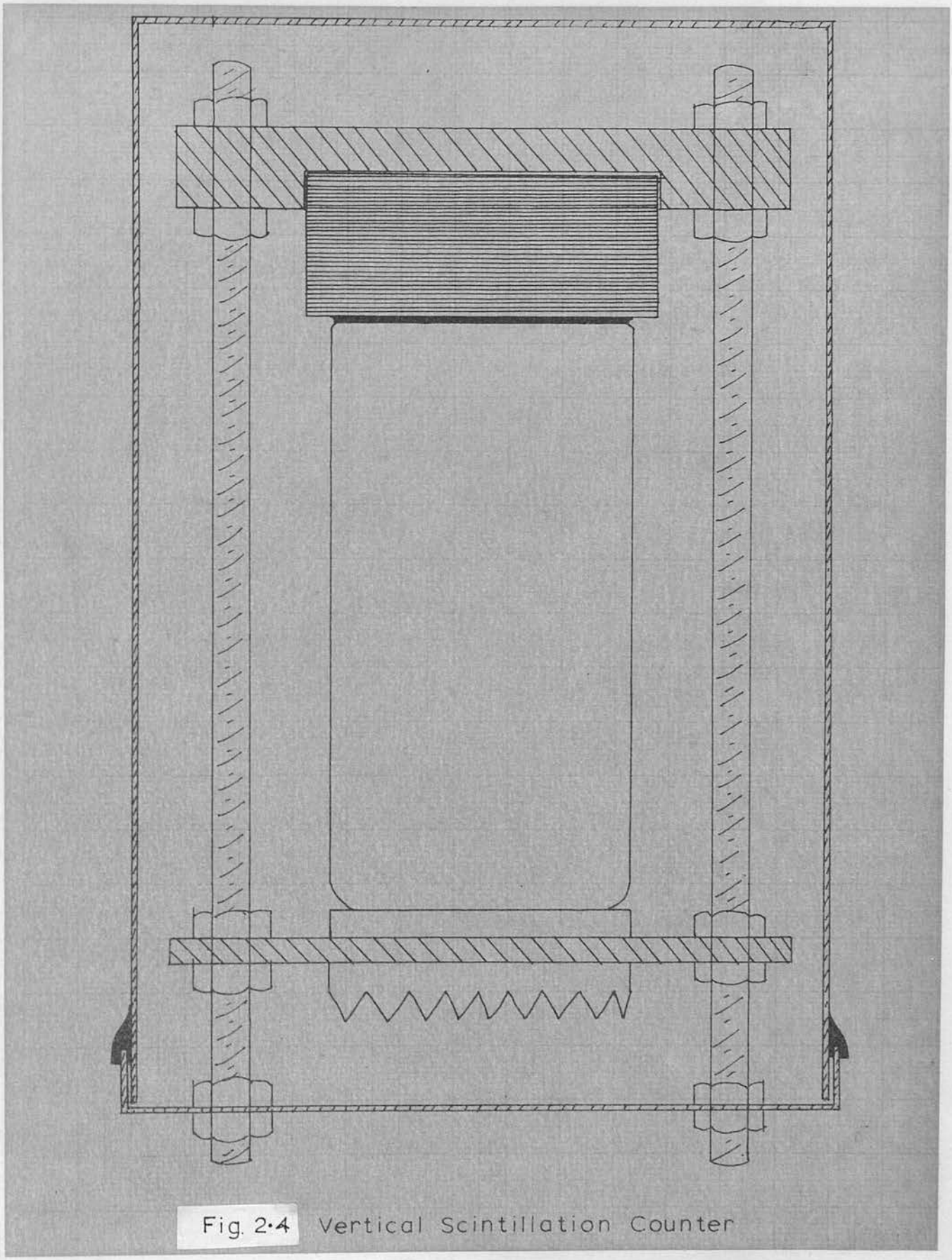

Fig. 2·4 Vertical Scintillation Counter

if a counter telescope is used, the distance between counters is determined by the length of the cylindrical boxes. Now, in some cases, two Čerenkov counters are required to be placed, one above the other, with a scintillation counter in between, and the distance between the base of the top Čerenkov counter and the top of the lower counter, should be as small as possible. For such situations, and in anti-coincidence counter experiments, another type of scintillation counter,was developed, in which the phototube is at right angles to the direction of the required particles. A diagram of this type of counter is shown in Figure (2.5). It will be seen from the diagram, that this counter is rectangular in cross-section, and has two steps lengthways. In the thicker part of the box, the photomultiplier is supported horizontally, and in the thinner part, there is the scintillating medium, also supported horizontally. The optical contact between the scintillator and the photocathode, is made by the edge of the scintillator, rather than the base, as was the case in the counter described previously.

The two types of counter are different, from the point of view of light collection. In the first type, the vertical counter, the photocathode subtends quite a large angle for direct light collection, and this angle is relatively independent of the position of the particle track in the scintillator. If the scintillator surface is covered with reflecting paint, except for the part in optical contact with the photocathode, nearly all the light reaches the photocathode after only a few reflections. Therefore, the amount of light lost on reflection, and absorption in the scintillator will be comparatively small. Thus, it is possible to

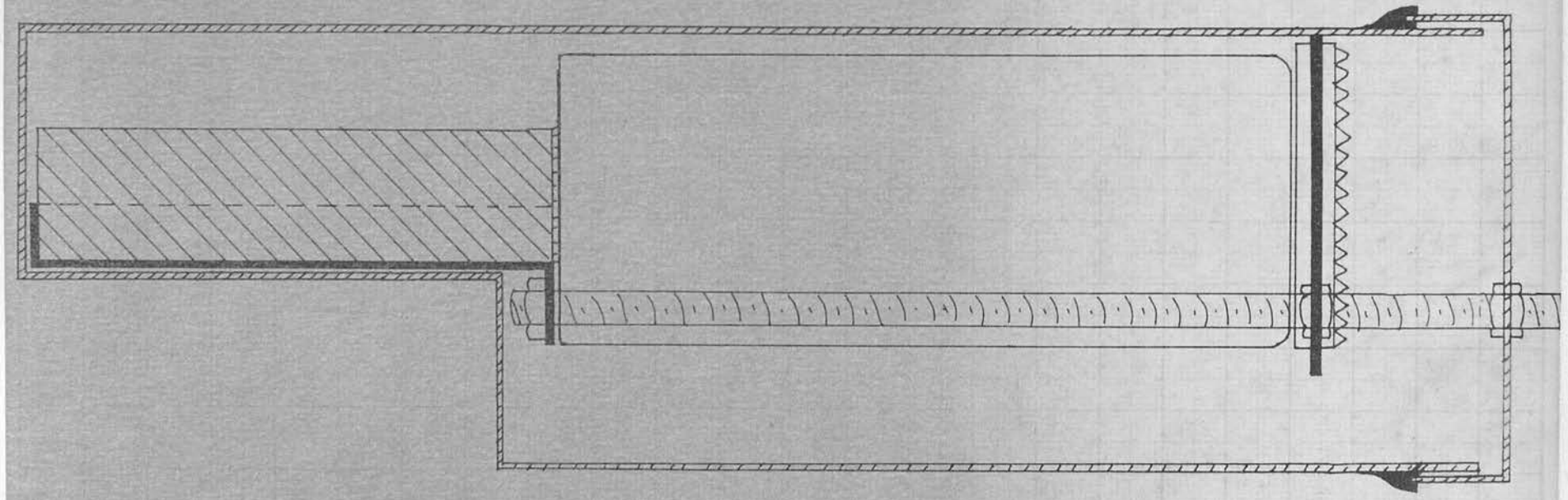

Fig.2·5 Horizontal Scintillation Counter

use this counter, in conjunction with a pulse height discriminator, to distinguish between particles losing different amounts of energy in the scintillating medium.

In the second type, the horizontal counter, the conditions are such that the photocathode only subtends a small solid angle, for the acceptance of direct light, and quite a large proportion of the light has to travel an appreciable distance and suffer numerous reflections, before it can enter the phototube. Thus, depending on the position of the particle track with reference to the photocathode, varying amounts of light can be lost due to absorption and on reflection. Thus, this type of counter could not be used for any pulse height resolution. However, in the cases in which this second type of counter is used, this is no disadvantage, as only a pulse, or no pulse is required, and pulse height discrimination is not needed. The light output in the scintillator is so large, that even in the worst position, enough light reaches the phototube to provide a count.

The scintillation pulses proceed to a cathode follower, similar to the ones described in the previous section. No further amplification is necessary in the case of scintillation pulses, as they are large enough to be counted directly.

The scintillation pulses and the amplified Čerenkov pulses are now applied to the inputs of a commercial coincidence unit (Dynatron Radio Coincidence Unit type 1036C). These were 3 channel units, which were capable of various combinations of coincidence and anti-coincidence mixing between the channels. The following variations were possible.

1. Channel 1 in coincidence with channel 2 (2-fold coincidence).
2. Channels 1, 2 and 3 in coincidence (3-fold coincidence).
3. Channels 1 and 2 in coincidence, with channel 3 in anti-coincidence (2-fold c + 1-fold a.c.).

Also, the single fold rates in each channel could be measured. Each channel had an input pulse height discriminator, which could be varied from 2 volts to 50 volts. The dead time of the amplitude discriminator, after a pulse had been received, could be set at various values between 5 and 500 microseconds. In general, this was set at the minimum paralysis time. The delays of the various channels with respect to each other could be varied from 0 to 1 microsecond, in steps of 0.05 microseconds. Before each experiment, the delays were matched correctly by replacing the counters by a pulse generator and finding the optimum delay position in each channel.

The resolution time between channels 1 and 2 was, in general, set at 100 nanoseconds, and that between the coincident output of channels 1 and 2 and channel 3 at 300 nanoseconds.

The output pulses from the coincidence unit vary depending on the combination of channels, but are approximately 20 volts high, positive and between 2.5 - 15 microseconds in width. These output pulses are then led into a scaler (Dynatron type 1009E), where the pulses are counted, and from which a standard output pulse is taken. This pulse is amplified to approximately 120 volts and is used to trigger a low pressure cloud chamber, in which the particle tracks can be photographed.

Chapter 3.

EFFICIENCY OF THE ČERENKOV COUNTERS.

The efficiency of the individual counters, the construction of which has been described in the previous chapter, must now be determined. This would be a simple procedure, if a reasonably mono-energetic beam of particles was available. If effects of contamination in the beam are neglected, all the particles would be travelling with effectively the same velocity v. The pressure of the counter could be varied, to give a range of threshold velocities about the value v, and the corresponding counting rate noted. The efficiency curve against pressure, (or velocity), could thus be obtained directly (Dumas et.al.). However, with no suitable beam available in this experiment, cosmic ray muons have to be used to determine the efficiency indirectly, from their spectrum.

The apparatus consists of a counter telescope for selecting single particles. It consists of the Čerenkov counter under investigation, and two scintillators, one placed immediately above, and the other immediately below the Čerenkov counter. The three counters are placed in a three-fold coincidence arrangement. With such an arrangement, the variation of the three-fold counting rate with increasing pressure can be obtained. For the large counter, the variation is shown in Figure (3.1). It should be noted that the x-axis is the pressure above atmospheric. If this is converted into absolute pressure values, it will be seen that at 15 lbs./sq. in., there is a background count of ~ 0.8/hr., and that the counting rate curve increases rapidly to a value of 2.8/hr., by

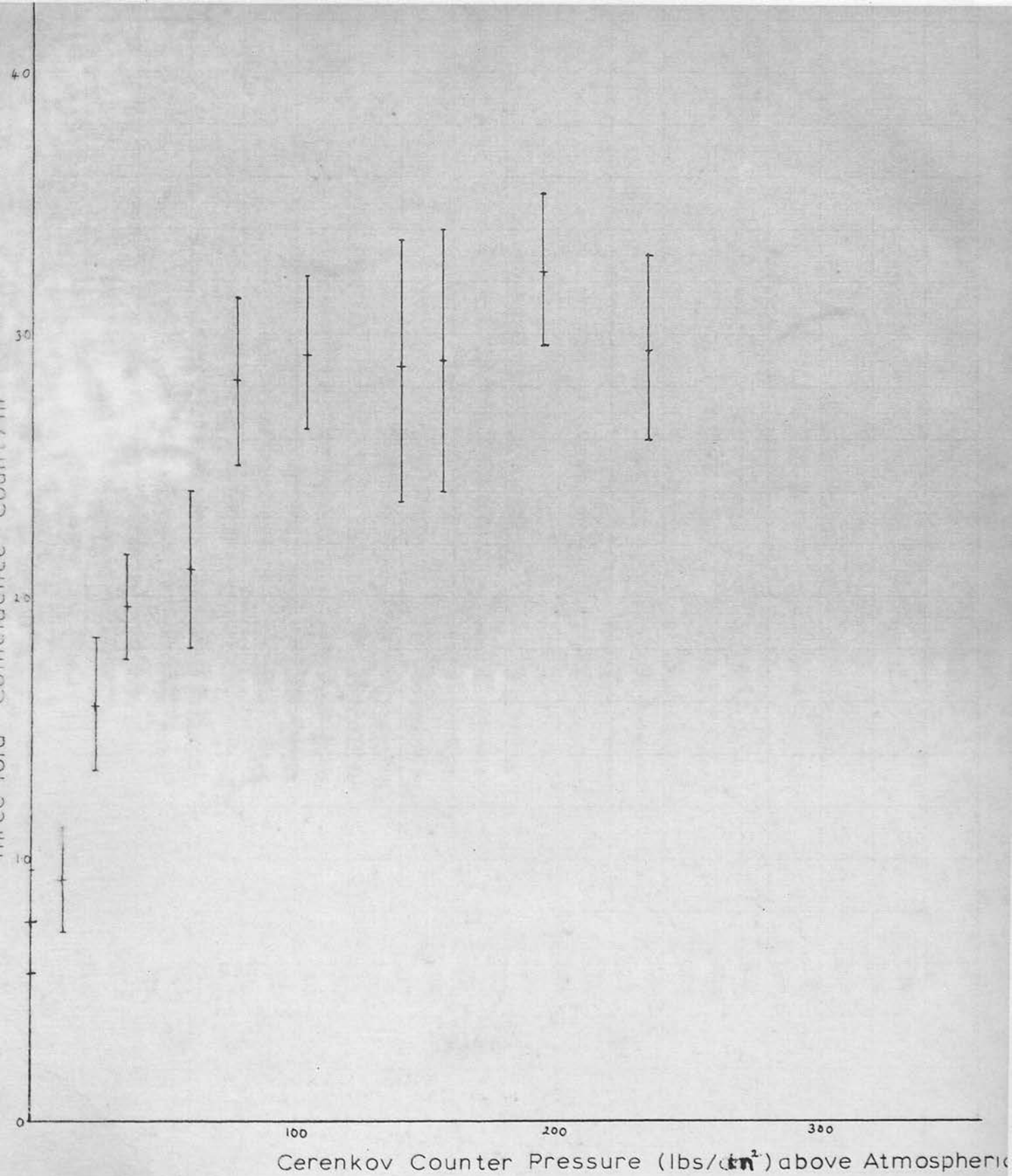

Fig.3·1 Cylindrical Mirror & Lens

a pressure of 94 lbs./sq. in. It will also be noted that by 215 lbs./sq. in., the curve has flattened out.

Before discussing the efficiency of the counters, there are several problems which must be considered. Firstly, it will be seen that there is a background count, and the magnitude and source of this spurious counting must be determined. Secondly, a theoretical curve, showing the relation between the muon counting rate and pressure, must be obtained, assuming that the counter is able to detect all those particles whose velocity is greater than the critical velocity. Thirdly, the effects of other cosmic ray particles on the counting rate have to be discussed.

3.1. The Background Count.

On consideration of Figure (3.1), it will be seen that there is what appears to be a background count at the lowest pressure of 1 atmosphere. This count could be produced by any one or combination of the following effects.

1. Single particles, the velocity of which is greater than 0.9997c, passing through the counter telescope. These particles could possibly count as their velocity is greater than the critical velocity at 1 atmosphere pressure.
2. Several particles, all with a velocity greater than 0.9997c, forming part of a shower. These would have a higher probability of counting than a single particle of the same velocity, as n times as many photons would be produced in this case, if n particles were present in the shower.

3. A single particle passing through the counter telescope, and being counted in the Čerenkov counter by the light produced in the glass lens.

4. A shower, in which one or more particles produce light in the glass lens. In this case, the particle could be travelling at any angle, and thus a count from this type of event is more likely than from case 3, where the single particle would have to be travelling approximately vertically.

5. A shower, in which one or more particles pass through the glass exit window.

6. A shower in which one or more particles pass through the phototube. It will be seen (Appendix 1), that such events can produce a count.

In the experiment, to be described, the contribution each of these effects make to the background count will be evaluated. In this subsiduary experiment, the sizes of the scintillators were slightly different from that in use in the experiment described in the previous section, so the counting rates are not directly comparable. The arrangement of the counters was as follows. The top scintillator was a 2" x 2" block and the lower scintillator was circular in shape, of diameter 2". The single fold counting rates were 240/min. in channel 1 (top scintillator), 280/min. in channel 2, (bottom scintillator), and 8000/min. in channel 3 (the Čerenkov counter). The calculated chance rate was 1.3×10^{-6}/hr., which is effectively zero. With the above single fold rates, a measurement of the three-fold coincidence rate (1 + 2 + 3) was made for the

following cases.

Case A:- The Čerenkov counter operating under its normal conditions at atmospheric pressure, with no black paper inserted anywhere (0.54 ± 0.10/hr.).

Case B:- Black paper was placed immediately above the glass lens, in such a way that any light produced in the gas, above the lens, would be absorbed and would not reach the phototube. (0.55 ± 0.09 /hr.).

Case C:- In this case, the black paper was placed below the lens, eliminating light produced in the lens, as well as the Čerenkov light produced in the gas further up the tube. (0.39 ± 0.10/hr.).

Case D:- In this final case, the black paper covered the photomultiplier, cutting out all light, except that produced in the photomultiplier envelope. (0.18 ± 0.10/hr.).

If count B is subtracted from count A, the contributions from all effects producing light in the gas are obtained. It will be seen that this contribution is zero, within the statistics. Thus, neither effect 1 nor effect 2, can be making any significant contribution to the background count. This is not surprising as all of the single particles would only be fractionally above the threshold velocity, and thus would only produce a small number of photons (maximum number of ~ 30 photons). Also, muons with an energy, higher than 4.3 Gev. (energy equivalent of v = 0.9997c) will be extremely rare. The contribution from showers has likewise proved to be negligible, and this too is not unexpected, as the number of showers containing several particles, all of velocity greater than 0.9997c, will be small. Thus, it can be said that

contributions from effects 1 and 2 are not significant.

If count C is now subtracted from count B, it will be seen that there might be a small difference in the counting rates but it is not significant. This difference gives the contributions from effects 3 and 4 (i.e. particles producing Čerenkov light in the glass lens). It appears unlikely that a single particle passing vertically through the counter telescope could produce light, at such an angle, that it could reach the phototube. It is possible, however, due to the position of the lens and the critical angle for glass, that a knock-on electron produced by the muon, might produce light in the lens which would give a count. Likewise, some of the shower particles might give a count in the lens. Thus, it appears that the contribution from these sources, if present at all, is small and better statistics would have to be obtained before any definite conclusion could be reached.

The difference between cases C and D, gives the contribution from the effects taking place in the mirror, the gas of the side tube, and the exit window. It is extremely unlikely that any contribution is made by the mirror, as it is aluminised on the front surface, and it is equally unlikely that the gas in the side tube contributes. This gas will be at the same pressure as the main body of gas in the sensitive region, which has already been shown to give no contribution at this pressure. Also, the length of the sensitive region is in the same direction as the particle's motion, in the case of the gas above the lens, and at right angles to the particle's motion in the case of the gas in the side tube. Thus, there is a considerable increase in the path length available

to the particle above the lens, compared to the side tube. It is thus taken, that the difference in counts C and D, gives the contribution from shower particles, producing Čerenkov light in the glass of the exit window (Effect 5).

It will be seen that there is a remaining background count D due to showers, in which one or more of the particles trigger the arrangement, by producing Čerenkov light in the glass envelope of the photomultiplier (Appendix 1), at the same time as other particles trigger the scintillators.

From the point of view of the efficiency calculation, the important result is that counts A and B are equal, and thus there is no contribution from particles whose velocity is greater than the critical velocity for one atmosphere. Thus, in considering Figure (3.1), the counting rate at 1 atmosphere can be taken to be the background rate, and will have to be subtracted from the total counting rate, in order to obtain the genuine counting rate, due to Čerenkov light produced in the gas. It has also been shown that this background is not dependent on the gas pressure, and will thus be a constant.

3.2. Counting Contaminations.

At sea level, approximately 70% of the charged cosmic ray particles are muons, all but 3% of the remainder being electrons. The differential muon spectrum at sea level is very well known {Owen & Wilson (1955), Hayman & Wolfendale (1962)}, and from this, the integral spectrum of counting rate against velocity or pressure, can be readily obtained. This is the curve which has to be

compared with the experimental curve. However, it will be apparent that as well as the muons counting, the effects of other particles, present in any reasonable concentration, must be considered. Firstly, within the statistics and accuracy of our experiment, the effects of protons, pions and other particles, besides electrons, can be neglected. The proton spectrum comprises only approximately 1% of the total flux, and this would not show significantly within the counting accuracy of the experiment. The proton component is also discriminated against by the velocity - energy relation, which demands that a proton should have an energy greater than ~ 11 Gev., before it would count in a perfectly efficient counter, at 10 atmospheres pressure. The velocity - energy relation does not play as great a role in the case of pions, as the pion - muon mass ratio is 1.319, whereas the proton - muon mass ratio is 8.869. However, the pion spectrum, although not known so accurately, is even less intence than the proton contribution and would also make no significant contribution. Thus, the only contamination which could significantly affect the shape of the counting rate curve is the electron contribution.

It is of interest to consider what effects occur when an electron passes through a thickness of material, (in our case the material concerned is iron). Any charged particle passing through a material loses energy by ionisation and radiation. Thus, the electron will lose energy by ionising the atoms of the material, the magnitude of the energy loss being given by the Bethe-Bloch formula for electrons.

$$K_{COL} = 2C m_e c^2 \left\{ \ln \left(\frac{\pi^2 (m_e c^2)^2}{(1-\beta^2)^{\frac{3}{2}} I^2(Z)} \right) - a \right\} \qquad (A)$$

where K_{COL} is the average ionisation loss per gm. $cm.^{-2}$ of the material.

C is $0.150 \frac{Z}{A}$ $gm.^{-1}$ $cm.^{2}$

I is the average ionisation potential for the medium.

a = 2.9 for electrons.

As well as the ionisation loss, the electron will produce photons by Bremsstrahlung. The loss due to radiation is given by the formula shown below for high energy electrons $[E \gg 137 m_e c^2 Z^{-\frac{1}{3}}]$

$$K_{RAD}(E) = \frac{4}{137} \frac{N}{A} Z^2 r_e^2 E \left\{ \ln (183 Z^{-\frac{1}{3}}) + \frac{1}{18} \right\} \quad (B)$$

where $K_{RAD}(E)$ is the average radiation loss per gm. $cm.^{-2}$ for an electron of incident energy E.

N is Avogadro's number. r_e is the classical radius of the electron.

The photons so produced, can in turn create positron - electron pairs, which will produce more photons etc.. Thus, the net effect will be the production of a shower of electrons, positrons and photons. The average energy of the particles will gradually be degraded, as the number of particles increases. The Bremsstrahlung loss will be more important at high electron energies, and the ionisation loss more important at low energies. The energy at which the two effects are of equal importance is called the critical energy E_c and is equal to 24 Mev. for iron. The probability of a particle emerging from the material obviously depends on the initial energy of the particle, and the thickness of the material being traversed. R. R. Wilson has treated the problem of shower production by a Monte-Carlo method, and has obtained an expression

for the mean range r, (in units of radiation lengths), of an electron of initial energy E_o.

$$r = \ln 2 \ln \left\{ \frac{E_o}{E_c \ln 2} + 1 \right\}$$

The distribution of ranges around r, is approximately Gaussian, and the root mean square straggling s, (in units of radiation lengths), is given by:-

$$s \approx (r \ln 2)^{\frac{1}{2}} \left(1 - \frac{1}{r} \frac{E_c}{E_o} \right)$$

In the calculation, Wilson has taken into account the fact that low energy γ-rays have a relatively long mean free path.

The electron spectrum at sea level, (Williams 1939), shows that the number of electrons above 300 Mev. is extremely small and that the number increases rapidly with decreasing energy. Thus, 83% of the electron contamination will be below 100 Mev. The counter system will automatically eliminate electrons, the energy of which is below 3 Mev. (3 Mev. corresponds to the threshold pressure of 25 atmospheres). Thus, we need only consider the range of electron energies from 3 - 300 Mev. If a particle is to traverse the complete counter system, it has to pass through 4 iron plates each 1½ cms. thick. If only one counter is being operated, the particle has two of the above iron plates to penetrate.

In Figure (3.2), the mean range r, the root mean square straggling s, and the average ionisation loss and radiation loss of energy in traversing one plate are tabulated for various incident electron energies. The first two quantities, r and s, are calculated from Wilson's shower theory and so should be accurate. The energy loss calculations are made from the formulae above, (A & B) and are not so accurate as an electron would certainly suffer multiplication and

Electron Energy (Mev.).	r (rad. lengths)	r (cm.)	s (rad. lengths)	s (cm.)	Average Radiation Loss in 1.5 cm. plate. (Mev.).	Average Ionisation Loss (Mev.).	Total Loss (Mev.)
300	2.138	3.75	1.041	1.822	123	28	151
38.7	0.8572	1.5	0.3659	0.6403	17.7	21	38.7
3	0.1159	0.20	0.0213	0.0373			

Fig. (3.2).

this has not been considered in these formulae. Thus, these results give the average energy loss of the incident electron after it has penetrated the plate and does not take into account the fact that the electron which leaves the plate might not be the one which was incident on it. Thus, good agreement between the two theories need not necessarily be expected. However, to give orders of magnitude, the energy loss results, as calculated by this rough method are included.

It will be seen that for one of the extremely high energy electrons (300 Mev.), the average range is 3.5 cms. in iron, so that it is to be expected that the majority of such particles will produce effects below a single plate. However, if the particle does penetrate the plate, it will have suffered, on average, an energy loss of ~ 150 Mev. The electron energy which corresponds to an average range equal to the thickness of the plate (1.5 cms.) is ~ 39 Mev. It is to be expected that 50% of the particles of such an initial energy will show effects below the plate. However, the outcoming particle or particles will probably have insufficient energy to produce a count. It will be seen that low energy electrons (3 Mev.), have an average range of 0.2 cm., and are extremely unlikely to penetrate the plate in any form. Thus, it will be seen that only electrons with energy above ~ 40 Mev. need be considered, if the criterion of passing through one plate is adopted. If the necessity to pass through more than one plate is considered as the criterion, the electron energy will be correspondingly increased. From the shape of the electron spectrum, it can be calculated that only ~ 38% of the electrons have an energy

greater than 40 Mev. In order to have a range equal to two plate thicknesses, (i.e. to have a 50% chance of penetrating one complete counter), the electron would require an energy of 180 Mev. Less than 8% of the electrons have an energy greater than this value, thus it would be expected that only 4%, at most, of the electron contamination would contribute. Thus, it will be seen that the higher the energy of the electron, the higher the probability of penetration. However, the frequency of occurrence decreases rapidly with increasing energy. The net effect of electrons on the apparatus is thus negligible within the statistics of the experiment.

The next source of electron contamination is knock-on electrons produced by muons passing through the counter system. The muon might trigger the scintillators but have insufficient energy to produce a Čerenkov count. However, if a knock-on electron was produced by the muon, in the top plate of the Čerenkov counter, it is possible that this might have sufficient energy for a count to be obtained. Of course, from previous considerations, the knock-on electron would have to have an energy greater than 3 Mev. From the results of Lloyd and Wolfendale, a figure of 9% can be taken, for the percentage of the total number of muons which leave an iron plate 7 cms. thick, accompanied by a knock-on electron. The overwhelming majority of these knock-ons will have an energy less than 3 Mev. Thus, this effect can likewise be neglected and will have no effect on the counting rate results, as the number of knock-on electrons decrease with decreasing plate thickness.

The remaining source of particle contamination is air showers

where some of the particles pass through the scintillators, at the same instant that, perhaps, several pass through the Čerenkov counter. These showers could count through two different effects. Firstly, the Čerenkov counter could be triggered by particles passing through the phototube. It is thought that this is a significant effect, and it has been discussed in a previous section. However, there is also possibly a contribution when several particles pass through the sensitive region of the Čerenkov counter at the same instant. This effect can best be described if we consider the example of the large counter of sensitive length 100 cms., and at a pressure of 10 atmospheres. Figure (3.3) shows the increase in photon number against increasing particle velocity for such a counter, and if a figure of 60 photons for 100% efficiency is assumed, curve 2 for a single particle is obtained. It will be seen that instead of the theoretical count starting at 0.9970c, a value of 0.9972c must be attained, before the efficiency curve becomes non-zero. Before 100% efficiency is attained, the particle must have a velocity of 0.9976c.

The effect of showers can be observed from consideration of curve 1. This curve has been drawn for two particles both with the same velocity, obviously doubling the photon number at any particular velocity. It will be observed that if two identical particles are present, the efficiency curve is displaced toward the theoretical threshold velocity, in this case giving figures of 0.9971c for the initial rise in the efficiency curve, and 0.9973c for the attainment of 100% efficiency. Thus, it will be noticed that if several particles of similar velocities are present, a count will be

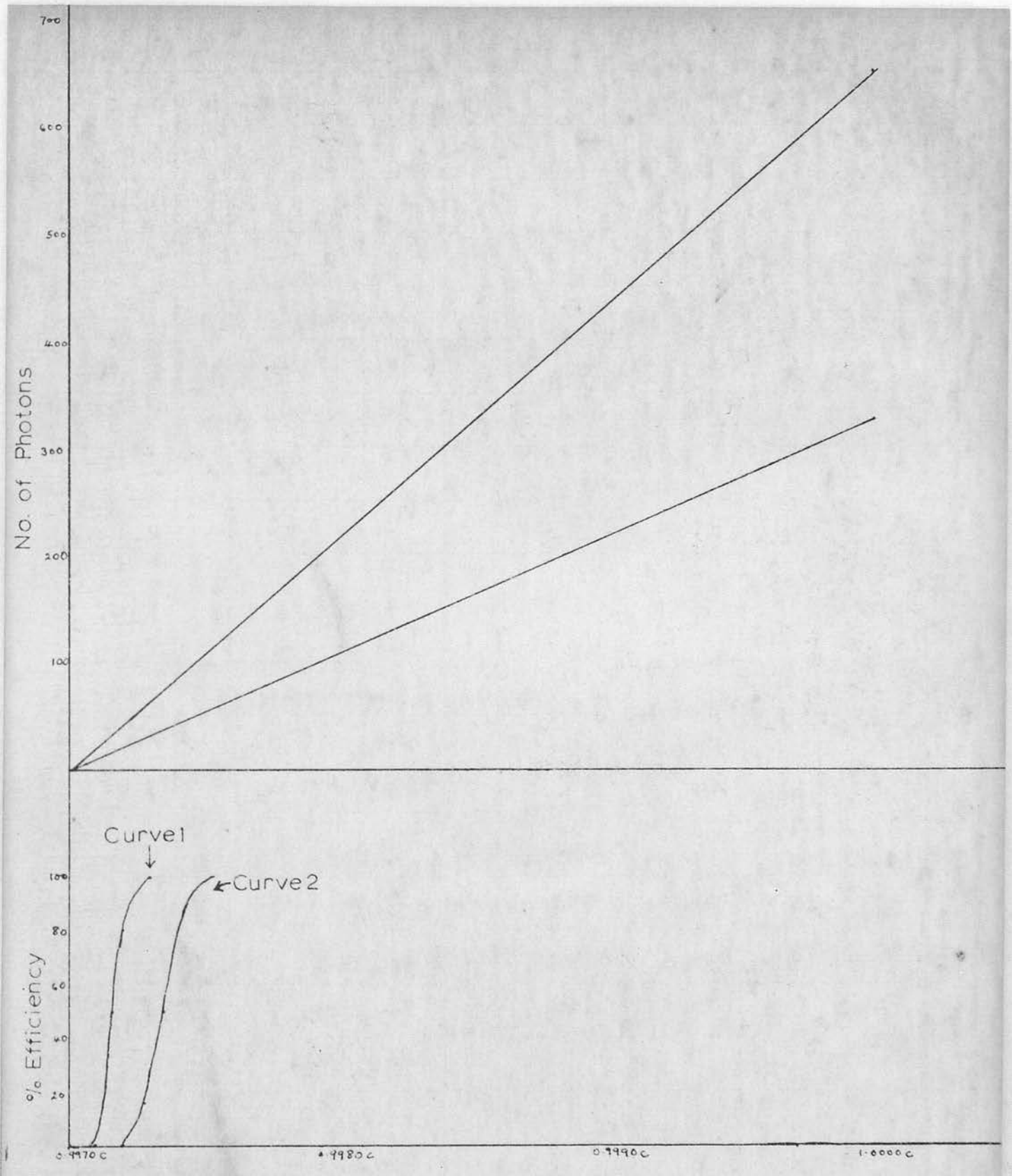
700
600
500
400
300
200
100
No. of Photons
Curve1
Curve2
100
80
60
40
20
% Efficiency
0·9970c
0·9980c
0·9990c
1·0000c
Particle Velocity

Fig. 3·3

possible, at pressures nearer the critical pressure, than would be the case if only one particle of the same velocity is present. Thus, showers should be detected at very low pressures, and one might expect an initial rise, due to this effect, before the muon spectrum contributed. It should also be noticed that as well as being displaced, the efficiency curve becomes steeper, when more particles are present.

3.3. Efficiency of Large Counter.

It now remains to compare the counting rate against pressure curve, Figure (3.1) with the integral muon spectrum Figure (3.4). Firstly, as has been shown in a previous section, a constant background count, equal to the counting rate at 1 atmosphere pressure, has to be subtracted from Figure (3.1). The value subtracted was 0.8/hr. and this left the genuine counting rate against pressure curve.

A comparison of the theoretical and genuine experimental curves can now be undertaken. Firstly, the experimental curve must be normalised to the theoretical one, and this is carried out as follows. It can be seen that both curves are flattening out to two different asymptotic values, and therefore the curves are normalised using these values at high pressures. The curves are flat enough, that normalising them at as low a figure as 25 atmospheres, does in fact not alter the result significantly, as the errors on the experimental curve are relatively large. The experimental curve is thus magnified, in such a way, that it coincides with theoretical curve at high values of the pressure. The flatness of the curves shows that very few additional particles are being added per unit pressure

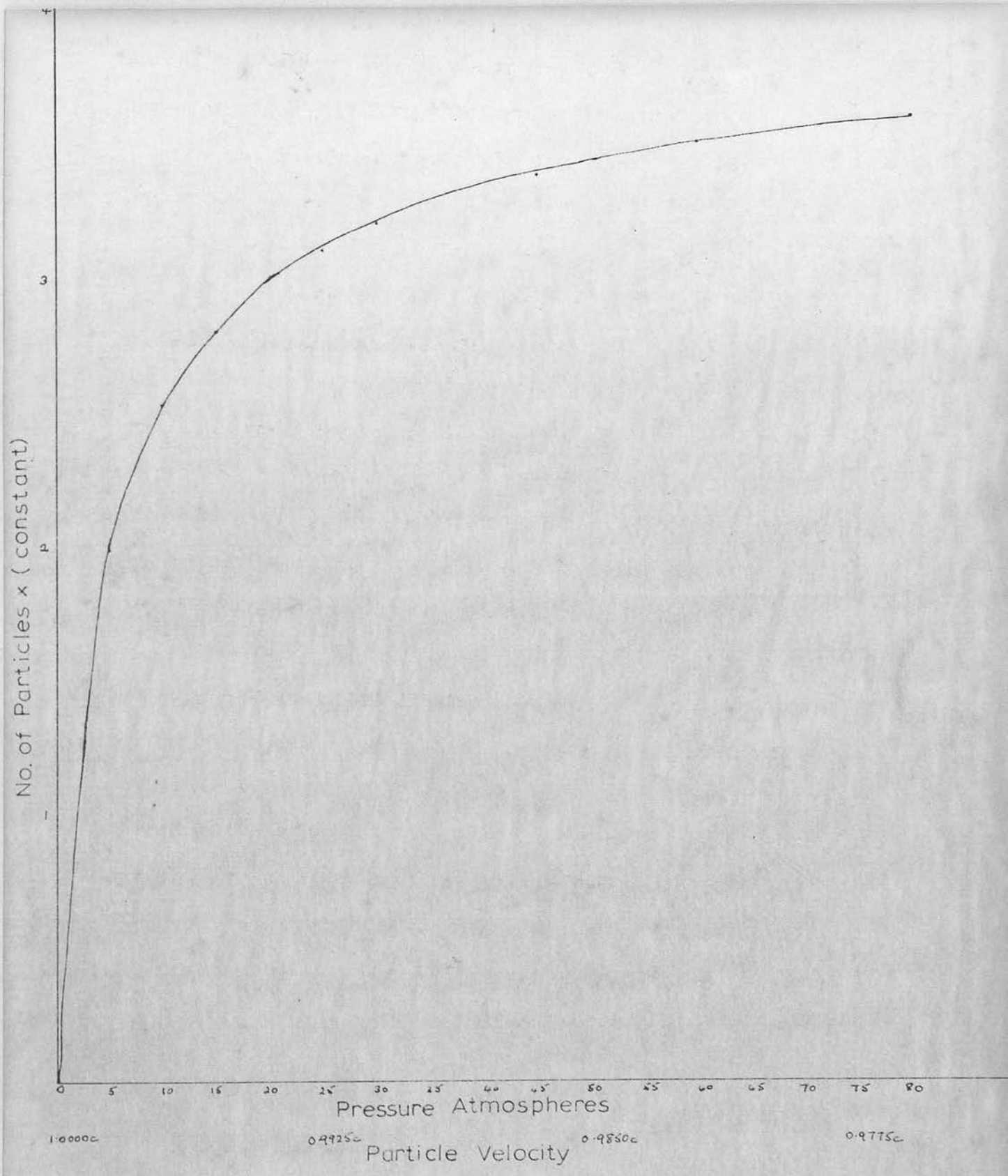
No. of Particles x (constant)
4
3
2
1
0
5
10
15
20
25
30
35
40
45
50
55
60
65
70
75
80
Pressure Atmospheres
1·0000c
0·9925c
0·9850c
0·9775c
Particle Velocity

Fig. 3·4

range at high pressures. Thus, two curves are obtained, as shown in Figure (3.5), curve 1 (theoretical) and curve 2 (experimental). It is now required to obtain a characteristic of efficiency against velocity above threshold, which will convert curve 1 into curve 2. This efficiency curve can be considered from two points of view. Firstly, it can be assumed that the experimental curve gives the muon contribution with pressure, and effects due to other particles and to showers can be neglected. In this case, a characteristic has to be obtained, which changes the theoretical curve into the experimental one directly. On the other hand, it might be thought, that the shape of the experimental and theoretical curves should be similar, and only displaced. In this case, the deviations from similarity at the low pressure end, could be due to showers, and should be subtracted from the experimental curve. Both of these possibilities will be considered in turn.

It will be seen that curve 1 rises immediately, from 0 atmospheres, whereas curve 2 does not rise until 1 atmosphere. This suggests that the characteristic must have such a form, that the efficiency is 0%, until a velocity corresponding to 1 atmosphere is reached above threshold. The first characteristic tried was one of type 3, Figure (3.5). It will be seen that this characteristic has an efficiency of 0%, up to a velocity of 0.0003c above threshold, and afterwards an efficiency of 100%. This has the effect of shifting the theoretical curve over by 1 atmosphere to the right, (curve 3), putting it nearer in agreement with the experimental curve. Various other efficiency characteristics were tried, and the corresponding counting rate curves against pressure, drawn. It

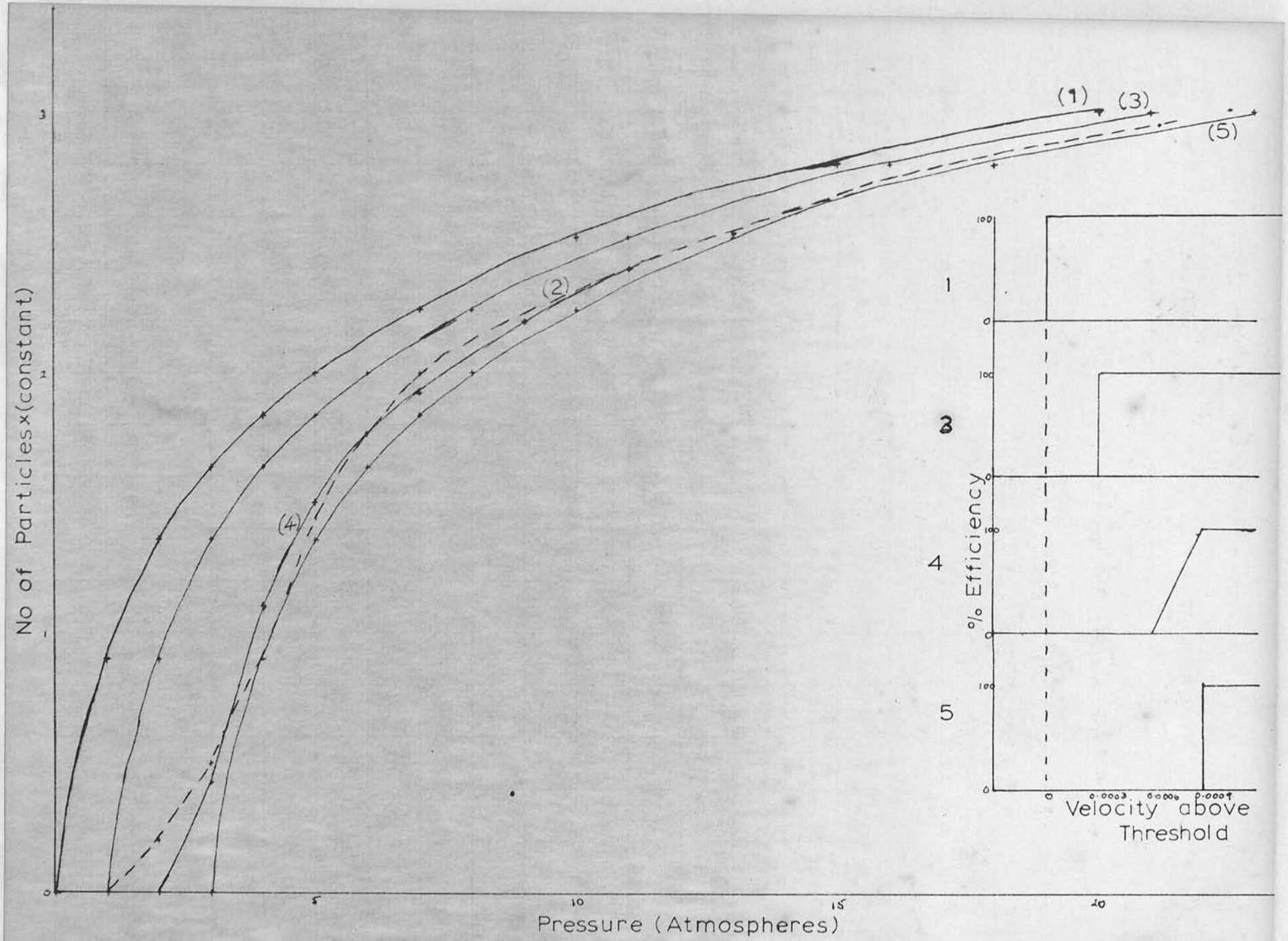
No of Particles x (constant)
Pressure (Atmospheres)
(1)
(2)
(3)
(4)
(5)
% Efficiency
Velocity above Threshold
1
2
4
5

Fig. 3·5

will be seen that the best curve is of type 4, and the characteristic of type 4, gives an extremely good fit at most values, except the very lowest pressures. Thus, if the effect of showers is negligible, we can consider the characteristic to have an efficiency of 0% up to a value of 0.0006c above threshold velocity, and then a linear increase to 100% by 0.0009c above threshold.

If on the other hand, both curves are assumed to be of similar shape but displaced, the best characteristic, which gives a good fit at higher pressure value is one of type 5. It will be seen that this characteristic has 0% efficiency up to 0.0009c above threshold, and thereafter 100% efficiency. This has the effect of shifting the theoretical curve, 3 atmospheres to the right. It will also be seen that at low pressure values, the experimental curve 2, gives a higher counting rate than curve 5. This is assumed to be the contribution due to showers. The reason the two curves come together at high values is that as the pressure is increased, some of the counts, which could only be obtained by showers, at the low pressure values, can now be produced by a single particle of the shower. Thus, the contribution from the showers will gradually be taken over by any muons which are present in the showers. Of course, there will always be a residual count due to electron showers and this explains the fact that curve 5 is tending to a slightly lower value than the experimental curve 2.

Within the accuracy of the experiment, it is impossible to differentiate between the two characteristics 4 and 5, described above. The efficiency characteristic of type 5, is therefore

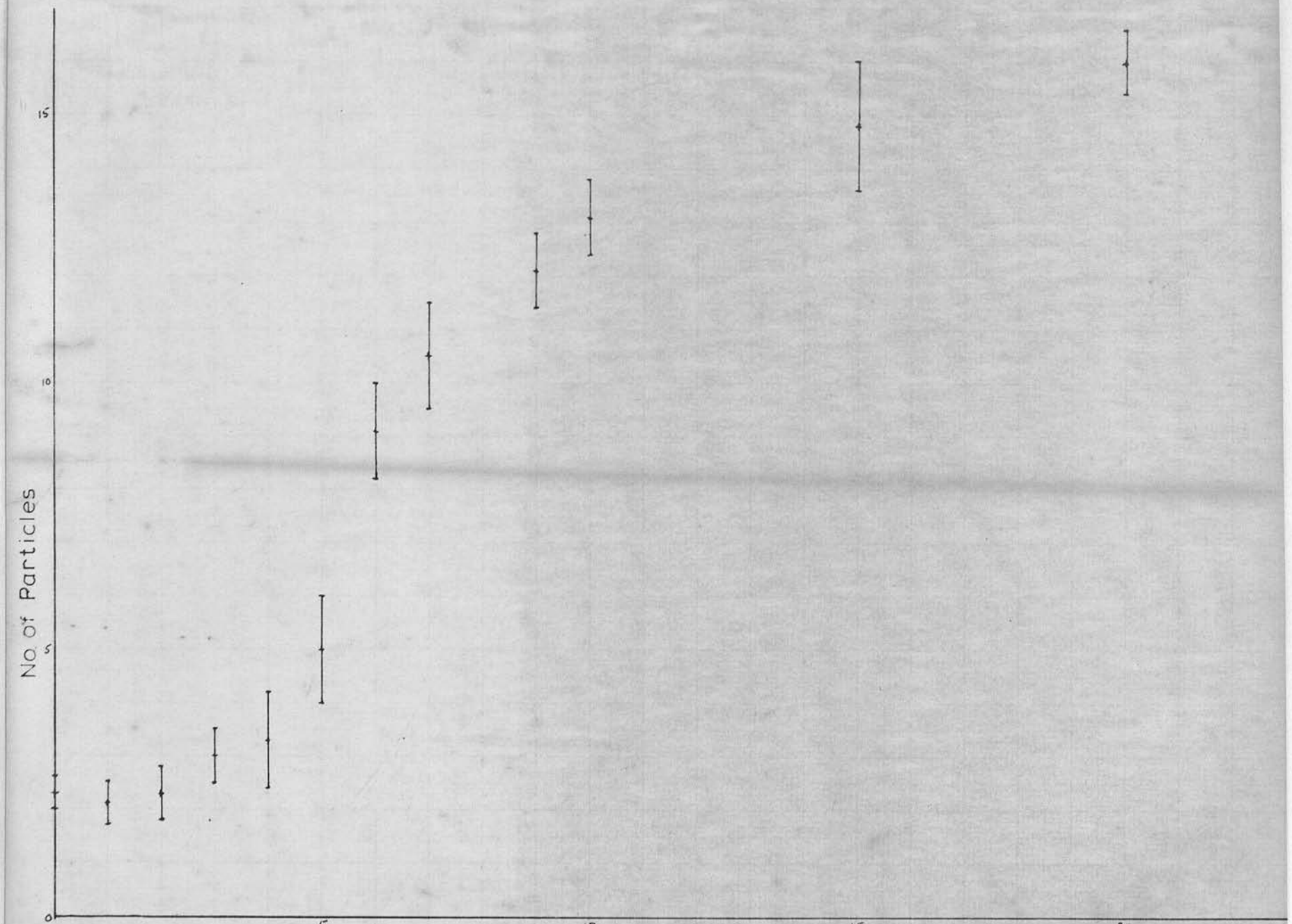

Fig. 3·6

taken for the large counter, as the minimum we should expect in using this counter. This also agrees with the ideas on showers discussed in the previous section.

3.4. Efficiency of the Small Counter.

A similar procedure was carried out with the small counter, replacing the large one in the counter telescope. The counting rate curve is shown in Figure (3.6). It will be noticed that the count per hr. is greater in this case, and this is due to the counter telescope being shorter and thus subtending a larger solid angle. The background count is subtracted, and the curve is normalised to the theoretical curve in the same way as in the previous section, and Figure (3.7) is obtained. If as an approximation, it is assumed that the range of the characteristic, itself, is small compared to the velocity range between the threshold velocity and the beginning of the characteristic rise, it will be expected that once more the curve of counting rate against pressure will just be moved over. In this case, a calculation of the efficiency characteristic produces curve type 2, where there is zero efficiency up to 0.0015c above threshold, due to the shorter length, and thereafter 100% efficiency.

3.5. Photon Efficiency.

It can now be shown that the previous estimate of 60 photons for 100% efficiency is rather low. In a previous section, an efficiency characteristic for the large counter has been obtained, by comparing the experimental and theoretical curves for counting rate against pressure. It will be remembered that a curve which gave a good representation of the efficiency curve, was one which gave 0% efficiency up to 3 atmospheres above threshold, and there-

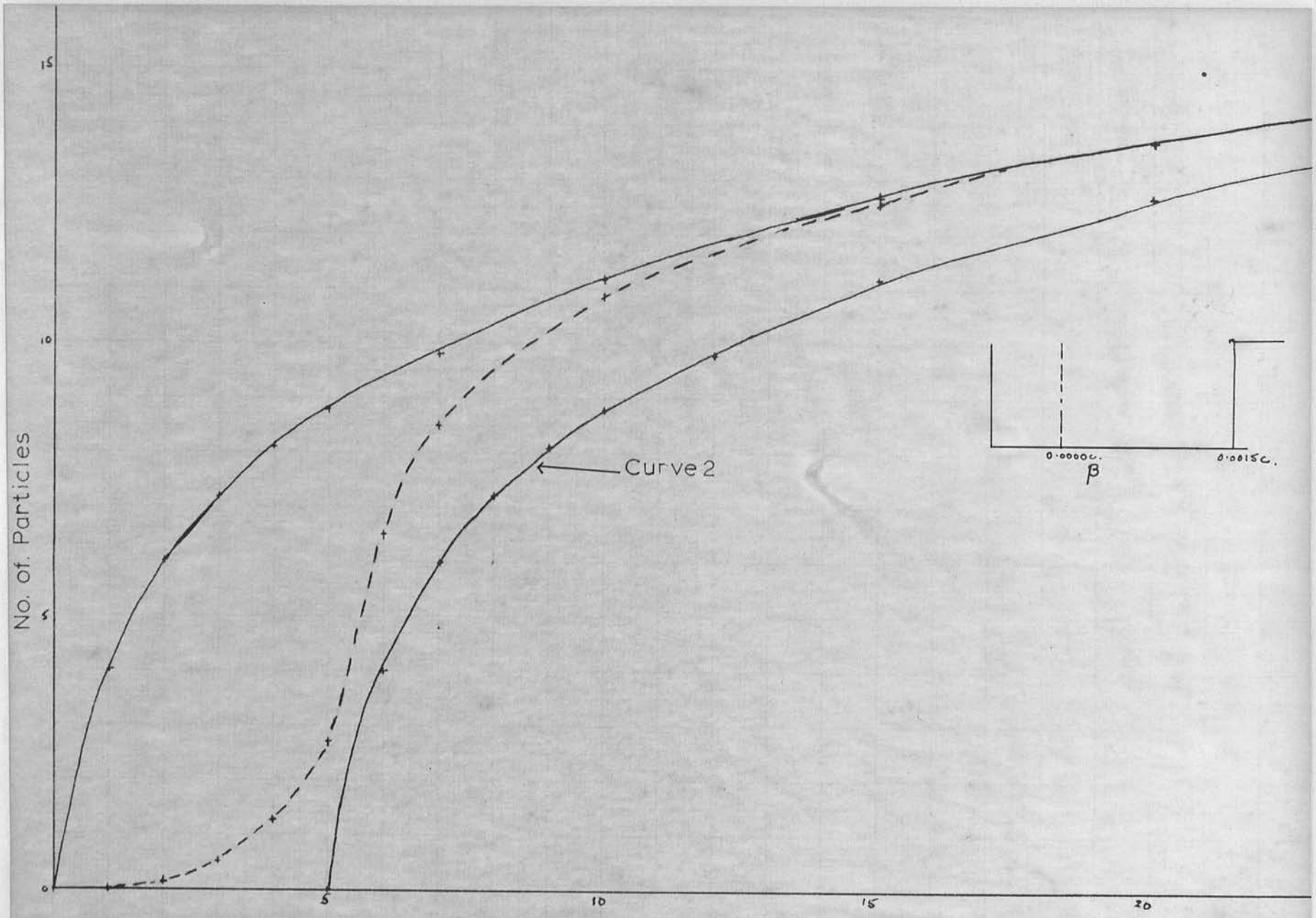
No. of Particles
0
5
10
15
5
10
15
20
Pressure (Atmospheres)
Curve 2
0·00000c.
0·00150c.
β

Fig. 3·7

after 100% efficiency. If the long counter and a wavelength range of 3800 - 5800Å is considered, the curve of photon number against particle velocity can be drawn for the threshold velocity of 0.9970c (10 atmospheres). From statistical considerations, an efficiency curve curve against particle velocity can be constructed, if a certain number of photons are assumed to produce a 50% probability of counting. An efficiency characteristic is required which corresponds to one or other of the characteristics obtained in section (3.3). These characteristics are shown in the full lines in Figure (3.8). It will be seen that if 76 photons are assumed to give an efficiency of 50%, curve 1 is obtained by taking the statistical probability, that various numbers of photons can produce counts. It will be seen that this curve does not correspond to the curve previously calculated which is the full vertical line (100% at 0.0009c above threshold). If on the other hand, a figure of 64 photons is assumed to give an efficiency of 50%, curve 2 is obtained and it can be calculated that 88 photons would give ~100% efficiency. It will be seen that this curve corresponds very well to the characteristic of type 4, (0% up to 0.0006c and thereafter a linear increase up to 100% at 0.0009c). Therefore, a figure of ~ 90 photons for 100% efficiency with the large counter is adopted. If a similar calculation is carried out for the small counter, it can be shown that the increase in the threshold gap, (i.e. the difference between theoretical and experimental thresholds), is counteracted by the smaller photon increase with particle velocity, and a figure of 70 photons for 100% efficiency is obtained. As the long counter is 2½ times as long as the small one, it will be seen

that fewer photons are required for 100% efficiency, in the case of the small counter, as we should expect. When 90 photons are produced in the large counter, most of them, ($\frac{6}{10}$), will be in the extension piece where the collection efficiency is not so great, as there is no silvered tube. Thus, we should expect a certain

Continued on Page 47.

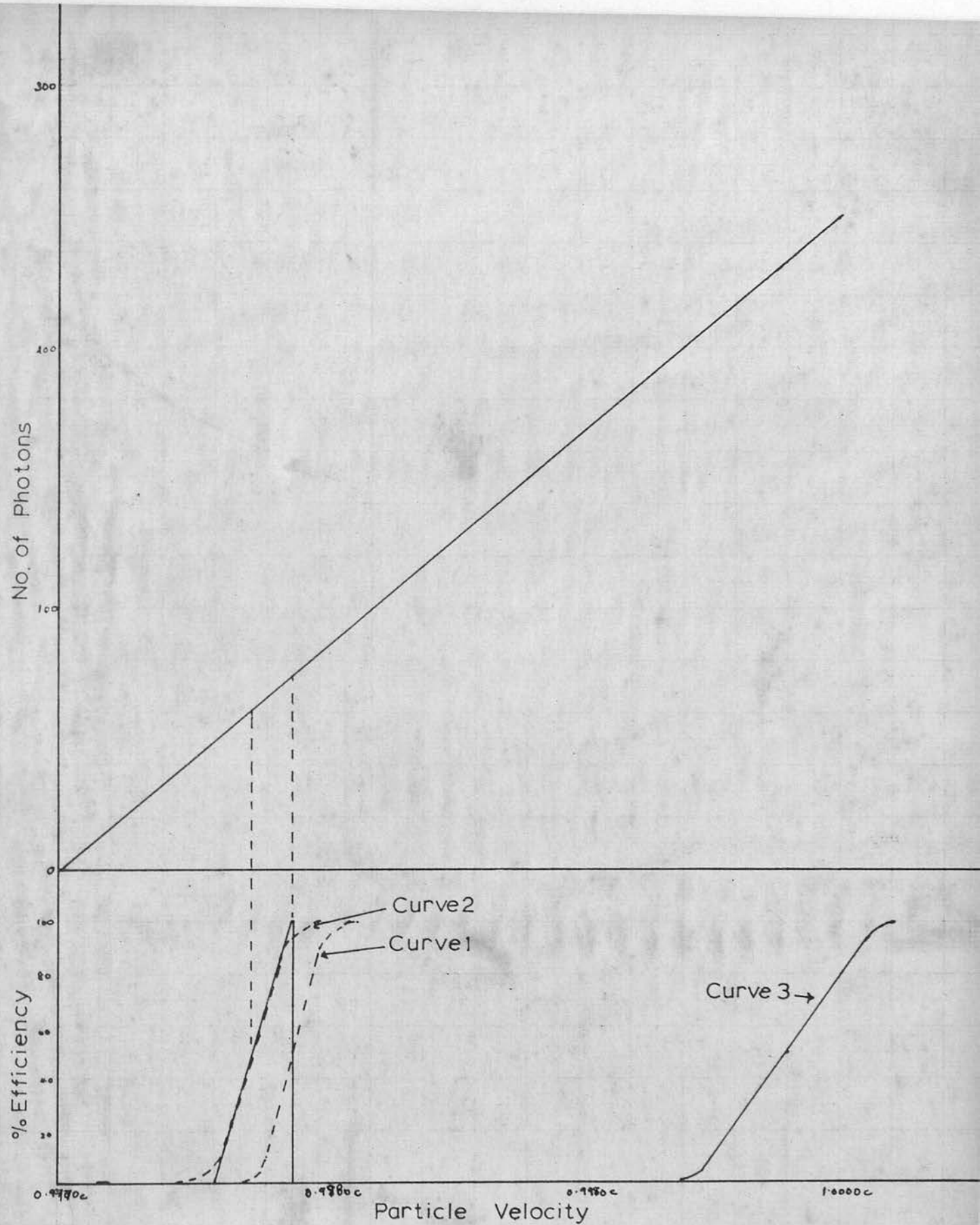
300
100
100
0
No. of Photons
Curve2
Curve1
Curve 3
% Efficiency
0·9880c
0·9880c
1·0000c
Particle Velocity

Fig. 3-8

proportion to be lost by absorption, at walls, which is not the case with the small counter.

These figures of 70 and 90 photons for 100% efficiency are in disagreement with the results of Perez-Mendez and Atkinson, who give an efficiency of 90%, when 270 photons are produced per particle, and 10% when 53 were produced. This difference can only be explained if the experimental curve of counting rate against pressure is incorrect. Where it was supposed that the large rise at ~ 3 atmospheres is due to the muon contribution, it is possible that this rise could be due to showers. If this is the case, the muon contribution might not occur until a higher velocity above threshold was attained. Thus, there would be a greater background (perhaps variable) to be subtracted from the experimental curve. Whereas previously, in obtaining the above curve, results were used from the counting rates, the position could be checked by using the number of single tracks passing through the multiplate chamber. If a particle passes through 3 lead plates without multiplication, it is almost certainly a muon. Sampling suggested that in fact, muons were being selected.

However, although without a significant number of the above measurements, a 100% efficiency with 90 photons cannot be completely justified, a better efficiency than that of Perez-Mendez and Atkinson can undoubtedly be claimed. If Figure (3.8) is considered once more, and 100% efficiency at 250 photons is assumed, this gives the characteristic, curve 3. Thus, at 10 atmospheres, particles of velocity c, should only just be counted with 100% efficiency, and particles of velocity 0.9991c should not be counted at all (muon

energy = 2.6 Gev.). Thus, at 10 atmospheres, the majority of the counts should be due to showers and electrons with only a small proportion of muons. This is in disagreement with the experimental results.

There are also, two other checks on the above efficiency figures. One is from the photomultiplier data which states that ~3 photoelectrons will be counted. If a figure of $\Delta\beta = 0.0009$ is assumed, and the wavelength range is split into subdivisions, the number of photoelectrons produced can be calculated from the photomultiplier conversion curve. The result of this calculation is 5.25 photoelectrons. Thus, it will be seen that this figure of 90 photons is reasonable for 100% efficiency with the large counter.

One further check is made from measurements made on the multiple scattering of muons in lead plates to be discussed in the next chapter.

3.6. The Complete Counter Telescope.

Previously, the operation of the individual Čerenkov counters has been discussed. In this next section, the operation of the counter telescope with both counters in position will be described. The counters were placed in a telescopic arrangement above the atmospheric cloud chamber, in such a way that the axis of the system passed vertically through the middle of the sensitive region of the cloud chamber. The telescope consisted of the two Čerenkov counters, placed one above the other, (large counter on top), with a scintillator, (horizontal type), in between. There were also two other scintillators, one placed above the large Čerenkov counter and the other below the small counter, immediately above the cloud

chamber. The small Čerenkov counter photomultiplier was normally shielded by an anti-coincidence counter, but when the large counter was being run by itself, the anti-coincidence counter was used to shield its phototube.

In the normal experimental set up, the three scintillators are run in coincidence, defining a cone of solid angle Θ, within which the particle trajectory must lie. The large Čerenkov counter, (on top), is put in anti-coincidence with this selection count, and the small Čerenkov counter is put in coincidence with the selection count. In case, the small counter is triggered spuriously by a particle passing through its phototube, the shielding counter is placed in anti-coincidence with the selection pulse. Thus, there is a 6 fold arrangement, 4 channels in coincidence and 2 in anti-coincidence.

Thus a particle would have to trigger all three scintillators, the small Čerenkov counter, (without setting off the anti-coincidence counter), and fail to set off the large counter, before a 6 fold count would be obtained. The highest pressure is always in the small counter, and therefore, with such an arrangement, particles are selected with a velocity which lies between the critical velocities of the two Čerenkov counters. By varying these pressures, various velocity ranges can be obtained. It must be remembered that the true velocity range selected, will not correspond exactly to the theoretical range, due to the efficiency characteristics of the counters.

In a preliminary experiment, it was decided to test the conclusions on the efficiency, derived in previous sections. This

experiment consisted of a 3-fold count,(coincidence between the 3 scintillators in the counter telescope), and a 5-fold count,(the above 3-fold count + large Čerenkov counter + anti-coincidence shield of phototube). If it is assumed that all muons of energy greater than 400 Mev. are counted if they pass through the system, the 3-fold count should represent all the muons present above this value. If muons of lower energy also count, they will make little difference to the calculation, as the muon spectrum decreases rapidly below this energy. The corresponding figure for the 5-fold count, should give the number of muons above a particular velocity. Thus, the ratio of these counts should give the ratio of muons above a particular threshold velocity, to the total number of muons. This, in turn, can be compared to the values as determined by Hayman and Wolfendale. In this experiment, only single particles were considered as the measurements were taken from the photographs in the cloud chamber. Only single particles travelling in the correct direction through the chamber, were used in the two counts. This eliminated the showers and blank photographs (spurious particles), and gave a more accurate determination than counting rates would have done. The photographic rate per hour, for coincidence between the three scintillators in the counter telescope was 0.83 $\pm$ 0.10. The corresponding counting rate for the 5-fold was 0.56 $\pm$ 0.05/hr. The pressure in the Čerenkov counter was 20.5 atmospheres and this corresponds to a theoretical threshold velocity of 0.9939c. However, the practical Δv of 0.0009c, due to the efficiency characteristic must be taken into account. Thus, all muons of energy greater than 780 Mev. are being selected in the 5-fold case.

The ratio of these counts is 0.68 $\pm$ 0.18 against the results of Hayman and Wolfendale of 0.86. It will be seen that the result just agrees with the above figure within the statistical error.

Chapter 4.

SCATTERING EXPERIMENT.

4.1. Introduction.

Having determined the characteristics of the Čerenkov counters, it was now possible to use the velocity selector in an experimental determination. The intention was to measure the scattering distribution of muons, on passing through a lead plate. The momentum of the muons could be determined from the velocity selector, while a multiplate cloud chamber was used to determine the scattering angles. It was also possible to use information obtained while testing the counters, as several runs with a single plate chamber had been obtained, at pressures suitable for the momentum range required. The efficiency of our counters will, of course, have to be taken into account, in selecting the required particles, and an estimate of the contamination which is not eliminated by the counter system will have to be made. Firstly, the reason for the experiment, and the previous work, both theoretical and experimental, which has been done on muon scattering in lead and other substances, will be discussed.

4.2. Scattering Theory.

Several scattering theories have been put forward, including those of Williams, Moliere, Snyder and Scott, Olbert, and Cooper and Rainwater. The first problem in producing a multiple scattering theory, is to obtain an expression for the probability of a single scattering through an angle between Θ and $\Theta + d\Theta$. The first expression obtained, was that due to Rutherford, in connection with α-particle scattering in foils.

$$I(\Theta) = \frac{Z^2 e^4}{4M^2 v^4 \sin^4 \Theta/2}$$

where Z is the charge on the scattering nucleus, and M and v are the mass and velocity of the scattered particles. This expression was obtained in a classical manner, but if small angle scatters are considered, i.e. the particle not approaching too close to the nucleus, a similar expression is obtained from relativistic quantum mechanical considerations

$$I(\Theta) = \frac{Z^2 e^4}{4M^2 v^4 \zeta^2 \sin^4 \Theta/2} \qquad \text{where } \zeta = (1 - \beta^2)^{-\frac{1}{2}}$$

For small angles, the above expression simplifies into William's function for the single scattering probability

$$P(\Theta)\, d\Theta = \frac{2k d\Theta}{\Theta^3} \quad \text{where } k = \frac{4\pi N t Z^2 e^4}{M^2 c^4 \beta^2 \zeta^2}$$

N being the number of nuclei/cc., and t is the thickness of the plate traversed. This angle Θ is the actual three dimensional scattering angle, and it is more usual to work in terms of φ, the scattering angle projected at right angles to the line of sight. In terms of this angle φ, the above expression becomes:-

$$P(\varphi)\, d\varphi = \frac{k\, d\varphi}{\varphi^3}$$

As the probability of scattering through small angles is very much greater than through large ones, from the above formula, it follows that the resultant multiple scattering angle will be the composition of a large number of small angles. As one direction is as probable as another, the resultant multiple scattering distribution will be very nearly a Gaussian distribution. Williams gives the expression for the distribution of multiple scattering

angles α, as:-

$$P(\alpha)\, d\alpha = \left(\frac{2}{\pi \alpha_m}\right) e^{-\frac{\alpha^2}{\pi \alpha_m^2}}$$

where α_m is the arithmetic mean value of α and α_m^2 is $\frac{2}{\pi}$ times the mean square of α.

In this theory, and in all the others, a small angle cut off is included i.e. it is assumed that single scatters below a minimum angle φ_{min} are impossible, due to the effects of electron screening of the nucleus. On the Williams theory, $\varphi_{min} \sim \frac{\lambda}{a}$ where λ is the De Broglie wavelength for the scattered particle, and a is of atomic dimensions.

Molière extended the Williams theory, postulating that the single scattering distribution was given by

$$P(\varphi)\, d\varphi = \frac{\frac{1}{2} Q\, d\varphi}{(\varphi^2 + \varphi_{min}^2)^{\frac{3}{2}}} \quad \text{where } Q = \frac{4\pi N t}{A} \left(\frac{Ze^2}{pc\beta}\right)^2$$

N being Avagadro's number t - thickness in gm. $cm.^{-2}$

The angle φ_{min} was the screening angle associated with the extra nucleur electrons and had a value on the Molière theory of

$$\varphi_{min} = \frac{1.14\, m_e\, c\, Z}{137\, p} \left\{ 1.13 + 3.76 \left(\frac{Z}{137\beta}\right)^2 \right\}^{\frac{1}{2}}$$

The multiple scattering on the Molière theory also approximates to a Gaussian distribution, and will therefore fall off exponentially with increasing angle . The single scattering distribution is decreasing as $\frac{1}{\varphi^3}$ with increasing φ, and therefore at small angles, the scattering will be multiple in nature, but at large angles the probability of single scattering will be much greater than that for multiple scattering. There will, of course, be a region where the two curves are "smoothed" together. On the Williams theory, the

point of intersection of the two curves is given by the angle θ_2. Typical values of some of these quantities in the case of a muon of 2 $\frac{GeV}{c}$ momentum, passing through a 2.5 cm. lead plate are as follows:-

Arithemetic mean deflection (William's theory)

$\alpha_m = 1.29 \times 10^{-2}$ radians.

Crossing point (William's theory) $= 4.634 \times 10^{-2}$ radians.

Electronic screening angle (Molière theory)

$= 1.455 \times 10^{-5}$ radians.

In the Molière theory, the nucleus is considered as a point charge, and there is no large angle cut off in the single scattering distribution due to the finite size of the nucleus. Thus, it would be expected that in the large angle region of single scattering, (well above θ_2 value), the Molière theory would give a higher value for the scattering probability than would be found experimentally, if a finite size nucleus is assumed.

The charge on the nucleus, is of course situated at various distinct regions, i.e. the protons, and when a particle passes the nucleus at relatively large distances, the scattering potential can be taken to be produced by the total charge at a fixed point. This is the case for small scattering angles. If, however, the particle passes the nucleus at distances of the order of nuclear dimensions, the secondary scattered wavelets from the various protons will interfere, and the scattering will therefore be reduced in this large angle scattering region. Thus, it would be expected that the Molière theory would over estimate the large angle single scattering probability.

In the theory of Olbert, the reduction in large angle single

scattering is taken into account, by no longer considering the nucleus as a point charge. In his theory, Olbert takes the following expression for the single scattering probability

$$f(\varphi', \varphi_0')\, d\varphi' = \frac{\frac{1}{2} Q\, d\varphi'}{(\varphi'^2 + \varphi_{min}'^2)^{\frac{3}{2}}} \qquad |\varphi'| < \varphi_0'$$

$$= 0 \qquad |\varphi'| > \varphi_0'$$

It will be seen from the above formula, that Olbert uses the same function as Molière, but assumes no single scattering through angles greater than φ_0' where φ_0' is related to the nuclear size. On Olbert's theory $\varphi_0' = \varphi_{min}' a r_n^{-1}$ where φ_{min}' is the screening angle, as previously defined, a is the Thomas-Fermi radius of the atom = $1.67 \times 10^{4}\, r_e Z^{-\frac{1}{3}}$ ($r_e = 2.82 \times 10^{-13}$ cm.).

$$r \sim 0.49\, r_e A^{\frac{1}{3}}$$

The multiple scattering function which is derived from the above single scattering distribution, again approximates to a Gaussian distribution. Now as φ_0' for a 2 $\frac{\text{Gev.}}{c}$ muon passing through a 2.5 cm. lead plate is 1.933×10^{-2} radians, it follows that any scatters above this value must be due to multiple scattering. Therefore, at large angles, the Olbert distribution falls off exponentially, as only the multiple scattering contributes, whereas the Molière theory gives a fall off of the order of $\frac{1}{\varphi'^3}$ in this region.

Of course, it is to be expected that the Olbert theory has overestimated the effect of the finite size of the nucleus, in imposing a sharp cut off at φ_0'. It would be expected that the cut off would be gradual in the region of φ_0'. However, Olbert's theory would be expected to correspond better to experimental results than

the theory of Molière.

Cooper and Rainwater have produced a theory which does not assume a sharp cut off as in the theory of Olbert. They modify Molière's single scattering distribution for large angles, by putting for the single scattering relation

$$F(\varphi) = \frac{\frac{1}{2} Q}{\left(\varphi^2 + \varphi_m^2\right)^{\frac{3}{2}}} F_N\left(\frac{\varphi}{\varphi_0}\right)$$

The result of this theory is to give a distribution curve between those of Olbert and Molière.

4.3. Previous Experiments on Muon Scattering.

A large number of experiments have been attempted on muon scattering and the results fall into two groups. Several experiments have given results which follow the Molière distribution, whereas others agree with the Olbert, or Cooper and Rainwater theory. The results which agree with Molière are unexpected, as it should be expected that this theory would over-estimate the scattering at large angles, and the results have been interpreted as implying the existence of anomalous scattering of the muon, due to muon-nuclear forces. The magnitude agreement with Molière's theory is fortuitous and has no real significance.

Most of the experiments have used magnetic fields for the determination of the momentum of the scattered particles. Among those who find agreement with the theory of Molière are Whittemore and Shutt, and Lloyd and Wolfendale.

In the experiment of Whittemore and Shutt, the momentum determination was by a spectrograph consisting of two cloud chambers separated by a magnetic field. The range of momenta considered was 0.3 - 3 $\frac{\text{Gev}}{c}$. The range was so chosen to ensure uncertainties in

momentum and deflection were negligible. It was found that their results followed the distribution of Snyder and Scott (Molière). The contributions from spurious scattering (pion, electron contamination etc.) was less than 10% of the observed excess scattering.

The method adopted in the experiment of Lloyd and Wolfendale was similar to that of the above experiment, i.e. that of momentum determination by deflections in a magnetic field, followed by scattering of the particle in a cloud chamber containing two plates, one of iron and the other of lead. The particles were divided into momentum categories from the momentum spectrograph results, and the projected scattering angles were measured. The momentum categories ranged from 0.63 - 11.8 $\frac{\text{Gev.}}{c}$.

Corrections were applied to the momentum spectrum, due to the finite width of the selecting counters, and the scattering in the counter trays etc., and to the scattering in the cloud chamber due to systematic distortion. The root mean square angle of scattering for each momentum category was calculated and compared with the predictions of both Molière and Olbert, using a large angle cut off equal to 3.5 times the root mean square angle found from the smaller angles. The ratios of observed to expected root mean square angles for 50.9 g/cm^2 of lead were

Molière's theory 0.995 ± 0.021.

Olbert's theory 1.066 ± 0.021.

The experimental results agreed with the Molière theory in the small angle region (less than 3.5 x r.m.s. angle) up to approximately 20 $\frac{\text{Gev.}}{c}$. In this region, there is not much variation between

Olbert's and Molière's theories, and it is the large angle scattering region which must be considered. In this region, it was found that the Molière distribution was followed up to a value of $p\varphi$ = 12 $\frac{Gev.}{c}$ deg. In all these calculations, the effects of protons were taken into account by adopting a cut off in the scattering distributions. Beyond this limit the number of muon events should be small on any reasonable theory, while within it the proton effect should be small. Contamination from Λ-mesons should be negligible.

There have however, been several observers whose results disagree with the conclusions of the above experiments.

Fukui et. al. (1959) had two large absorber blocks of iron, one above, and the other below, a multiplate cloud chamber. Trays of counters were placed underneath both absorber blocks. The top absorber was 1 metre of iron, and it served to reduce the number of spurious particles entering the chamber, whereas the second absorber, (75 cm. of iron), served to define the residual range of the muons. After traversing the iron, the mesons stopped and decayed in one or other of two carbon slabs placed below the lower absorber. The momentum could be calculated if such an event occurred, and the scattering distributions found in this experiment agreed with the Cooper and Rainwater theory and not with that of Molière.

All these previous experiments suffered from the disadvantage of being cosmic ray experiments, and thus, large errors were involved in the momentum determination and the spread of momentum, contamination and the identification of the muons. Also, an important factor was the low counting rate, even within wide momentum ranges. These difficulties were surmounted in the machine

experiment of Masek et. al. They used 2 $\frac{Gev.}{c}$ muons produced by the decay of pions from the Bevatron. The muons were separated magnetically from the higher momentum pions and also passed through a Čerenkov counter to reduce any residual contamination. With this arrangement, they obtained muons of momentum 2.00 ± 0.03 $\frac{Gev.}{c}$, with a pion contamination of 4.9×10^{-6} (which is negligible from the scattering distribution point of view). The beam was scattered from carbon and lead targets, the number of incident particles in the case with the lead target being 3.4×10^{6}. The distribution so obtained for the scattered particles, which were detected by means of scintillators, agreed with the Cooper and Rainwater theory. It seems possible that with the better experimental conditions available in this experiment, that the agreement with Cooper and Rainwater is correct, and the other experiments underestimated the errors involved.

4.4. Counter Efficiencies.

In the experiment to be undertaken, the arrangement discussed previously for selecting particles within a certain band width, was in operation. Theoretically, this band width could be reduced to a very small value, but in practice, using cosmic radiation as the particle source, this range had to be kept relatively wide, in order to obtain a suitable particle flux. Thus, particles will be selected within a finite momentum range, and the shape of the muon spectrum within this range will be used. The choice of range of momentum is determined by two factors. Firstly, in order to distinguish between the scattering theories, high enough momentum must be chosen to obtain a significant difference. The high energy cut off of the counter system is determined by the Čerenkov counter

efficiency. The counters were in fact set at pressures of 25 atmospheres (small counter) and 10 atmospheres (large counter). Theoretically, this would give the selected velocity range as v = 0.9925c - 0.9970c, but the actual range would be higher than this, due to the shape of the efficiency characteristic. With the described experimental arrangement, it was eventually found impossible to distinguish between the two theories and the results were used to check the counter efficiencies. It will be remembered that the efficiency of the counters for selecting numbers of particles has already been discussed in a previous chapter. However, in this case, the efficiency of counting single particles is required. It has been shown in a previous section, that when a particle produces approximately 90 photons in the large counter, or 70 photons in the small counter, it has almost 100% probability of being counted. Thus, the important point in this connection is how far above threshold velocity the particle velocity must be, in order to produce the required number of photons in the sensitive length of the counter. This can be directly calculated from the formula $N = K \left(1 - \frac{1}{\beta^2 n^2} \right) l$, where $K = \frac{2\pi}{137} \frac{\Delta\lambda}{\lambda^2}$, l is the sensitive length and N the number of photons.

From this formula, curves can be constructed of the variation of number of photons produced, against increasing momentum for various threshold pressures. The results of these calculations is shown in Figure (4.1). It will be seen that with a threshold momentum of 680 $\frac{\text{Mev.}}{c}$, (pressure in the counter of 30 atmospheres), the curve for a 100 cm. long counter, (large counter), rises almost vertically at first. The momentum at which 90 photons are produced

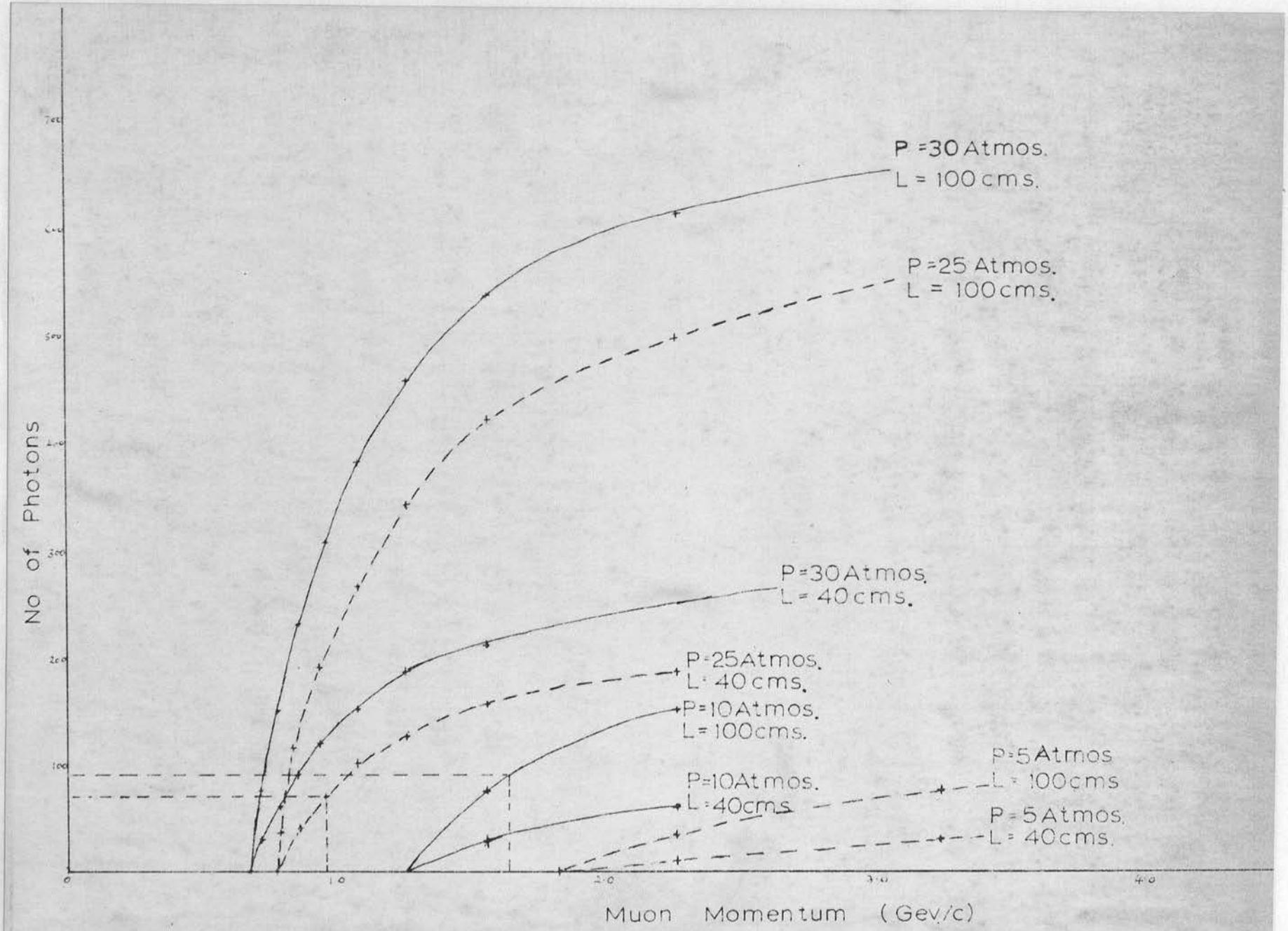
P =30 Atmos.
L = 100 cms.
P =25 Atmos.
L = 100cms.
P=30Atmos.
L = 40cms.
P=25Atmos.
L = 40 cms.
P=10Atmos.
L=100cms.
P=5Atmos
L = 100cms
P=10Atmos.
L=40cms
P=5Atmos.
L = 40cms.
No of Photons
Muon Momentum (Gev/c)

Fig. 4·1

is $\sim$ 740 $\frac{\text{Mev.}}{c}$. Thus, all muons with momentum greater than 740 $\frac{\text{Mev.}}{c}$ should count in this practical counter, whereas in the theoretical case of a perfect characteristic, all particles of momentum greater than 680 $\frac{\text{Mev.}}{c}$ would count. As the difference in momentum is very small, an approximation to the counter efficiency characteristic can be made by assuming a zero efficiency for 60 $\frac{\text{Mev.}}{c}$ above the theoretical threshold and then a 100% efficiency at 740 $\frac{\text{Mev.}}{c}$. This is an approximation, but is the worst case, as the change will be gradual over this range. If the counter, with a pressure of 30 atmospheres is only 40 cms. long, (small counter), the rise of the curve is more gradual and there will be 100% efficiency obtained when 70 photons are reached. In actual fact, consideration of Figure (4.1) shows that the required momentum value in this case is 810 $\frac{\text{Mev.}}{c}$. Corresponding graphs are drawn for two such counters, (one large and one small), for pressures of 25, 10 and 5 atmospheres. It will be seen, that as the pressures are decreased, the curves become less and less steep, the shorter counter, of course, always providing the lower curve at any particular pressure. The efficiency becomes particularly bad at low pressures, For example, the large counter, with a pressure of 5 atmospheres has a practical threshold of 3.7 $\frac{\text{Gev.}}{c}$ against the theoretical threshold of 1.82 $\frac{\text{Gev.}}{c}$. In the case of the smaller counter, at this pressure, the number of photons never becomes as large as 70, even if the particle is travelling with the velocity of light. Thus, this counter under these conditions, would never give anything approaching a 100% efficiency. Thus, this effect limits the upper velocity cut off that can be obtained from the counters. Of course, the inferior

counter, (the small one), must be the one operated at the higher pressure, to minimise this effect as much as possible.

The conditions under which the experiment was run, were that the counters contained nitrogen, the large one being at a pressure of 10 atmospheres, and the small one at a pressure of 25 atmospheres. Theoretically, this would give a momentum range of 780 $\frac{\text{Mev.}}{c} < p <$ 126 $\frac{\text{Gev.}}{c}$. However, by consideration of the curves, it will be seen that using the above criterion, the practical momentum range approximates to 960 $\frac{\text{Mev.}}{c} < p < 1.64$ $\frac{\text{Gev.}}{c}$. To obtain such a range, the large counter must be run in anti-coincidence with the counter telescope.

4.5. Effects of Contamination.

The major sources of contamination in the experiment are the effects due to protons, pions and electrons being identified as muons, and there is also the probability that muons of lower momentum, than that selected by the counters will be present. We shall consider each of these possibilities in turn. In a previous section, the particle contamination has been discussed from the point of view of efficiency characteristic calculations. It was found that from that point of view, the effects of other single particles could be neglected and only showers would play a significant role. However, in the scattering measurements, a small contamination could be sufficient to upset the results.

The proton contamination in the experiment is small, due to the fact that a velocity discrimination system is being operated. The important feature is that the particle must have a velocity higher than the threshold velocity, and this therefore, requires that a

proton which produces a count, should have an energy in the range 8.5 - 14.5 Gev. The ratio of protons in this range to the genuine counting rate is extremely small. Thus, in this experiment, there is a better discrimination against proton contamination, than in magnetic spectrograph experiments, where the discrimination is on a momentum basis.

The pion contamination will not, however, be greatly affected by the type of selection, as the masses of the muon and the pion are close together. The corresponding range of allowed pion energies is 1.27 - 2.16 Gev. The pion flux can, of course be reduced, by placing an absorber in the flight path, in which case pion-nucleon interactions will reduce the ratio of pions to muons. Thus, the multiplate cloud chamber should reduce the pion contamination to a greater extent than the single plate chamber, as a larger proportion of the pions would be seen to interact in the chamber. However, this contamination will, in general, still be present and will have to be taken into consideration. The total thickness of lead present in the cloud chamber was 63 gm. $cm.^{-2}$, and this should reduce the incident pion flux considerably. Thus, while not eliminating the pion contamination, it should be approximately reduced to 69% of the incident flux. The inclusion of a thick absorbing block of lead placed above the top scintillator, to shield the whole counter telescope from pions, is a possible method, for calculating the residual effect of the pions. Any difference between the scattering results from the shielded and unshielded systems could then be attributed to pion contamination.

The electron flux at sea level is the largest of the unwanted

particles. However, from the point of view of the scattering experiment, all electron effects should be eliminated. Firstly, the selected electron energy range as theoretically detected by the counter system is 4.6 - 7.9 Mev. Electrons of such energies could not be detected as they would be unable to penetrate the complete telescope system. If any spurious electron did enter the chamber, it would be recognised as it would either produce a shower or be absorbed in the lead plates. It would have zero probability of passing through the lead plates and being mistaken for a muon. In the selection of events, only particles which passed through all three plates were considered as genuine.

The most difficult contamination to eliminate is that where the muons are slower than the required velocity range. It has already been shown that some of the six-fold counts are spurious, i.e. caused by two or more particles interacting with the counters, in such a way as to obtain a six-fold count. It is possible that such an occurrence can happen simultaneously with the arrival of a slow muon, or perhaps a slow muon sets off some of the counters itself, and the Čerenkov counters are triggered by another particle, travelling at such a large angle, that it is not visible in the chamber. In such an occurrence, the slow meson would have a higher probability of being scattered into the region of large angle scattering.. Thus, this effect could seriously interfere with the results. The multiplate chamber, however, enables a certain correction to be made. Firstly, all particles which are travelling at an angle, which makes it impossible, for it to have traversed the counter telescope, are eliminated. Secondly, any particle which is

accompanied by a second one, which could also have traversed the system is rejected. A number of both of these events were found. The third check is one imposed on all large angle scatters. If there is a large angle scatter in one of the plates, the corresponding scattering angle in the other two plates is compared carefully. If the large scattering is due to a fast particle receiving a large single scatter, it is improbable that there will be large angle scatters in the other two plates as well. If, however, it is a slow particle which has slipped through the counter system, there will be a larger probability of large angle scatters in the other plates. Thus, any photograph which has three large scatters associated with the particle will be discarded. In fact, no such events were found and this effect cannot be significant.

It has already been shown that on the Olbert theory, there is a maximum angle for single scattering. If it is assumed that all the particles have an energy greater than 1.6 $\frac{\text{Gev.}}{c}$ (approx. 5 fold case), it can be shown that the maximum scattering angle for such particles is $\sim 1.5^{\circ}$. Thus, on the Olbert theory any scatters which are greater than this angle must be due to multiple scattering. From the Olbert theory, it can be shown that for such a particle, the number of scatters greater than 4° would be approximately 1 out of every 6000 scatterings.

On the Molière theory, the scattering at large angles would be predominately single with a small contribution due to multiple scattering and on this theory for a 1.6 $\frac{\text{Gev.}}{c}$ muon, we should expect 1 scatter greater than 4° out of every 200 scatters. It was considered that if $\sim$ 2000 scatters could be obtained, it should be

possible to distinguish between the theories, even if the contamination was as high as 0.1% of the incident particle flux. In actual fact, from considerations discussed in a previous chapter, this should be an upper limit, and it would be expected that the contamination would be much lower than this figure. The obtaining of 2000 scatters was found to be impossible on the grounds of time, due to a combination of low counting rate and chamber distortion. Out of 38, five-fold events, no scatters greater than 4° were observed. The statistics on this, are, of course, insufficient to draw any conclusion. A similar calculation was carried out for 6-fold events and it was found that the same figures as above would apply to scatters greater than 6°. Thus, on the Olbert theory we should expect 0.3 scatters greater than 6° out of 2000, whereas the Molière theory predicts 10. In fact, out of 97 measured 6-fold scatters, only 1 was greater than 6°, (single plate chamber).

4.6. Photographic Measurements.

The camera used in this experiment possessed two Dallmeyer anastigmatic lenses selected to form a stereoscopic pair. The maximum aperture of the lenses is f/3.5, their focal length is 3.5 cm., and the separation of the axes of the lenses is two inches. The position of the camera is so arranged, that the plane of best focus occurs approximately at the centre of the illuminated part of the chamber. This, in turn, is the region selected by the counter telescope. The camera details and the wind-on mechanism are discussed in the Ph.D. thesis of Dr. R.M. Hudson. A maximum of approximately 80 photographs can be taken in any single run.

The only modification to the system is the inclusion, in the

camera field of view, of a neon bulb, which is switched on by a 6-fold triggered pulse, but not by a 5-fold pulse. It will be remembered that a 6-fold pulse denotes a particle, the velocity of which lies between the critical velocities of the two Čerenkov counters, while a 5-fold pulse denotes a particle with a velocity greater than the higher critical velocity.

The photographic measurements involved examining the negatives by means of a Cambridge Universal Measuring Machine, by which the co-ordinates of various points along the track could be obtained. As stated previously, the required parameter is the scattering angle, projected on the plane at right angles to the line of sight. This can be determined from the negative in the following way.

In Figure (4.2), AB is the actual track position, projected on the plane at right angles to the line of sight. The angle γ is the angle required. $(x_1 y_1 , x_1' y_1')$ and $(x_2 y_2 , x_2' y_2')$ are the corresponding track sections on the two stereoscopic views, and O and O′ are the pole positions of the two lenses. The co-ordinates of these points are shown in the diagram. Therefore:-

$$\text{Tan } \gamma = \frac{BC}{AC} = \frac{ON - OM}{AM - CM} = \frac{\frac{x_1'}{m'} - \frac{x_1}{m}}{\frac{y_1}{m} - \frac{y_1'}{m'}}$$

$$\text{where } m = \frac{D - L}{L} \quad \text{and} \quad m' = \frac{D' - L}{L}$$

$$\text{therefore } \tan \gamma = \frac{\frac{(m)}{(m')} x_1' - x_1}{\frac{(m')}{(m)} y_1 - y_1'}$$

$$= \frac{x_1' - x_1 + \frac{(m)}{(m')} x_1' - x_1'}{y_1 - y_1'}$$

$$= \frac{x_1' - x_1}{y_1 - y_1'} + \frac{\left(\frac{m}{m'} - 1\right) x_1'}{y_1 - y_1'}$$

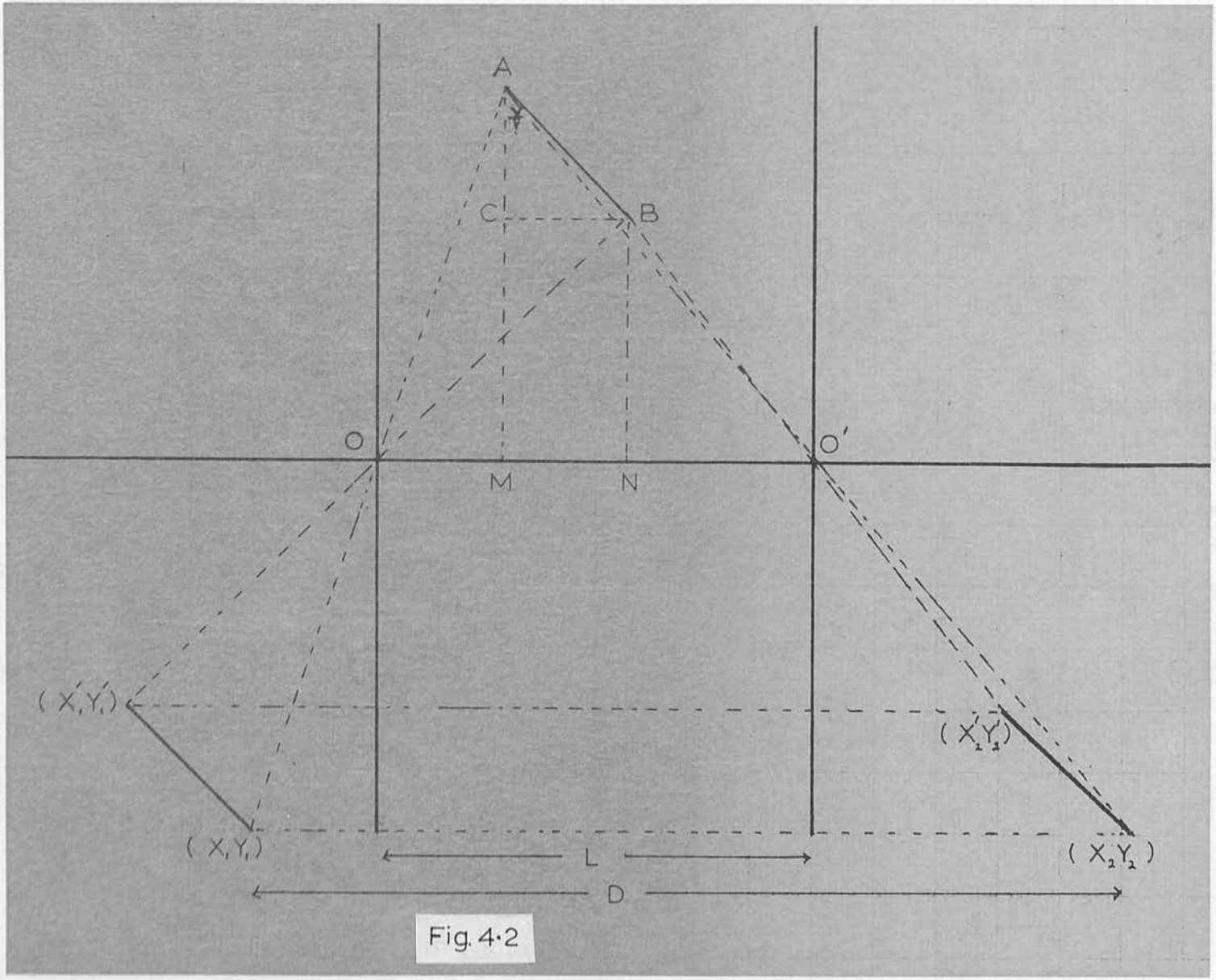

Fig. 4·2

$$\gamma = \alpha + \frac{(D - D')}{(D' - L)} \frac{x_1'}{y_1 - y_1'}$$

as the angles are small $\tan\gamma = \gamma$

L is the separation of the lens' positions = 5 cm. Thus for this analysis, a knowledge of the x co-ordinates of the pole positions, and the co-ordinates of two or more points along the track, on either side of the scattering plate is required. An error was introduced in the centering of the crosswire on the track. It was found that if the crosswire was brought up from one side rather than the other, an error of as much as 0.005 mm. could be made. Thus, in all measurements, the reading was obtained twice from each side, and the results averaged. The instrument itself could be read to 0.002 mm.

To eliminate distortion as far as possible, at least, three points were taken on each portion of the track, and it was required that they fell on a straight line within the experimental error, before they were accepted. Most of the later tracks satisfied this criterion.

Approximately 120 scatters were taken with the single 2.5 cm. thick lead plate in the chamber, with a particle momentum range lying between 0.96 and 1.64 $\frac{\text{Gev.}}{c}$. Any tracks showing chamber distortion were eliminated. Similar readings were taken of 21 6-fold and 38 5-fold tracks obtained in the multiplate chamber, (three 2 cm. thick lead plates). These were better from the point of view of eliminating contamination.

4.7. Small Angle Multiple Scattering Experiment.

With such a low counting rate, the scattering results were used to check the selection efficiencies of the Čerenkov counters.

It will be remembered that our counters were calculated to be selecting muons, the energy of which was within a range of 0.96 - 1.64 Gev. This range could be checked by calculating the mean angle of scattering and the mean square angle of scattering from the experimental results, and comparing them with those predicted by theory for the above range. It has already been stated that the various scattering theories only diverge in the region of large angle scattering, and in the small angle region they are roughly equivalent. Thus, in calculating the mean angle in this region, any of the theories can be used, and it was found to be convenient to use the theory of Olbert for this purpose.

In calculating the experimental mean angle, any angle which was greater than 3.5 times the mean angle, as obtained from the smaller angles, was rejected. This is the usual criterion applied to this calculation, and it also rejects any large nuclear scattering of pions or protons which might be present as contamination. This contamination has already been discussed in connection with the large angle scattering and in this case its effects are completely negligible, as so many more scatters are being considered. The application of the 3.5 times the mean angle criterion, only eliminated one scatter in the case of the 6-fold counts and two in the 5-fold case.

To obtain the corresponding theoretical mean angle, the shape of the sea-level muon spectrum in the above range (Owen and Wilson, 1955) had to be taken into account. The spectrum was split into ranges of width 100 Mev., and the mean scattering angle for the mid-point of each range was calculated. The results were then

weighed according to the muon spectrum and the final result obtained by averaging. On Olbert's theory, the mean scattering angle is given by.

$$\langle|\varphi|\rangle_{Av} = \left(\frac{2GQ}{\pi}\right)^{\frac{1}{2}}\left[1 + \frac{1}{2G}\left(1 - \alpha_0(x_0) + \frac{1 - \exp.(-x_0^2) - \sqrt{\pi}\,\Phi(x_0)}{x_0^2}\right)\right]$$

$$\text{where } \Phi(x_0) = \frac{2}{\pi^{\frac{1}{2}}}\int_0^{x_0} \exp.(-t^2)\,dt$$

$$Q = \left(\frac{4\pi Nt}{A}\right)\left(\frac{Ze^2}{pc\beta}\right)^2$$

$$G = 5.66 + 1.24 \log_{10}\left[\frac{Z^{\frac{4}{3}}A^{-1}t}{\left(1.13\beta^2 + 3.76\left(\frac{Z}{137}\right)^2\right)}\right]$$

$$\alpha_0(x_0) = \tfrac{1}{2}\left[\gamma(\tfrac{1}{2}) + \frac{1 - \exp.(-x_0^2)}{x_0^2} - Ei(-x_0^2)\right]$$

$$x = \varphi(2GQ)^{-\frac{1}{2}}$$

where φ is the projected scattering angle. φ_0 is the cut-off angle, N Avogadro's number, t - the thickness of the scattering plate in gm./cm^2.

The results for the above calculation are shown in Figure (4.3). It will be seen that results give a value for the theoretical mean angle for the six-fold muons of 0.0193 radians, and the corresponding value for the experimental results was 0.0191 $\pm$ 0.0040 radians. The experimental results are shown in Figure (4.4). It will be noticed that the agreement is excellent, and thus, it can be considered that the previous calculation, in obtaining the practical range of momentum, selected by the counters, is substantially correct. Further, the mean square angle according to Olbert's theory is given by

$$\langle\varphi^2\rangle_{AV} = Q\left[\ln 2\frac{\varphi_0}{\varphi_m} - 1\right] = 6.024 \times 10^{-4} \text{ radians}^2.$$

The experimental value is once more in good agreement, being

Six-fold Results.

(0.96 - 1.64 $\frac{\text{Gev.}}{c}$ Muons).

Momentum Range. $\frac{\text{Gev.}}{c}$	Weight from Spectrum.	Q radians^2 x 10^{-4}	$\langle\varphi\rangle_{Av}$ radians	$\langle\varphi^2\rangle_{Av}$ radians^2 x 10^{-4}
0.96 - 1.05	14.8	1.173	0.02254	8.072
1.05 - 1.15	12.5	0.9679	0.02047	6.661
1.15 - 1.25	10.2	0.8123	0.01876	5.590
1.25 - 1.35	8.0	0.6918	0.01731	4.761
1.35 - 1.45	5.6	0.5961	0.01607	4.102
1.45 - 1.55	3.4	0.5187	0.01499	3.570
1.55 - 1.64	1.1	0.4559	0.01406	3.137

$\langle\varphi\rangle_{Av}$ = 0.0193 radians. $\langle\varphi^2\rangle_{Av}$ = 6.024 x 10^{-4} radians^2.

Fig. (4.3).

Plate No.	α_1 rad.	γ_1 rad.	α_1 rad.	γ_1 rad.	Scatt.-Angle. rad.
216 - 1 - 2	+0.0270	+0.0286	-0.0110	-0.0058	+0.0344
216 - 1 - 3	-0.0110	-0.0058	-0.0420	-0.0363	+0.0305
216 - 2 - 1	-0.0400	-0.0282	-0.0280	-0.0358	+0.0076
216 - 2 - 2	-0.0280	-0.0358	-0.0620	-0.0310	-0.0048
216 - 2 - 3	-0.0620	-0.0310	+0.0380	-0.0120	-0.0190
216 - 3 - 1	+0.0500	+0.0124	0.0000	+0.0072	+0.0052
216 - 3 - 2	0.0000	+0.0072	-0.0180	-0.0200	+0.0272
216 - 3 - 3	-0.0180	-0.0200	-0.0160	+0.0096	-0.0296
217 - 1 - 2	+0.0480	+0.0601	-0.0160	-0.0123	+0.0724
217 - 2 - 1	-0.0540	-0.0414	-0.0820	-0.0558	+0.0144
217 - 2 - 2	-0.0820	-0.0558	-0.0060	-0.0137	-0.0421
217 - 2 - 3	-0.0060	-0.0137	-0.0400	-0.0409	+0.0272

Fig. (4.4).

6.292×10^{-4} radians^2.

When a similar calculation is carried out for the 5-fold case, the following results were obtained. For the average scattering angle, the experimental value was 0.0105 $\pm$ 0.0020 radians, as compared with the theoretical value of 0.0065 radians. It will be seen that the agreement is not so good in this case, however the difference between 5-fold and 6-fold is significant (see page 74).

4.8. Knock-on Electron Ratio.

The photographs obtained for the scattering experiment were also used to measure the ratio of knock-on electrons produced in the lead plates, to the number of muon traversals. The criterion adopted was that the muon had to leave the plate accompanied by an electron which was within 1 radiation length of the muon's emergent position. Two electrons satisfying this condition would count as two, but in fact no such event was observed, as the probability for such an event would be the square of the probability for a single knock-on.

Several experiments have been undertaken on the knock-on electron ratio, including those of Lloyd and Wolfendale, and Viswanathan et. al. Lloyd and Wolfendale used a cloud chamber containing nine 1 cm. lead plates, and selected the muons by means of a magnetic spectrograph. They found that the probability of a muon emerging from a 1 cm. lead plate, accompanied by a single electronic secondary was 5.8 $\pm$ 0.15%. Viswanathan et. al. used a counter experiment and summarised the present position with regard to knock-on production. They showed that the angular distribution of emergent secondaries should follow a $\cos^{2.5}\theta$ distribution and that

the ratio of knock-ons produced, should not depend on the energy of the primary particle, at least in the high energy range, (the case in the present experiment). Brown et.al., and Lovati et. al. have shown that back scattering from 1 cm. thick lead plates should occur in approximately 1% of the traversals. No such event was recognised in our experiment.

The relation between the production probability and the thickness of the lead plate being traversed is given by

$$P(t) = A \ln (1 + b\,t)$$

where P(t) is the probability of knock-on production from a plate of thickness t gm. cm^{-2}

$$A = 0.0177 \pm 0.0006 \text{ and } b = 3.0 \pm 0.4.$$

Thus, this gives a probability for knock-on production of $(7.5 \pm 0.5)\%$ for a 2 cm. thick lead plate, (multiplate chamber) and $(7.9 \pm 0.5)\%$ for a 2.5 cm. lead plate, (single plate chamber). The results obtained in the multiplate cloud chamber gave a value of $(3.2 \pm 0.7)\%$, well below the quoted figures. However, when the results of the single plate chamber were considered, better agreement was found. For the 5-fold muons (> 1.65 $\frac{\text{Gev.}}{c}$), a ratio of $(4.8 \pm 2.0)\%$ was obtained, and the corresponding figure for 6-fold muons ($0.95 - 1.65$ $\frac{\text{Gev.}}{c}$) was $(7.0 \pm 1.5)\%$. It will be seen that these results agree within the statistics with the theoretical value and with the non-dependence on momentum of the incident particle.

If all the results are included, a knock-on ratio of $(5.9 \pm 1.2)\%$ is obtained, in agreement with the results of Viswanathan.

Thus, it will be seen that in the experiments described in this chapter, the selected 6-fold range as calculated from the assumed

characteristics has proved to be substantially correct. The experimental 6-fold average scattering angle showed remarkable agreement with the calculated value. The 5-fold average angle did not show such good agreement and this could be taken to be a measurement of the distortion and measuring errors. It was found in the 5-fold scattering runs that there was a slight excess of negative scattering angles over positive, and this would suggest that there was a degree of systematic distortion. If the difference between the calculated and experimental 5-fold scattering angles is taken as the maximum distortion, this would give a value for the 6-fold average scattering angle of 0.0151 radians, still agreeing with the calculated value within the statistics.

The knock-on electron results will be seen to just agree with the calculated values although, one particular run is very low.

Chapter 5.

PHOTOGRAPHIC DETAILS.

5.1. Introduction.

In this chapter, the photographs obtained with the various experimental arrangements will be discussed. These photographs can be divided into three categories. Firstly, those photographs taken with the high pressure cloud chamber when acting in its dual capacity as chamber and detector. Secondly, the atmospheric chamber photographs with the single lead plate, and thirdly, the same chamber with the multiplate arrangement.

5.2. High Pressure Chamber Photographs.

These photographs were taken with an arrangement discussed in Appendix 2. The photographs were taken with the scintillator placed above the chamber, and an anti-coincidence counter shielding the Čerenkov photomultiplier. Such a photograph is shown in Plate 1. It will be seen that the particle track is inclined to the vertical, and the reasons for this are discussed in the section mentioned above. Great care had to be taken in interpreting the photographs obtained with this arrangement. Particle tracks produced up to 2 secs. before the expansion will be visible in the chamber, as well as post expansion tracks, so it is vital to ensure that the tracks studied are counter controlled. This can best be done by considering the sharpness of the tracks in relation to field separated tracks, which are in focus in the same part of the chamber. In order to ensure that the tracks are in the same plane of focus in the chamber, the distances D between the same point on the two stereoscopic views should always be of the order of 62.15

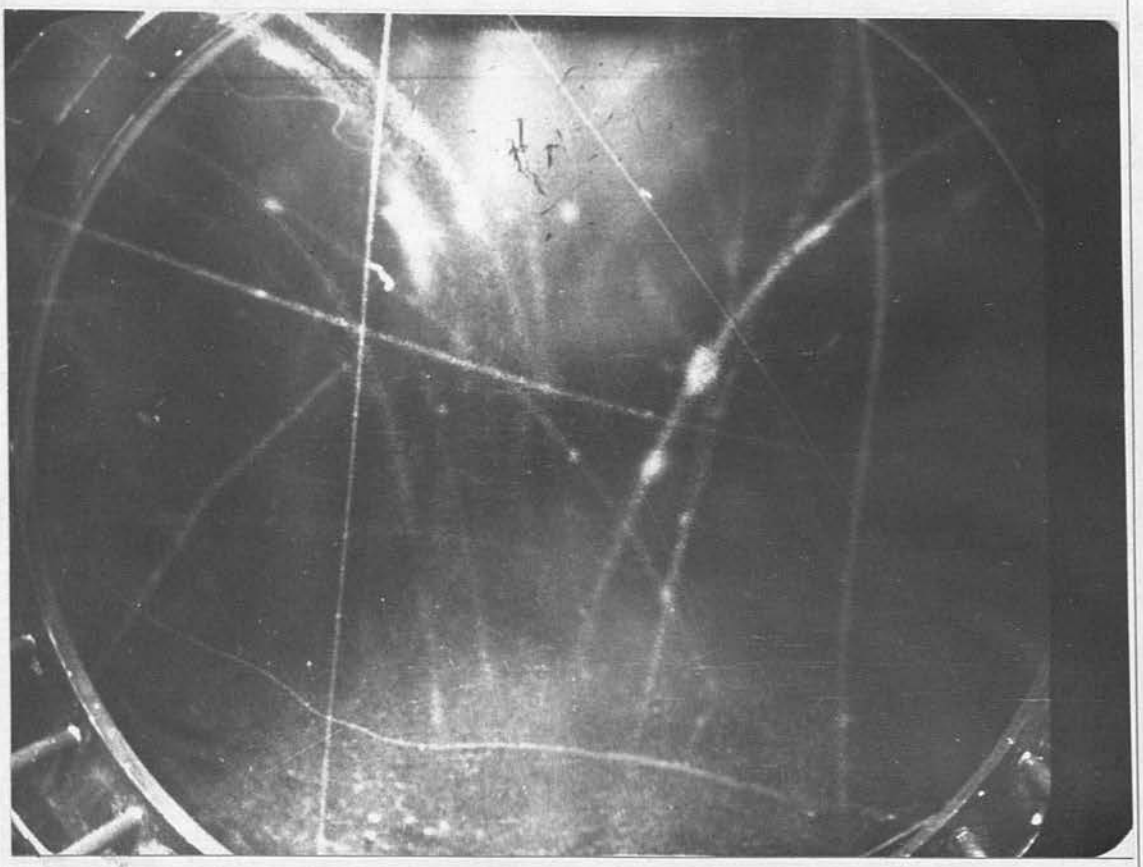

Plate 1

mms. The other point which had to be checked was that light from the track could in fact pass through the bottom window of the chamber onto the photomultiplier. The details of this calculation are given in the following section.

5.3. Calculation of Track Position.

In this section, the position of the Čerenkov cone with respect to the chamber window will be calculated. In order to determine this, the co-ordinates of the lens pole positions, two points at the extremities of the considered track and also the co-ordinates of some point which can be identified in the chamber, are required. These co-ordinates are measured on the Cambridge Universal Measuring Machine. The point chosen as the identifiable position is a piece of cotton attached to the chamber velvet back piece. The results of these measurements are shown in Figure (5.1).

The first requirement is to find the distance the two track points, (Points 1 and 2), are from the back of the chamber (Cotton Point). This can be calculated in the following way Figure (5.2).

Magnification in first case M_1 is v/z_1, and in second case $M_2 = v/z_2$

$$z_1 - z_2 = \Delta z = v\,(1/M_1 - 1/M_2).$$

	Left Hand Plate.	Right Hand Plate.
Pole Position.	(91.05, 25.85)	(141.05, 25.85)
Top End of Track (Point 1).	(80.89, 35.85)	(143.03, 35.85)
Bottom End of Track (Point 2).	(79.12, 15.85)	(141.03, 15.85)
Piece of Cotton.	(93.210, 14.21)	(151.780, 14.21)

Figure (5.1).

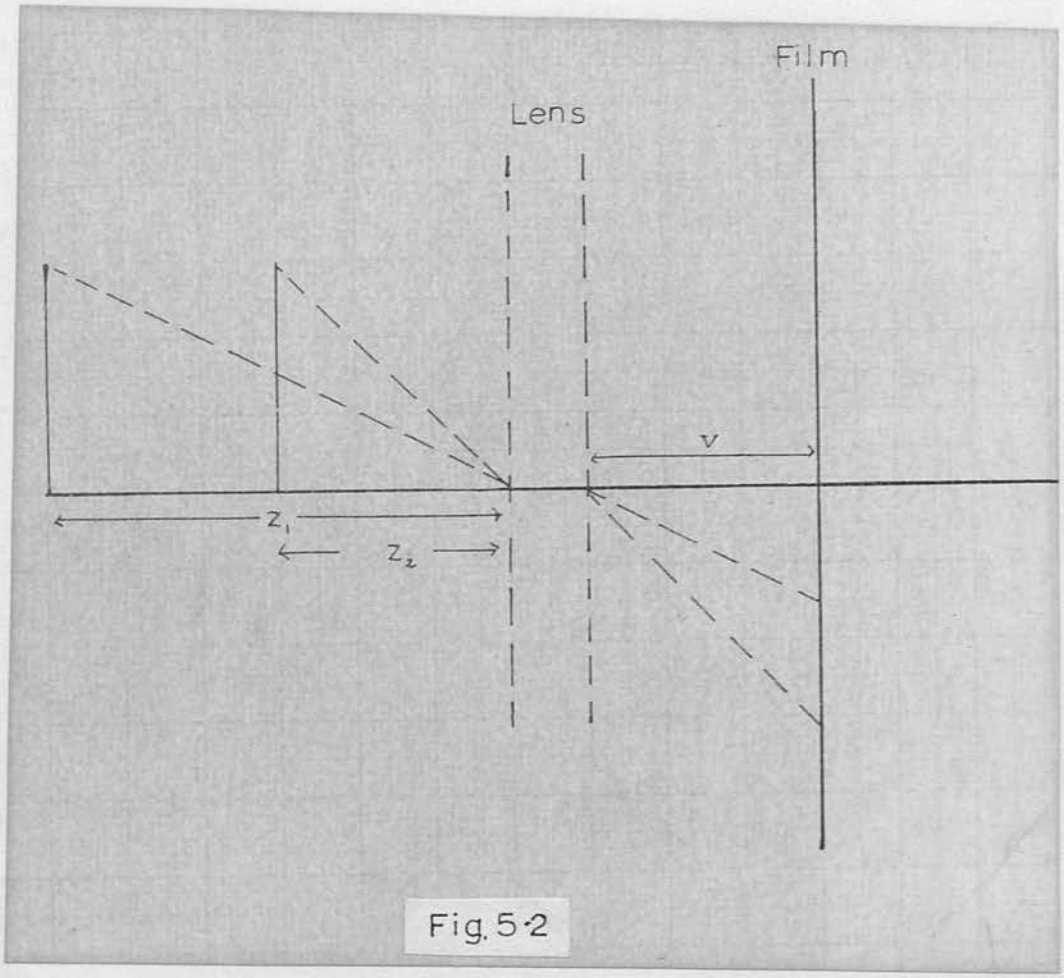

Fig. 5-2

From previous considerations Figure (4.2) $M_1 = (D_1 - L)/L$ etc. with the same notation as previously. Thus, if the cotton point figures are inserted for z_1, and the top end of track (Point 1) for z_2, Δz the distance of Point 1 from the back of the chamber can be found, (v is known to be 4.78 cms.). A similar calculation gives the distance of (point 2) from the back of the chamber. These give values of 8.403 cms. and 7.814 cms. respectively. The spacial lines parallel to the back of the chamber on which the 2 points lie, are known but their position along this line is still not known. This can be calculated by considering once more Figure (4.2). The distances OM and ON are required and these are respectively x_1/M_1 and x_2/M_2. Thus, knowing OM and ON′ and the fact that OO′ = L = 5 cms., the results that Point 1 is 1.64 cms. to right of centre line, and Point 2 is 2.5 cms. to right of centre line are obtained. The position of the window can be measured with respect to the chamber velvet and hence Figure (5.3) is obtained, where the points previous denoted as 1 and 2 are now designated B and A. Due to inversion, the top point on the film is the lower spacial point and thus point B is the lower of the two points in the chamber.

The vertical distance of points A and B above and below the centre line is now required, these distances being given by y_1/M_1 and y_2/M_2 respectively. These calculations give A as 4.199 cms. above the centre line, and B 4.076 cms. below it. The centre line itself is 12.5 cms. above the plane of the chamber window and thus from similar triangles, AB can be extrapolated to the point C, where the particle path meets the plane of the window. If the angle the path makes with the vertical is calculated, (as in section 4.6), it is

found that the inclination is only $\sim 3^{\circ}$. Thus, an approximation to the elliptic cross-section of the cone on the window plane can be made, by taking a circle of radius 20 tan Θ about C, where Θ is the Čerenkov angle (20 cm. being the path length in the chamber). The maximum radius is for a particle with v = c ($\Theta = 9^{\circ}\ 30'$). This case is the one shown in Figure (5.3). If the particle is slower, the radius of the circle will decrease with decreasing velocity, until it becomes the point C itself at threshold velocity.

5.4. Single Plate Atmospheric Chamber Photographs.

With the single plate atmospheric chamber, a large number of photographs were taken with the six-fold and five-fold arrangements. The results were included with the multiplate results in the scattering measurements. There was some distortion in some of the photographs and an error would have been introduced here. The distortion however, was not sufficient to affect results as the photographs considered were those with the least distortion. Care was taken to measure only on undistorted sections of the particle track. An example of a muon traversing the chamber is shown in Plate 2. This particle has been selected by two Čerenkov counters at pressures 10 atmospheres and 25 atmospheres. These photographs only enabled a single scattering measurement to be obtained per photograph. There was also the possibility that slower muons might not be eliminated. These difficulties were resolved by using the multiplate chamber for the next series of photographs.

5.5. Atmospheric, Multiplate Chamber Photographs.

The photographs initially taken with this chamber had considerable distortions, especially below the middle plate. Also,

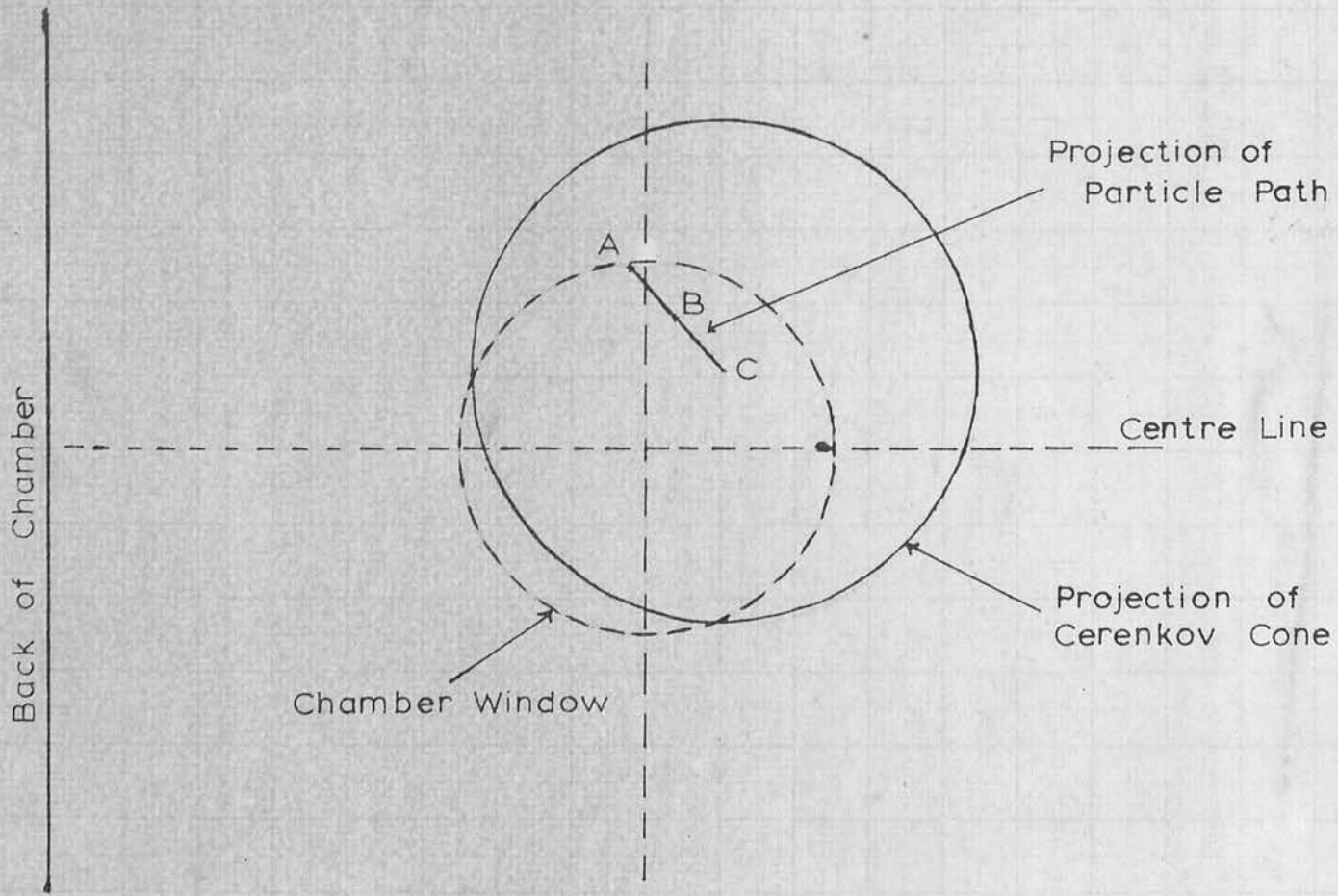

Fig.5·3

Position of Light Cone
with Respect to Chamber Window

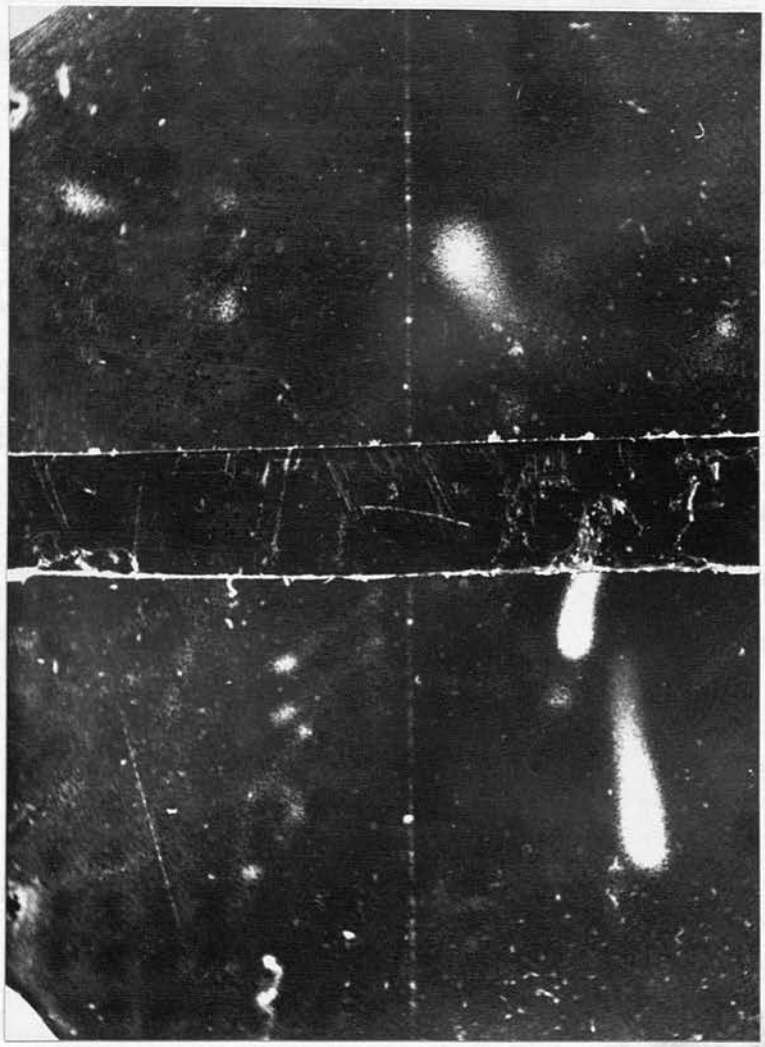

Plate 2

the introduction of the three plates had cut down the light entering the chamber in the top and bottom gaps. It was found almost impossible initially to measure the scattering angles. An example of the chamber distortion is shown in Plate 3. The lighting was improved by reducing the size of the top and bottom electrodes allowing more light into the top and bottom gaps. The distortion was due to a temperature gradient through the working volume of the chamber, and this distortion was eventually eliminated by enclosing the chamber and counters in a hut complete with thermostat (21° C). Previously, there were quite large temperature fluctuations. Plate 4 shows one of the later photographs, (with hut), where the distortion has been reduced.

Plates 5 and 6 are also examples of photographs taken with this arrangement, while running on the 5-fold, (no neon lamp showing), and 6-fold, (neon switched on), triggering arrangement. The difference between the two photographs is obvious, and they are easily distinguished by this method. It will be seen from all these photographs that the background of velvet is not up to the best standards. The reason for this is that the atmospheric chamber is shallow and the Čerenkov counter cross-section takes up nearly the whole depth. Thus, in order to obtain tracks over the complete chamber depth, the photoflash has to be allowed to spread and naturally some of the light falls on the back velvet.

Plate 7 shows two knock-on electrons, one produced in the middle plate and one in the bottom plate. This was an uncommon event as in measuring the ratio of knock-on events per track a ratio of 3.2% was found. Any electron which had been selected

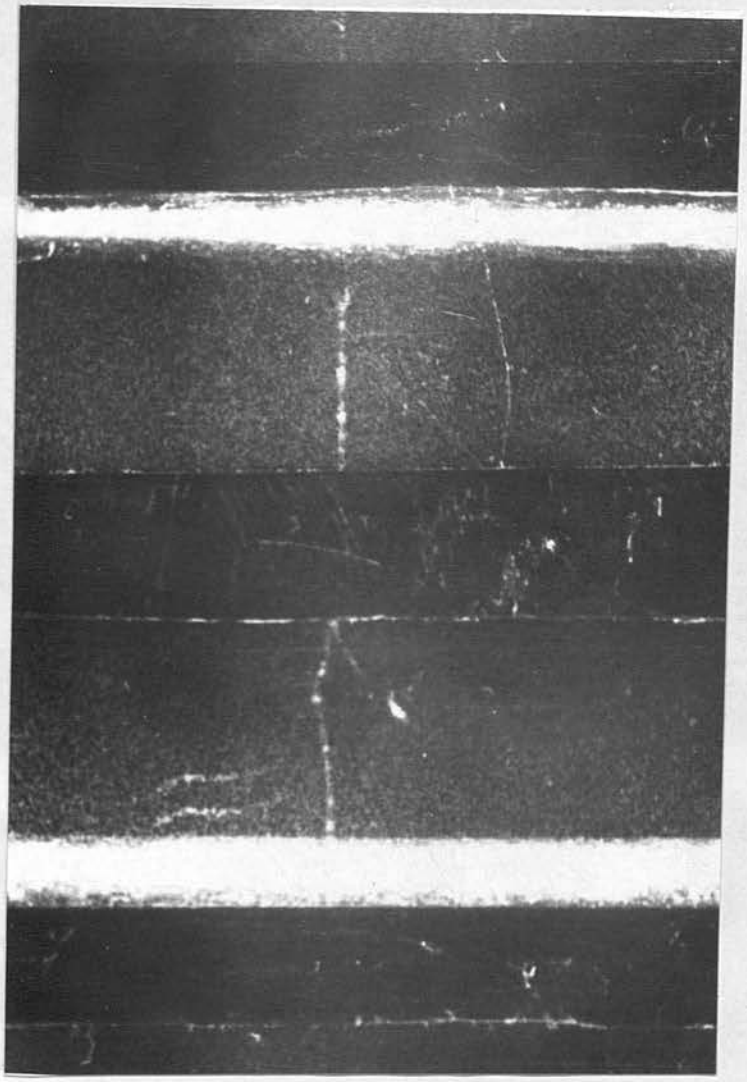

Plate 3

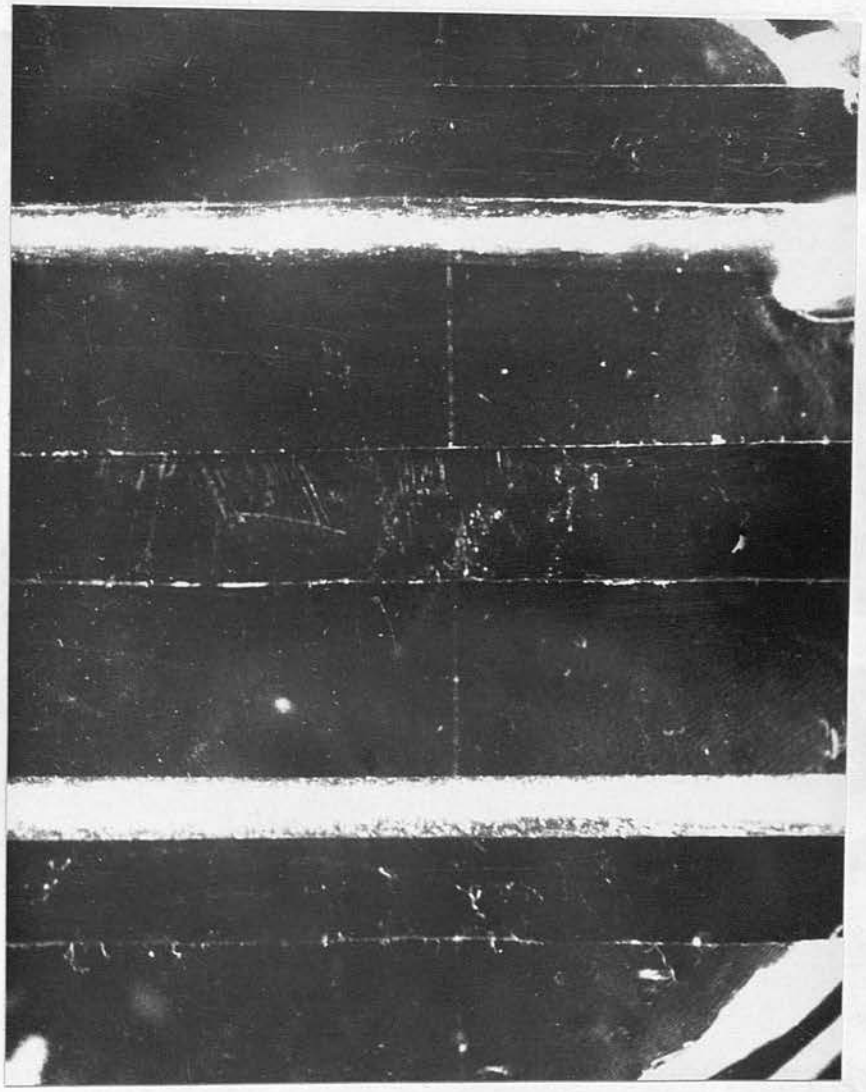

Plate 4

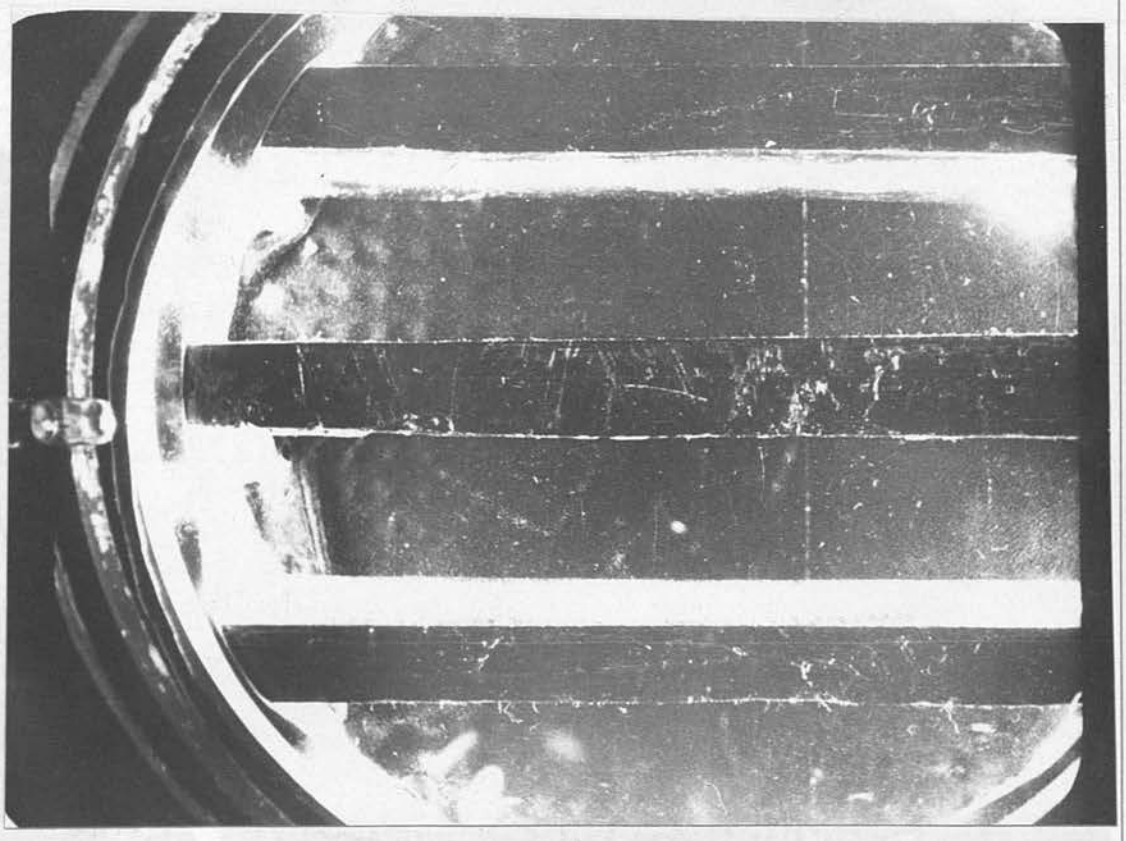

Plate 5

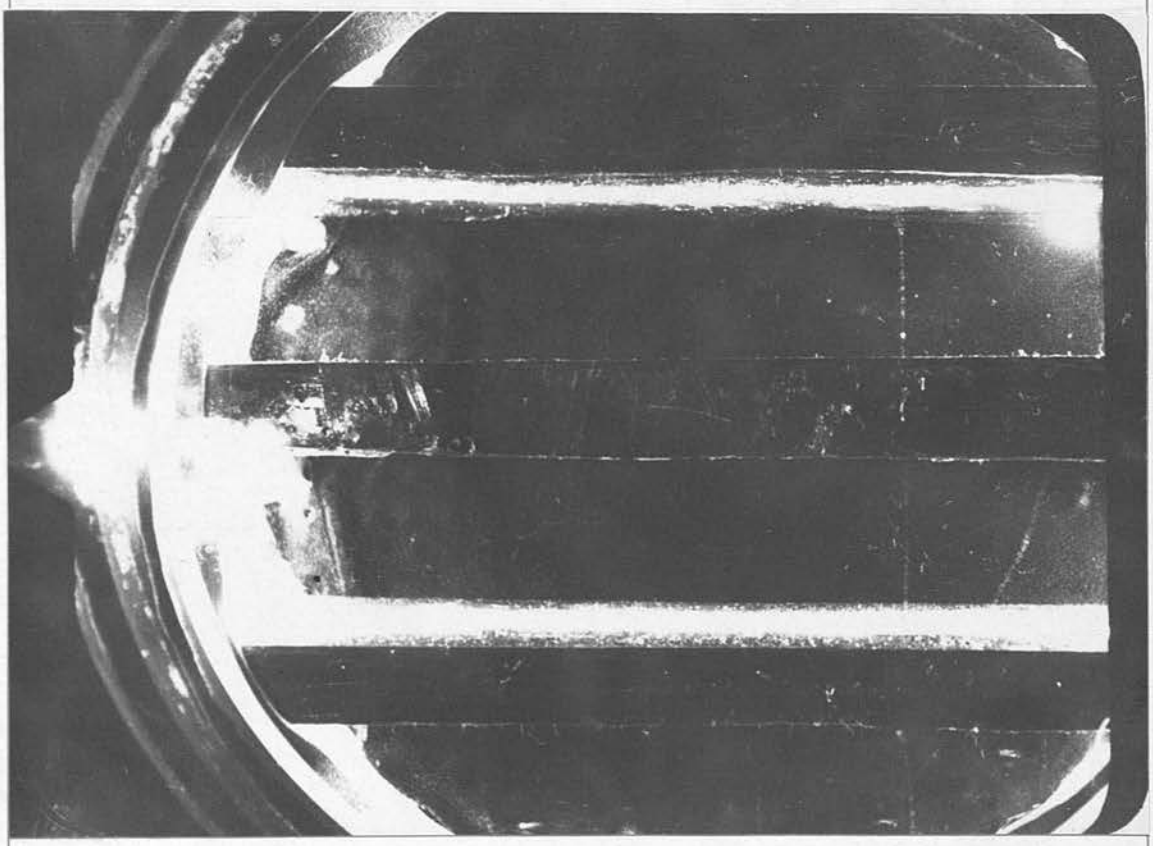

Plate 6

would produce multiplication and would be eliminated from the experiment.

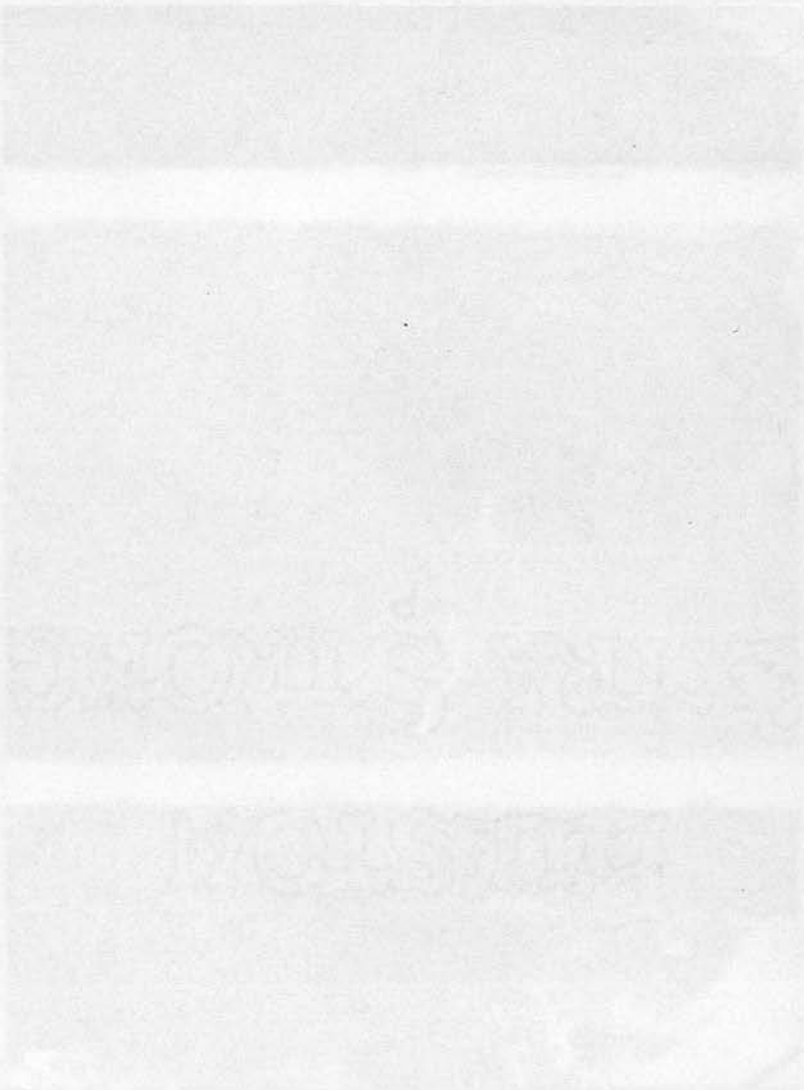

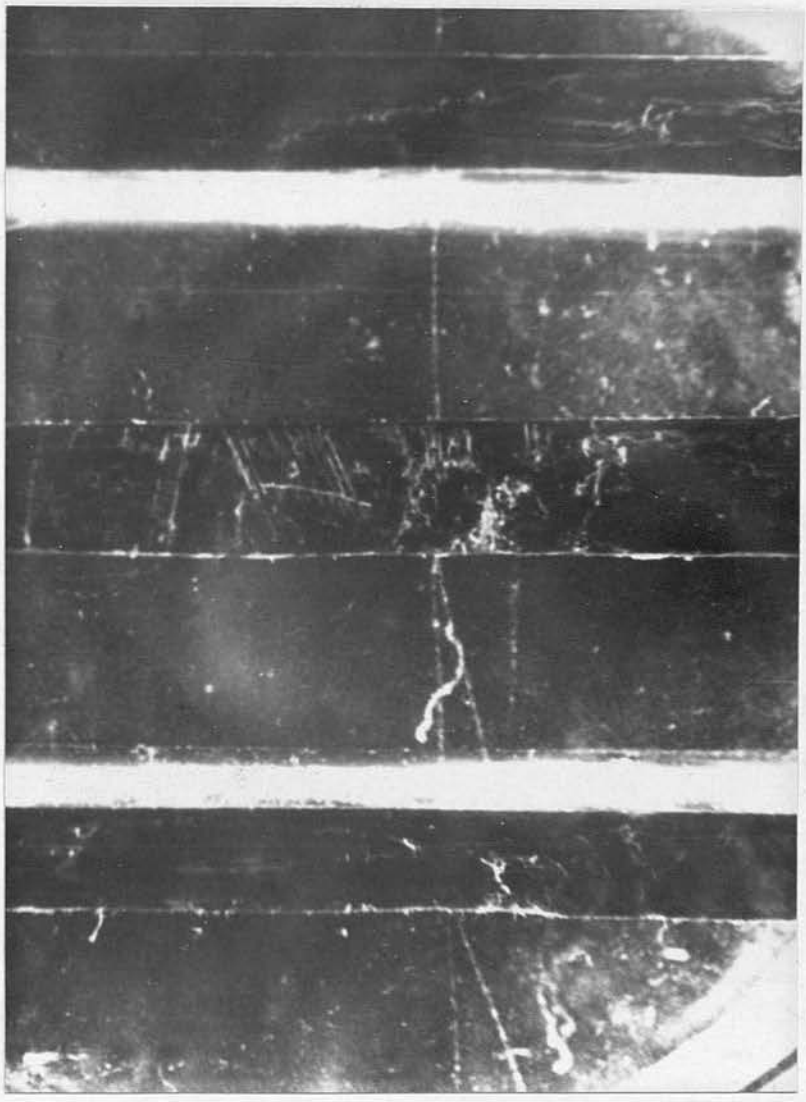

Plate 7

Chapter 6.

CONCLUSION.

6.1. Limitations of the Counter System.

In this chapter, the conclusions drawn from the experiments will be stated, and the future uses of the counter system will be discussed.

It will be obvious from the results, that a gas Čerenkov counter system of the type described, is an extremely useful tool for the detection of muons in the high energy range. The most useful property of the counter is of course, its velocity dependence. This has certain advantages over other selecting arrangements, which select on a momentum basis, e.g. elimination of contamination in beam experiments.

It had been shown that at 10 atmospheres pressure, the large Čerenkov counter can select particles which are 0.0009c above the threshold velocity. This threshold is set by the least number of photons which can be detected by the photomultiplier (90). If Figure (6.1) is considered the properties and limitations of the Čerenkov counters can be seen over a wide range of momenta.

The table shown below has been calculated from Figure (4.1), which shows the increase in photon number with increasing momentum. It is calculated on the basis of a 100 cm. long sensitive length. As has been stated before, the practical threshold momentum is displaced further from the theoretical threshold with increasing momentum. In fact, with such a counter, it is possible that even if the particle is travelling with the velocity of light, insufficient photons will be produced to give a count. The only thing which can

Pressure (Atmos.).	Theoretical Threshold Momentum. $\frac{Gev.}{c}$	Practical Threshold Momentum $\frac{Gev.}{c}$
30	0.68	0.72
25	0.78	0.82
10	1.26	1.50
5	1.80	2.70

Figure (6.1).

be done to rectify this situation is to increase the length of the counters. If, for example, a particle of momentum as high as 20 $\frac{Gev.}{c}$ was to be selected with an atmospheric pressure counter, it would have to be 4.8 metres long, and of such design to collect all the photons produced in the sensitive region. Of course, such a counter should theoretically select all particles above 4.5 $\frac{Gev.}{c}$, and thus the spread is becoming very large. It is this effect which puts a practical high momentum limit on the counters, and 20 $\frac{Gev.}{c}$ would certainly be the upper limit to any type of counter which we would consider possible to design.

Pulse height discrimination at these higher momentum values is also impossible, as can be seen from Figure (4.1), as the curves flatten out after a sharp initial rise. At the higher momentum values the increase in photon number with increasing momentum is extremely slow.

The experiments using cosmic radiation are at a great disadvantage compared to experiments using machine intensities. Therefore, the fundamental interest is in being able to select particles

in an energy range above the limits of the present accelerators. It does not therefore, appear possible to do this with a Čerenkov counter system alone. A combination of Čerenkov counters and ionisation counters using the relativistic rise in the latter, is being considered for future use. With such an arrangement, it might be found possible to select muons with an energy greater than those produced by accelerators.

---oOo---

APPENDIX 1.

Experiments on the Design of the Čerenkov Counters.

In this appendix, some of the preliminary experiments on the design of the Čerenkov counters will be discussed. It has been stated previously, that the distinctive property of the Čerenkov counter is the emission of light in the forward direction of particle motion. In this, it is different from a scintillation counter, where the light is emitted in all directions. It is possible, therefore, to distinguish between scintillations and Čerenkov light, by using the above difference, as will be seen in some of the experiments described below. This indeed, is the first problem; proving that the light produced in the gas is Čerenkov light, and not scintillation light, or some other non-directional effect.

As the counters had to be designed to withold a pressure of up to ~30 atmospheres, it is obvious that the light detecting device, the photomultiplier tube, must be placed outside the counter. This means that the counter must have an exit window through which the Čerenkov light can leave. Armoured plate glass was used as the material for this window. It must, therefore, be ensured that neither scintillation light, nor Čerenkov light produced in the glass, can reach the photomultiplier.

The third problem concerns the photomultiplier tube itself. It was discovered in preliminary experiments, that the photo-multiplier tube when covered with black paper, could still detect particles. It was necessary to investigate this phenomenon and discover the mechanism through which these counts were obtained.

Connected with this problem is the positioning of the reflecting mirror.

A 1.1. Scintillation and Čerenkov Effects in the Gas.

The gas used in all the experiments was nitrogen. In the first experiment, the high pressure Wilson cloud chamber was used as the gas holding device. It can be thought of as a light tight cylinder, capable of holding a pressure of up to ~ 100 atmospheres. Light produced in the gas, could leave the chamber by a glass window set at the lowest point. This light was reflected by a mirror onto a horizontal phototube. This mirror could be rotated, in such a way as to reflect all the light back into the chamber when required. The counter photomultiplier was run in coincidence with a scintillator, placed vertically above the glass window of the chamber.

In order to show that Čerenkov radiation was being detected, the variation of the two-fold counting rate, with increasing pressure was measured. As the pressure is increased, the counting rate should be expected to increase also, as more particles will have a velocity above the critical velocity. For an increase of 1 atmosphere in pressure, the critical velocity drops by $\Delta v = 0.0003c$. Thus, an increased counting rate should be expected, on decreasing the critical velocity from v_1, to v_2, if Čerenkov light is being detected. Also, as the critical velocity is lowered, particles which counted previously, with low efficiency, will be detected with a higher efficiency, as they will now produce more photons of Čerenkov light. Thus, not all the increase in counting rate will be due to particles whose velocity lies between v_1, and v_2, as some extra counts will be obtained from particles with velocity $> v_1$,

which are now counting with a higher efficiency,

The results of this experiment are shown in Figure (A 1.1). It will be seen that the upper curve does show an increase with increasing pressure. This upper curve is the counting rate when the mirror is set at 45°. The effects which can, therefore, contribute to this curve are

(1). Čerenkov light produced in the gas.

(2). Scintillations from the gas.

(3). Čerenkov and/or scintillation light produced in the glass window.

(4). "Background" counts due to effects in the photo-multiplier.

As the increase in counting rate is purely a function of the gas pressure, as every other quantity is kept constant, it can be taken that the increase must be due to effects (1) and (2).

The lower curve is associated with the "background count", when the mirror is horizontal, thus reflecting all the light due to effects (1), (2) and (3) back into the chamber, to be absorbed by the chamber walls. In this case, it will be seen that no significant increase in counting rate with pressure is observed. It should also be noticed that the upper and lower curves come together at the low pressure end. At the low values of the pressure, it should be expected that effects (1) and (2) would be negligible, thus, leaving only effects (3) and (4). As the two curves tend to the same value, this suggests that effect (3) is not a significant process.

Although it has been shown that increasing the pressure of the

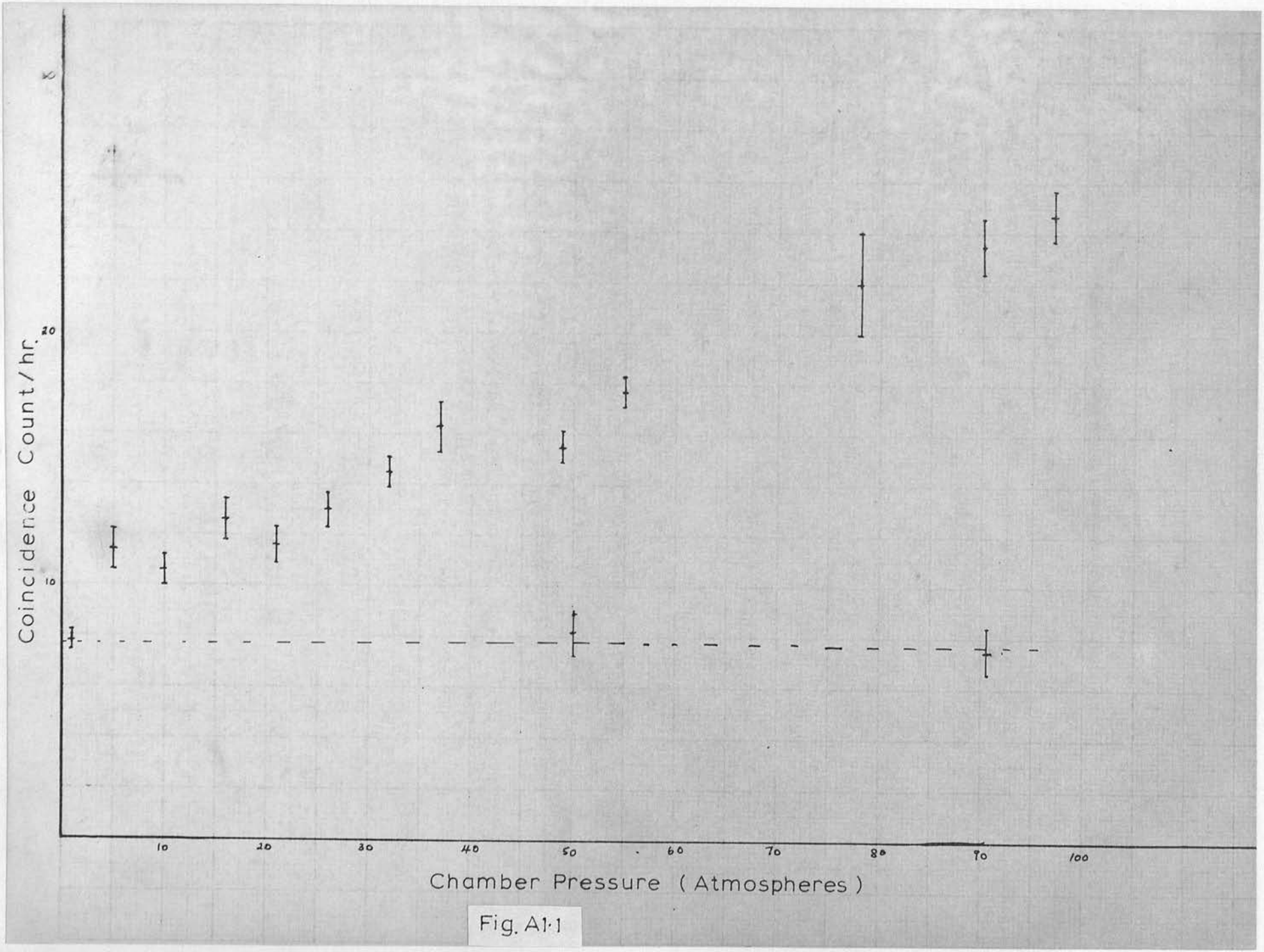
Coincidence Count / hr.
20
10
10
20
30
40
50
60
70
80
90
100
Chamber Pressure (Atmospheres)

Fig. A1·1

gas, increases the counting rate, it has yet to be shown that the light produced in the gas is Čerenkov light and not scintillations. It would be expected that if scintillations were being produced in the gas, the counting rate would likewise increase with gas pressure. When the counter is placed in the upright position, both Čerenkov and scintillation light produced in the gas would be capable of passing through the exit window and being reflected by the mirror onto the phototube. However, when the whole apparatus is turned through 180°, in such a way as to put the photomultiplier on top, and the scintillator beneath, the contribution from any Čerenkov light produced in the gas, can be calculated. In this upside down position, the Čerenkov light is directed downwards, away from the exit window, and it is absorbed by the black chamber walls. This, of course, assumes that the number of particles travelling vertically downwards, is very much greater than the number travelling in an upward direction. Therefore, in this second (upside down) position, the count should be solely due to any scintillation light produced, and should be considerably decreased, if most of the previous counts were due to Čerenkov light.

With the gas pressure fixed at 40 atmospheres, which corresponds to a critical velocity of $v_c = 0.9880c$, the coincidence counting rate, in both positions was measured. In position 1, (the upright position), a count of 16.0 ± 1.0/hr. was obtained, while in position 2 (upside down), there were 7.8 ± 0.6 counts/hr. This value of 40 atmospheres, for the gas pressure, was selected in order to make the critical velocity low enough, to obtain a significant difference in a short time. If atmospheric pressure had been chosen, the

counts in the two positions would have been more difficult to resolve, as there would have been fewer particles above the critical velocity.

From the above results, it will be seen that the difference in the two counts (i.e. 8.2/hr.) would be attributed to Čerenkov radiation in the gas. It will also be seen that the count in the upside down position is statistically the same as the "background" count due to effects in the phototube. Thus, it would appear that all the light from the gas was Čerenkov light and the remainder was due to the background count. Therefore, it can be assumed that there is no significant contribution from scintillation phenomena in the gas.

A 1.2. Scintillation and Čerenkov Effects in the Glass Window.

It has been shown in the previous section, that no significant counts were obtained from light, whether scintillation or Čerenkov, produced in the glass outlet window. However, this problem must be considered in more detail. If the glass of the window were to scintillate, this effect would be very serious from the point of view of the experiment to be undertaken.

In the experiments to determine the magnitudes of these effects, a photomultiplier was placed in a light tight box, and a piece of armoured plate glass replaced the scintillator. The glass was optically connected to the photocathode by a layer of glycerine. The single fold count was then taken in the following four cases. Firstly, the count for the photomultiplier alone, (glass removed) was taken in the upright position. This was found to be 23 $\pm$ 2/min. The photomultiplier was then turned upside down, with the photo-

cathode pointing downwards. In this case a counting rate of 22 ± 2/min. was obtained. This suggests that the count due to the photomultiplier alone, is not Čerenkov radiation, as in that case, a drop would be expected on turning the tube upside down. This point will be discussed in more detail, however, in the next section. It is sufficient to state that as far as the photomultiplier alone is concerned, no significant change in the counting rate is observed, on turning it upside down.

The experiment was then repeated, with the glass clamped in position, firstly in the upright position, (44 ± 3/min.), and finally upside down, (27 ± 2/min.). The difference between these two counts is attributed to Čerenkov radiation produced in the glass window. The small difference in the upside down position when the glass is added, would normally be attributed to scintillations in the glass. However, if the effects taking place at the glass-air boundary are considered, it would appear more likely that this increase is due to Čerenkov light. In the upside down position, the Čerenkov light produced in the glass is directed downwards, away from the photocathode and towards the glass-air boundary. If the angles are such that this light is reflected at this boundary, some of the light will manage to reach the photocathode and give a count. The amount of light reaching the photocathode will, however, be very much less than the amount produced, as the glass window had ground edges from which a large proportion of the reflected light would escape. This explains the difference in counting rate between cases 3 and 4. The reason for the reflection at the glass-air surface is discussed below.

In any practical counter, there is, therefore, a rather

complicated problem to be overcome. It is known that any particle which produces Čerenkov light in the gas ($\beta_c = 0.9880$ for 40 atmospheres), must also produce Čerenkov light in the glass bottom window, if it passes through it (β_c glass = 0.67). Also, by consideration of formula (1.2), it will be seen that the number of photons produced in $\frac{3}{4}$ inch of glass, (the thickness of the window), will be approximately twice the number produced in 30 cms. of gas, at 40 atmospheres, (for a particle with v = c). Therefore, it would appear that the radiation in the bottom window would swamp that produced in the gas. The outlook is improved, however, if the angle at which the Čerenkov light is produced in the window, is considered. In the glass, it can be assumed that all the relevant particles will have velocities, which can be considered as effectively $\beta = 1$. From relation (1.1), this gives a value of 48° 11', for the Čerenkov angle in the glass. This is also the angle of incidence upon the glass-air surface, and as the critical angle for such a boundary is 41° 49', (n = 1.5), the Čerenkov light will be internally reflected.

When the Čerenkov-cloud chamber and scintillator combination is being used, the geometry is such, that on tracing out the possible light rays, it can be shown that the contribution to the counting rate, from Čerenkov light produced in the glass, which is not reflected at the boundary, is very small. This agrees with the experimental result discussed in Section A 1.1.

However, at this stage, only fast particles have been considered, i.e. those that would give Čerenkov light in the gas. There are, however, slower particles ($0.6667 < \beta < 0.9880$), which, although

not counting in the gas, would still produce Čerenkov light in the glass window. It must also be considered, that these particles would emit Čerenkov light at smaller angles, the lower their velocity, and thus the critical angle cut off would no longer occur. By consideration of the curve of Čerenkov angle against velocity above threshold, it will be seen that at high velocities, the angle is fairly constant over a wide range and then drops rapidly. Thus, it will be seen that a particle would have to have a velocity $\leq 0.90c$, before the Čerenkov angle was less than the critical angle. Electrons of this velocity would be unable to traverse the counter, so effects of slow electrons need not be considered. Muons near this upper limit could count, and therefore the modification described below is made to the designed counters.

Thus, it has been shown that it is unlikely that any significant scintillation effect is produced in the glass window, although Čerenkov light is emitted. However, in a counter arrangement, this Čerenkov light would be internally reflected, at the glass-air boundary for most of the fast particles, and most of the slower particles could not traverse the counter telescope. However, to cut out the slow muon contribution, it appears better to place the glass window out of the direct particle path. This can be accomplished by placing the window in the side wall of the counter, and using a 45° mirror inside the counter, to reflect the light through 90° onto the photomultiplier lying horizontally outside the counter. It will be shown in a later section that there is another advantage with this design, with the mirror inside the counter.

A. 1.3. Effects in the Photomultiplier Envelope.

In the previous sections, the "background" count, due to particles passing through the envelope of the photomultiplier tube have been mentioned. In this section, the experiments carried out to investigate the mechanism by which such particles count, will be discussed.

The previous experiments were undertaken using single fold rates, but the arrangement was now returned to coincidence measurements, between a scintillator and a photomultiplier, enclosed in a light tight box. Firstly, the coincidence counting rate, between the scintillation counter and the upright photomultiplier was measured, when they were placed in a vertical line, scintillator above phototube (0.61 $\pm$ 0.08/min.). The photomultiplier was now inverted, in such a way that the photocathode was in the same place as in the previous count. This was to keep the geometry the same in the two cases. The count in this position was (0.38 $\pm$ 0.1/min.) It will be seen from these results that there is a significant difference, which is attributed to the loss of Čerenkov light after reflection (in second case) through the side of the photomultiplier envelope. It will be seen, however, that there is still a counting rate in the upside down case which is greater than half the upright. count. This is attributed to a proportion of the Čerenkov light being reflected back onto the photocathode.

That such effects are occurring can be shown more clearly in the following experiment, using a disc of black paper. The disc is placed on the glass-air boundary, good optical contact being made by a layer of glycerine. The photomultiplier-scintillation counter

coincidence counts were then repeated, firstly with the photomultiplier upright (0.70 ± 0.10/min.), and secondly, with the photomultiplier upside down (0.07 ± 0.02). From these results, it will be seen that when upright, the black paper makes no significant difference to the count, as the Čerenkov light is directed onto the photocathode. When upside down, however, the black paper reduces the counting rate very greatly. This is because the Čerenkov light is emitted away from the photocathode and is absorbed by the black paper. The small residual count is statistically the same as the chance counting rate which was determined by placing the two counters at the same level with a large separation (0.04 ± 0.02/min.). Any small difference is thought to be due to Čerenkov light, produced by cosmic particles travelling at large angles, where some of the light may strike the photocathode directly.

Thus, this experiment shows that the mechanism, by which particles are detected by the photomultiplier alone, is Čerenkov radiation emitted in the glass envelope of the phototube. Contributions from other sources are very small if present at all. It will be seen, therefore, that it is essential to place the phototube out of the direct particle path, and thus, it is necessary to employ a mirror to reflect the light.

A 1.4. Position of the Mirror.

Previously, it has been shown that it is preferable to have the reflecting mirror inside the pressure chamber, as in this case, the glass window through which the light leaves the chamber, can be placed out of the direct particle path. In the experiments described in(A 1.1), this condition was not satisfied, and it was

possible that Čerenkov light produced by particles in the glass window was contributing on a small, (but not significant), scale.

With the Čerenkov - cloud chamber, there is a more serious difficulty, however, which is dependent on the efficiency of collection of the genuine Čerenkov light, i.e. that produced in the sensitive gas volume. If it is assumed that none of the light produced in the glass can escape, and the particle velocity is such that no light can be produced in the atmosphere, between the window and the mirror, a situation is produced which can be represented by Figure (A 1.2). In this diagram, the situation has been exaggerated, as the Čerenkov angle is small in practice. However, it will be seen that the Čerenkov cone, falling on the mirror, is now hollow, as no light is produced, below the top surface of the glass. Thus, the light is striking the mirror round the circumference, rather than at the centre, If the rays are traced out on a scale diagram, it can be shown that a large proportion of the Čerenkov light does not reach the photomultiplier, but is reflected at such an angle as to absorbed by the container walls. This effect is most serious at high pressures, when the Čerenkov angle is greatest.

If the mirror was placed inside the pressure chamber, the Čerenkov cone would be solid, as light would be produced right down to the surface of the mirror. In this case, the whole mirror surface could be used for reflection, and the spread of light after reflection, would be such, as to ensure greater proportion of it reached the photomultiplier.

The other property desired in the mirror, is that it should be aluminised on the top surface. If the photomultiplier is placed out of

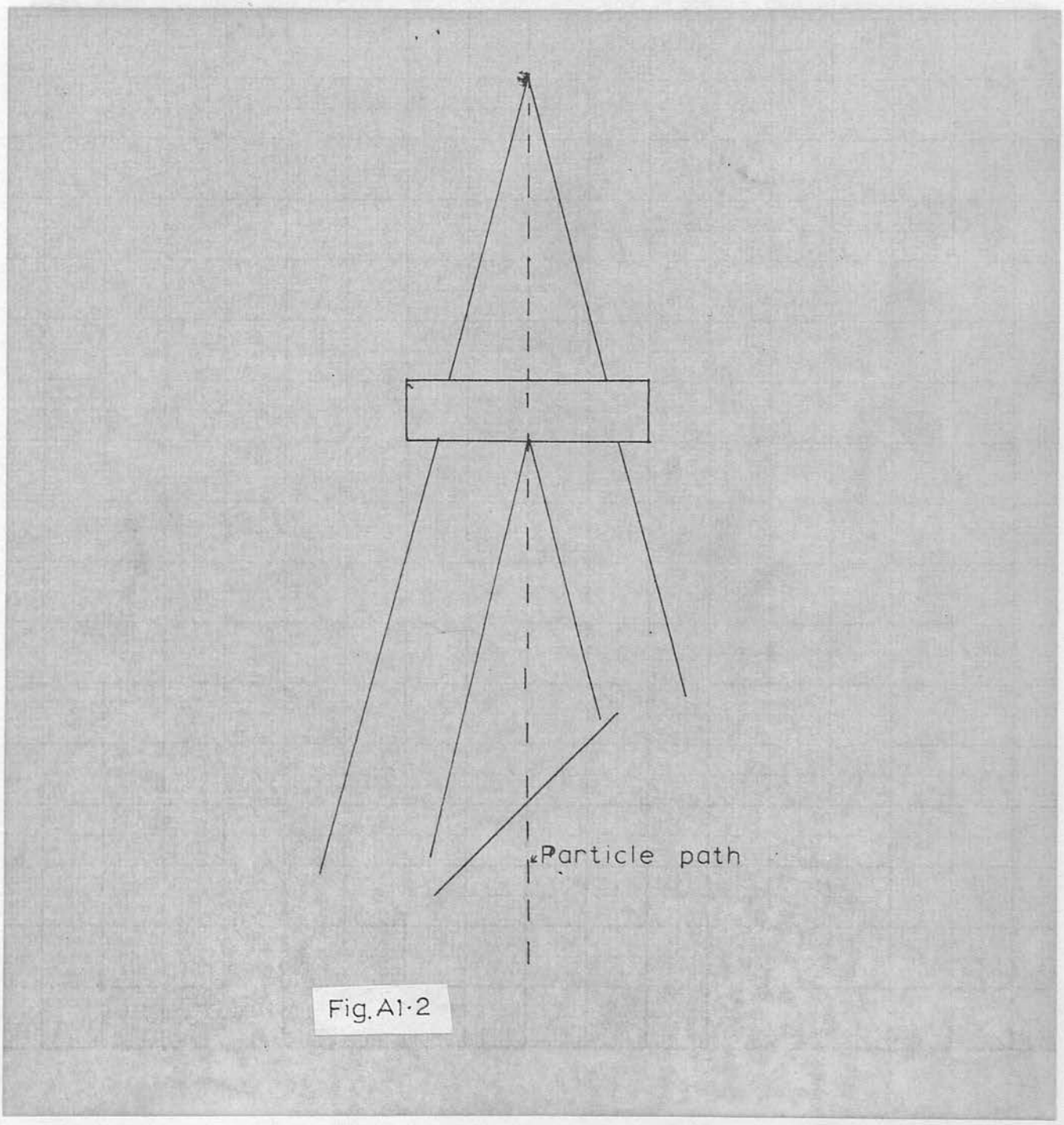

Fig. A1·2

the direct particle path, this means that the selected particle must pass through the mirror, producing Čerenkov light in the glass. If the aluminised surface was behind the glass, the Čerenkov light from the mirror would be reflected, and might contribute to the unwanted counting rate.

Thus, to sum up these preliminary experiments, it can be said that the required Čerenkov counter should be designed to have a front aluminised mirror, placed inside the pressure chamber, which will reflect the Čerenkov light, through a side window onto a horizontal phototube. Both the window and the phototube should be well removed from the particle path. It will be seen that the designed counters, described in chapter 2, satisfy these conditions.

Appendix 2.

In this appendix, experiments using the high pressure Wilson cloud chamber, in its capacity as a track recording device, and also as a Čerenkov counter will be described. This experiment is of interest as it enables the track position in the Čerenkov detector to be observed.

When operating in its dual capacity, certain modifications had to be made to the cloud chamber. Firstly, the chamber had to be made light tight, in order that only Čerenkov light produced in the gas will be collected by the photomultiplier. The other major modification concerns the positions of the lower flash tube and the photomultiplier. It will be remembered that when acting solely as a Čerenkov counter, the lower window of the chamber was used as a light output to the photomultiplier, which was placed below it, whereas when acting as a cloud chamber, the lower window was the light input for the lower photoflash tube.

This difficulty was overcome by having a shutter arrangement as shown in Figure (A 2.1). This shutter could be considered as a rectangular box, divided into two separate compartments, one containing the photoflash tube and the other a circular hole cut in the base of the box. In the waiting position, this hole was in position immediately below the lower chamber window. Thus, while in this position, any light produced in the chamber gas would pass through the window, through the shutter hole onto the mirror below, and be reflected through 90° onto the photomultiplier, placed horizontally out of the direct particle path. While in this position, no light from any other source could reach the phototube.

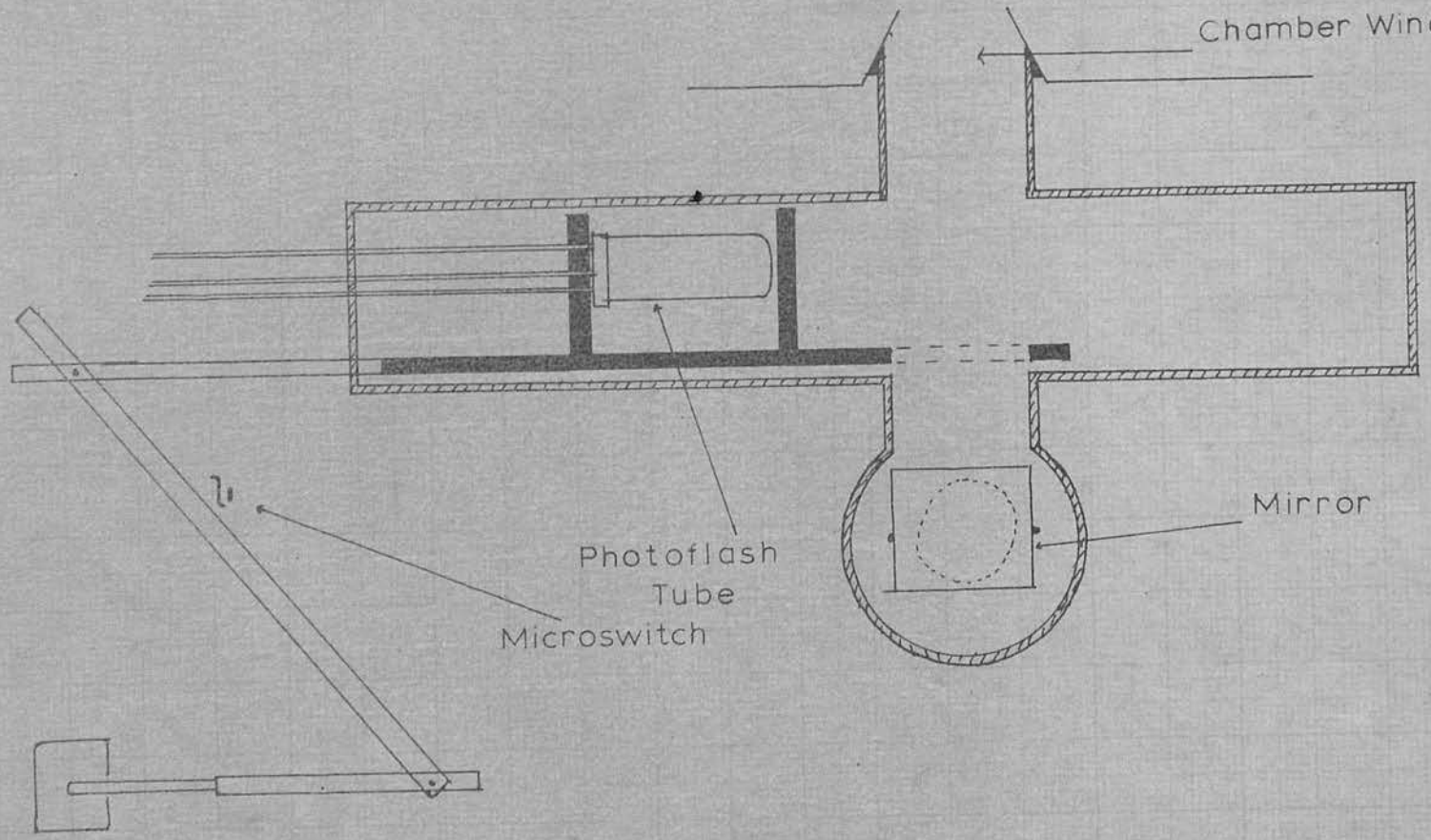

Fig. A2·1 Shutter Arrangement

When the chamber was expanded, a magnet pulled the shutter into the second position, where the photoflash tube lies immediately below the chamber window. When in this position, the photomultiplier is shielded completely from the photoflash, by the base of the shutter. There is also a safety circuit to ensure that the E.H.T. is removed from the phototube before the photoflash takes place.

There were obviously certain disadvantages in this arrangement. For example, the lower flash tube could no longer be placed as near the lower window, when in position, as it was in the case of operation as a chamber alone. Also, the photomultiplier was farther away, thus, cutting down the efficiency of light collection. It must also be remembered, that this arrangement had the fundamental defect of not being wholly automatic, and could therefore, not be left overnight to take photographs. However, it did have the advantage of photographing the particle, as it actually passed through the detecting medium and was on the whole an effective instrument.

It was found, by considering the initial photographs, that the most efficient track position for Čerenkov detection appeared to be such, that a proportion of the light emitted by the particle was travelling vertically downwards. This required that the particle was inclined to the vertical by an amount equal to the Čerenkov angle. It was also found that quite a large proportion of the photographs did not have a track travelling in the correct direction. In order to clarify this position, a counting rate experiment was undertaken.

The particles which produce a count, can be divided into 3

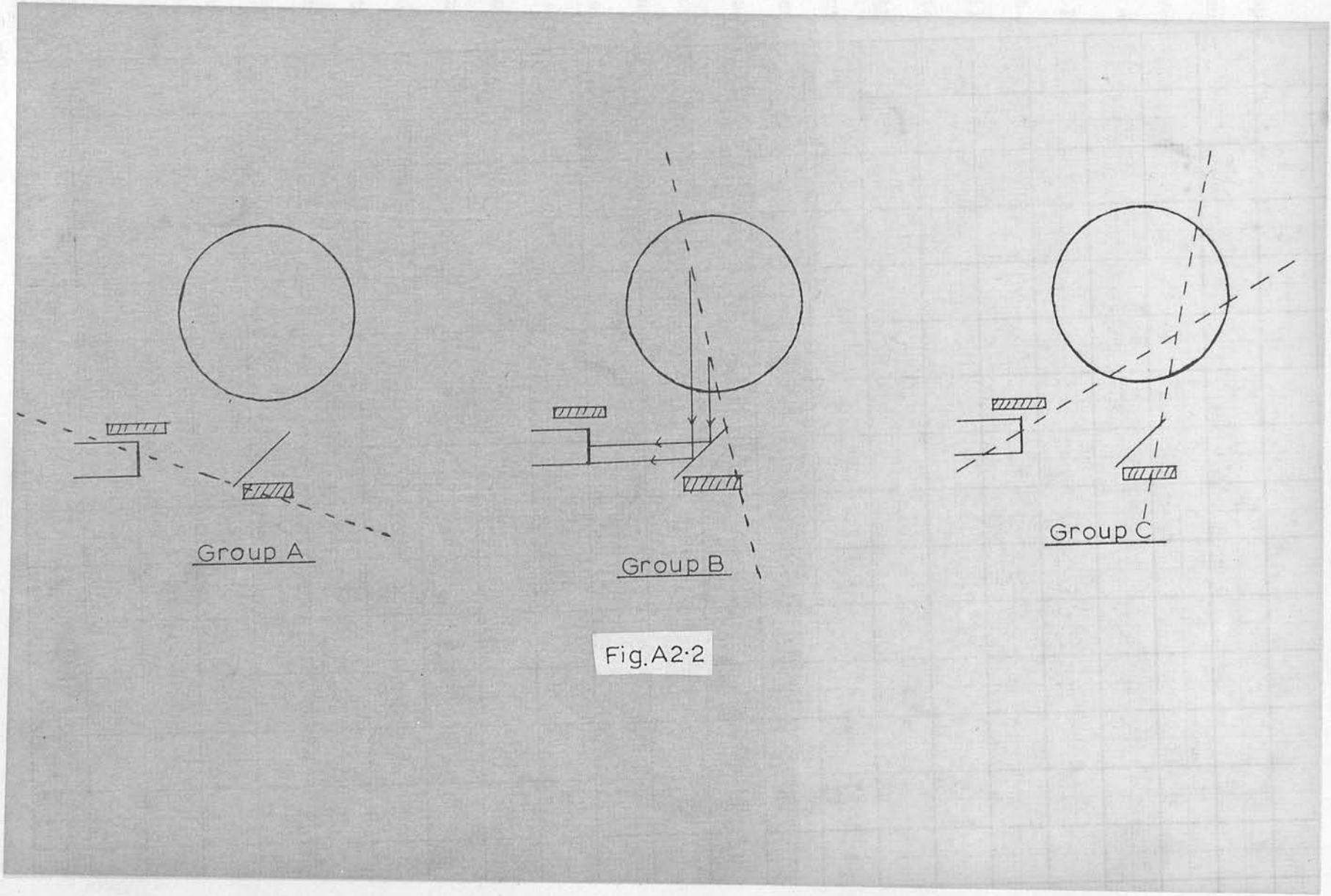

Fig. A2·2

groups. Group A are those single particles passing through the Čerenkov photomultiplier envelope and the scintillator, placed above the chamber, vertically above the exit window. Group B are the "genuine" particles i.e. those which produce Čerenkov light in the pressure chamber, which reaches the phototube, and which also pass through the scintillator. The remaining group C are those similtaneous particles, one of which passes through the Čerenkov phototube, as the other penetrates the scintillator. The pressure in the chamber was set at 46 atmospheres and with an anti-coincidence counter shielding the Čerenkov phototube, the following counts were taken. Count 1 was a two-fold count between scintillator and Čerenkov counter, with the shutter open. (23/hr.). In this count, all three types of count will be selected (A + B + C = 23). Count 2 was a identical count, with the shutter closed this time. This cuts off the Čerenkov light and thus eliminates the genuine particles (A + C = 8.5/hr.). Three fold counts (Čerenkov counter + scintillator - shielding counter) were also taken, both with window open (16.5/hr.), and with it closed (2.5/hr.). In case 3, with the window open, it can be approximately taken that, the anti-coincidence unit will eliminate group A, and not seriously reduce group C. Therefore, we have (B + C = 16.5). Finally in count 4, only group C will remain (C = 2.5). On solving these equations, the following results are obtained.

$$A = 6/\text{hr.} \qquad B = 14/\text{hr.} \qquad C = 2.5/\text{hr.}$$

It will also be seen that the 4 equations are consistent. Having determined these rates, the system was now used to trigger the chamber to obtain photographs.

These photographs were all taken at 46 atmospheres pressure, but varied in the value of the clearing field and flash delay time. Taking the criterion for a positive photograph, one in which there was a track which would pass through the top scintillator and which was travelling in the correct direction for Čerenkov light to reach the scintillator, 58 positive to 10 negative photographs were obtained with the window open, and 5 positive and 7 negative with the window shut. It would thus appear that the spurious photographs consist of equal numbers of obviously spurious events and events which appear to be genuine. Thus, it should be expected in the window open run, that 10 of the positive events were in fact spurious, so that there should be 48 genuine events, 10 obviously spurious and 10 spurious but not showing obviously. The large number of the latter group can only be explained as due to an inefficiency in the anti-coincidence counter. The detailed calculation proving that the particle track direction is such as to enable Čerenkov light to leave the chamber is given in Chapter 5.

ACKNOWLEDGEMENTS.

I wish to thank Professor N. Feather, F.R.S. for the use of the facilities of his laboratory.

I am very much indebted to Dr. G. R. Evans, F.R.S.E. for suggesting the subjects for this thesis and for much helpful advice and encouragement throughout the course of the work.

I am grateful to Dr. R. M. Hudson for his help in the initial stages of the work.

I also wish to acknowledge the valuable help given by Mr. A. Headridge and his staff in the construction of apparatus.

I am indebted to the Department of Scientific and Industrial Research for the award of a Research Studentship during the first two years of this work.

23). Lloyd J.L. & A.W. Wolfendale:- Proc. Phys. Soc. 73, 178 (1959).

24). Lloyd J.L., B. Rossle & A. W. Wolfendale:- Proc. Phys. Soc. A70, 421 (1957).

25). Lovati, A., A. Mura and C. Succi:- Nuovo Cim. 11, 92 (1954).

26). Mallet L. :- C. R. Acad. Sci. 183, 274 (1926).

27). Mallet L. :- C. R. Acad. Sci. 187, 222 (1928).

28). Mallet L. :- C. R. Acad. Sci. 188, 445 (1929).

29). Marshall J. :- Phys. Rev. 81, 275 (1951).

30). Masek G.E., L.D. Heggie, Y.B. Kim & R.W. Williams:- Phys. Rev. 122, 937 (1961).

31). Moliere G. :- Zeit. Naturf. 2a, 113 (1947).

32). Moliere G. :- Zeit. Naturf. 3a, 78, (1947).

33). McDiarmid B. :- Phil. Mag. 45, 933 (1954).

34). Olbert S. :- Phys. Rev. 87, 319 (1952).

35). Owen B.G. & J.G. Wilson :- Proc. Phys. Soc. A68, 409 (1955).

36). Perez-Mendez V. & J.H. Atkinson :- Rev. Sci. Instr. 30, 864 (1959).

37). Rossi B. & K. Greisen :- Rev. Mod. Phys. 13, 240 (1941).

38). Snyder H.S. & W.T. Scott :- Phys. Rev. 76, 220 (1949).

39). Viswanathan S.P., R. Mace & E.D. Palmatier:- Nuovo Cim. 28, 850 (1963).

40). Whittemore & Shutt:- Phys. Rev. 88, 1312 (1952).

41). Williams E.J. :- Proc. Roy. Soc. 169, 531 (1939).

42). Wilson J.G. :- Princ. of Cloud Chamber Technique (C.U.P.) (1951).